

# **Design of biosensors exploiting conformational changes in biomolecules**

**By**

**Frank Jeyson Hernández**

**Submitted in partial fulfillment of the requirements for the degree of  
Doctor in Chemical and process Engineering**



Departament d'Enginyeria Química  
Escola Tècnica Superior d'Enginyeria Química  
**Universitat Rovira i Virgili**

**Tarragona, 2008**

Dr. Ioanis Katakis , professor titular del Departament d'Enginyeria Química de la Universitat Rovira i Virgili, Dr. Ciara O'sullivan ICREA Research Professor de la Universitat Rovira i Virgili, Dr. Cengiz Ozalp Marie Curie Research de la Universitat Rovira i Virgili.

FAIG CONSTAR

que el present treball que porta el títol

Desing of biosensor exploiting conformational changes in biomolecules

que presenta en/na Frank Jeyson Hernández Hincapie per optar al grau de Doctor per la Universitat Rovira i Virgili, ha estat realitzat sota la seva direcció en els laboratoris del Departament d'Enginyeria Química de la Universitat Rovira i Virgili, i que tots els resultats presentats i la seva anàlisi són fruit de la investigació realitzada per l'esmentat/da doctorant.

I per a que se'n prengui coneixement i tingui els efectes que correspongui, signo aquesta certificació.

Dr. Ioanis Katakis

Dr. Ciara O'sullivan

Dr. Cengiz Ozalp

## Acknowledgements

*“What matters in life is not what happens to you but what you remember and how you remember it.”*

Gabriel García Marquez

### **For my little Sofi with love**

With many thanks for the support and scientific assistance from  
Dr. Katakis, Dr. O’sullivan and Dr. Ozalp, without  
Whom none of this would be here

Special thanks to everyone in BBG and NBG  
For their constant enthusiasm and help

Luiza, for her unconditional love and support

My *fratelo* Alesandro,  
So easy to be your friend

Alexandra, my little piece of Colombia in TGN,  
Because I feel myself when we are together

My friends: Christos, Cengiz, Salvatore, Edus, Vivi, Dunia,  
Montsant, Nuria, Ramon, Magda<sup>2</sup>, Zamorano, Jordi,  
and all the others with whom  
I shared my time in TGN

## Contents

1. Chapter one: Critical points in Biosensor development
  - 1.1 Introduction
  - 1.2. Biosensor classification
    - 1.2.1. Biosensors according to the biorecognition element:
      - 1.2.1.1 Enzymatic biosensors:
      - 1.2.1.2 Immunosenors:
      - 1.2.1.3 Whole-Cells or organelles based biosensors:
      - 1.2.1.4 DNA based biosensors:
      - 1.2.1.5 Protein based biosensors:
      - 1.2.1.6 Aptamer based biosensors:
    - 1.2.2 Biosensors according to the transduction method
      - 1.2.2.1 Optical biosensors
      - 1.2.2.2 Electrochemical biosensors
        - 1.2.2.2.1 Potentiometric
        - 1.2.2.2.2 Amperometric
        - 1.2.2.2.3 Conductimetric / impedimetric
  - 1.3 Biorecognition process
  - 1.4 Integrated biosensor development
  - 1.5 Bibliography
  
2. Chapter two: Towards Direct Electrochemical Detection of Maltose-Dependent Conformational Changes of Maltose Binding Protein
  - 2.1 Abstract
  - 2.2 Introduction
  - 2.3 Review of related literature
  - 2.4 Hypothesis
  - 2.5 Objectives
  - 2.6 Experimental Methods
    - 2.6.1 Protein Expression

2.6.2	Protein Purification
2.6.3	Additional Biosensor Reagents
2.6.4	Attachment of the ruthenium complex to MBP-MT
2.6.5	Attachment of the MBP-MT-Ru to gold electrodes
2.6.6	Electrochemical measurements
2.7	Results and discussion
2.8	Conclusion
2.9	Bibliography
3.	Selection of transduction-incorporating avidin-aptamer by a novel partitioning mechanism termed “Soluble-SELEX”
3.1	Abstract
3.2	Introduction
3.2.1	SELEX principle
3.2.1.1	Target molecule
3.2.1.2	Design of the oligonucleotide library
3.2.1.3	Interaction between library members and target molecule
3.2.1.4	Partitioning
3.2.1.5	Amplification
3.2.1.6	Conditioning
3.2.1.7	Cloning and Sequencing
3.2.1.8	Analysis of consensus sequences
3.3	Hypothesis
3.4	Objectives
3.5	Experimental Methods
3.5.1	Design of the SELEX Library.
3.5.2	Soluble-SELEX method:
3.5.2.1	Evolution monitoring of the Soluble-SELEX method.
3.5.2.2	Cloning

- 3.5.2.2.1 Bacteria Transformation:
- 3.5.2.2.2 Inoculation on media-LB agar plates:
- 3.5.2.2.3 Inoculation of single colonies in LB liquid media.
- 3.5.2.2.4 Plasmid extraction
- 3.5.2.2.5 Plasmid analysis by PCR
- 3.5.2.3 Sequencing
- 3.5.2.4 Alignment and analysis of sequence:
- 3.5.2.5 Evaluation of aptamer-candidates
- 3.5.2.6 Thermodynamics by BIAcore T100:
- 3.6 Results and discussion
- 3.6.1 SELEX
- 3.6.2 Candidate-aptamer evaluation
- 3.6.2.1 Surface Plasmon Resonance (SPR)
- 3.6.2.2 Thermodynamic information by Surface Plasmon Resonance Analysis
- 3.7 Conclusions
- 3.8 Bibliography
  
- 4. H18-avidin aptamer based biosensors
- 4.1 Abstract
- 4.2 Introduction
- 4.2.1 Biosensing
- 4.3 Experimental Methods
- 4.3.1 Fluorescence experiment
- 4.3.1.1 Synthesis of the oligonucleotide.
- 4.3.1.2 Reagents.
- 4.3.1.3 Measurement of fluorescence spectra.
- 4.3.2 Electrochemical experiments
- 4.3.2.1 Synthesis of the oligonucleotide
- 4.3.2.2 Reagents
- 4.3.2.3 Modification of gold electrode:
- 4.3.2.4 Electrochemical measurement:

4.4	Results and discussion
4.4.1	Aptamer characterization
4.4.1.1	Fluorescence
4.4.1.2	Electrochemistry
4.5	Conclusion
4.6	Bibliography
5.	Overall conclusions and future perspectives

## List of Figures and Tables

### Chapter one: Critical points in Biosensor development

**Figure 1.** Design and prediction of the SELEX library. The prediction was performed by mfold software.

### Chapter two: Towards Direct Electrochemical Detection of Maltose-Dependent Conformational Changes of Maltose Binding Protein

**Figure 1.** The use of MBP as biorecognition molecule for biosensing.

**Figure 2.** Four different mutations sites where cysteine is used to attach Ru<sup>II</sup> complex on the MBP-MT surface in order to study the effect of reporter location on transduction efficiency.

**Figure 3.** Optical properties of MBP-MT ruthenium attached. The protein and Ru<sup>II</sup> complex concentrations were evaluated by absorbance at 280 nm and 490 nm respectively. The percentage of protein labeling can be estimated in relation with both values. Experimental conditions have been described previously.

**Figure 4.** MALDI-TOF mass determination. Masses of N282C-MBP-MT and N282C-MBP-MT modified with [Ru<sup>II</sup>(1,10-phenanthroline-5-maleimide)(NH<sub>3</sub>)<sub>4</sub>][(PF<sub>6</sub>)<sub>2</sub>] were analyzed.

**Figure 5.** Cyclic voltammogram of [Ru<sup>II</sup>(1,10-phenanthroline-5-maleimide)(NH<sub>3</sub>)<sub>4</sub>][(PF<sub>6</sub>)<sub>2</sub>] complex.

**Figure 6.** Square wave voltammograms of Ru<sup>II</sup> modified MBP-MTs (**A**, N282C; **B**, K25C; **C**, Q72C; **D**, K46C) adsorbed to the Au electrode: -m) initial scan before maltose addition; +m) after maltose addition (10 μM, final). Baseline corrected current calculation outlined in the experimental section.

**Figure 7.** Maltose-dependent changes in baseline corrected current observed from Ru<sup>II</sup>-modified N282C MBP-MT adsorbed Au working electrodes.

**Figure 8. Maltose titration:** Amperometric titration data using SWV was able to detect small variations of maltose concentration. The corresponding titration curve has shown progressive decrease of current as a function of maltose concentrations.



**Figure 9.** The selectivity studies of MBP-MT based biosensor were performed by square wave voltammetry.

### **Chapter Three. Selection of transduction-incorporating avidin-aptamer by a novel partitioning mechanism termed “Soluble-SELEX”**

**Scheme 1.** Scheme of SELEX method (systematic evolution of ligands by exponential enrichment).

**Table 1.** List of several aptamer target-molecules and different separation methods

**Table 2.** Soluble methods for SELEX and their limitations.

**Figure 1.** Design and prediction of the SELEX library. The prediction was performed by mfold software.

**Fig 2.** Design of “Soluble-SELEX” method.

**Figure 3.** Hybridization analysis by fluorescence and time optimization.

**Figure 4.** Emulation of a round of “Soluble-SELEX”. Wherein, hybridization works as partitioning mechanism.

**Figure 5.** Electrophoresis of the first round of “Soluble-SELEX” using hybridization as partitioning mechanism.

**Figure 6.** Evolution of “Soluble-SELEX” by the binding of DNA library members.

**Figure 7.** Alignments by the candidate-aptamers by a bioinformatic tool (T-Coffee).

**Table 3.** Comparison between “Soluble-SELEX” and two additional aptamers performed by standard SELEX.

**Figure 8.** Prediction of secondary structure of the six candidate aptamers by mfold program.

**Figure 9.** BIAcore binding curves for 500 nM of six candidate aptamer.

**Figure 11.** Evaluation of specificity of H18-avidin aptamer by SPR.

**Figure 12.** Studies of stability and reproducibility of H18hp avidin-aptamer by BIAcore (T100) technology.

**Table 4.** Thermodynamic parameters of the interaction between H18hp avidin-aptamer and its target

**Figure 13.** van't Hoff plot of H18hp avidin-aptamer at 10, 20, 25 and 35°C.

**Figure 14.** High-resolution kinetic analysis of the binding of avidin to H18hp avidin-aptamer surface using BIAcore T100.

#### **Chapter four: H18-avidin aptamer based biosensors**

**Table 1.** Comparison between antibodies and aptamers.

**Figure 1.** Optimization of the H18hp avidin-aptamer fluorescence signal at two different conditions

**Figure 2.** Evaluation of buffer TBS-T dilution in the fluorescence-quenching signal.

**Figure 3.** Avidin-dependent changes in fluorescence-quenching of H18-aptamer.

**Figure 4.** Fluorescent signal Effect of KCl and NaCl on H18 avidin-aptamer.

**Figure 5.** Ferrocene-aptamer characterization of H18-avidin aptamer by square wave voltammetry.

## NOTATION/ABBREVIATIONS

AC	alternating current
$\theta$	Fractional coverage = $\Gamma/\Gamma_m$
$\Gamma$	Coverage of MBP-MT
$\Gamma_m$	$\text{Ru}^{\text{II}}$ -MBP-MT maximum coverage
Ab	Antibody
AFM	Atomic force microscopy
Ag	Antigen
ASP	Aptamer switch probe
Au	Gold
BHQ	Black hole quencher
bPBP	Bacterial periplasmic binding protein
BSA	Bovine serum albumin
cDNA	complementary DNA
CdSe	Cadmium Selenide
CE	Capillary electrophoresis
$c_o$	bulk maltose concentration
CV	Cyclic voltammetry
Da	Dalton
DNA	Deoxyribonucleic acid
dsDNA	Doble-strand DNA
	1-Ethyl-3-[3-dimethylaminopropyl]carbodiimide
EDC	Hydrochloride
EQCM	Electrochemical quartz crystal microbalance
ESPR	Electrochemical surface plasmon resonance
FAM	Carboxyfluorescein

Fc	Ferrocene
HEL	Hen Egg Lysozyme
<i>I</i>	Current
<i>I<sub>m</sub></i>	Maximum current
IPTG	Isopropyl β-D-1-thiogalactopyranoside
K25C-MBP-MT	Mutation K25C on MBP-MT surface
K46C-MBP-MT	Mutation K46C on MBP-MT surface
<i>K<sub>A</sub></i>	Association constant
<i>K<sub>D</sub></i>	Dissociation constant
LB media	Luria-Bertani media
LNA	Locked Nucleic Acids
LSPR	Localized surface plasmon resonance
MALDI-TOF	Matrix Assisted Laser Desorption /Ionization- Time Of Flight
MB	Magnetic-bead
MBP	Maltose binding protein
MBP-MT	Maltose binding protein – Metallothionein
MS	mass spectrometry
N282C-MBP-MT	Mutation N282C on MBP-MT surface
NHS	N-hydroxysulfosuccinimide
Nt	Nucleotide
PBPs	Periplasmic binding proteins
PCR	Polymerase chain reaction
PSA	Prostate specific antigen
Q72C-MBP-MT	Mutation Q72C on MBP-MT surface
QCM	Quartz crystal microbalance
RNA	Ribonucleic acid
RT-PCR	Reverse transcription - PCR
Ru <sup>II</sup> complex	[Ru <sup>II</sup> (1,10-phenanthroline-5-maleimide)(NH <sub>3</sub> ) <sub>4</sub> ][(PF <sub>6</sub> ) <sub>2</sub> ]
Ru <sup>II</sup> -MBP-MT	Ruthenium complex attached to MBP-MT
SELEX	Systematic evolution of ligand by exponential enrichment
SPR	Surface plasmon resonance

ssDNA	Single-strand DNA
SWV	Square wave voltammetry
TBS-t	Tris-Buffered Saline tween-20
UV	Ultraviolet
$\Delta G$	Free energy
$\Delta H$	Entropy
$\Delta S$	Enthalpy

# Diseño de biosensores explorando cambios conformacionales en biomoléculas

## *Resumen:*

El presente estudio utiliza dos moléculas diferentes como elementos de bio-reconocimiento. En el primer caso, un biosensor basado en proteínas fue desarrollado utilizando la proteína periplásmica de unión a maltosa (MBP = maltose-binding protein). La habilidad para manipular racionalmente la función de una proteína también ofrece la posibilidad de crear nuevas proteínas con valor biotecnológico. Nuestro diseño proteico ha sido usado para evaluar cambios alostéricos en proteínas. Este estudio evalúa un simple cambio conformacional el cual puede ser usado como el principio transductivo para un biosensor. Diferentes estrategias de transducción usando fluorescencia y electroquímica en eventos de reconocimiento entre la proteínas periplásmicas de unión y el ligando, han sido previamente reportadas. Esta investigación inicia con el estudio de los cambios conformacionales de MBP, continuando con el desarrollo de un biosensor electroquímico para maltosa. La señal de cuatro diferentes mutantes (K46C-MBP-MT, N282C MBP-MT, Q72C-MBP-MT; y K25C-MBP-MT) fue evaluada usando voltimetría de onda cuadrada. La posibilidad de usar este tipo de transducción mecánica (distancia) para la configuración de biosensores y la respectiva especificidad analítica es discutida.

La segunda parte de este trabajo incluye el método SELEX (systematic evolution of ligands by exponential enrichment) y aptámeros como moléculas de bio-reconocimiento.

Como resultado de el método SELEX, podemos obtener secuencias de oligonucleótidos (aptameros) con propiedades de reconocimiento similares a los anticuerpos. Estos elementos sintéticos, tienen un importante papel en el reconocimiento molecular por su capacidad de unión específica a la molécula blanco. Un nuevo mecanismo en el paso de separación ha sido realizado, y denominado “SELEX-Soluble”. Este nuevo método SELEX usa la hibridización como mecanismo de separación para dividir los oligonucleótidos de DNA que no se unen y los que se unen a la molécula blanco. El procedimiento de hibridización y su uso como mecanismo de separación en el método SELEX ha sido evaluado a través de estudios de fluorescencia. Este estudio también explora la incorporación de un aptamero como elemento de reconocimiento en un biosensor. Tres diferentes mecanismos de transducción has sido evaluados: fluorescencia, electroquímica y resonancia de plasmon superficial (SPR). En los tres casos una excelente señal fue reportada.

En conclusión, esta investigación ha evaluado la transferencia de una biosensor de fluorescencia a un biosensor electroquímico, utilizando la proteína periplásmica de unión a maltosa como elemento de bioreconocimiento. De otro lado, un nuevo método SELEX ha sido desarrollado. Sin embargo, futuras mejoras son requeridas para optimizar el método. Como resultado del método SELEX realizado un nuevo aptamero que reconoce específicamente avidina ha sido seleccionado y tres diferentes sistemas de transducción ha sido empleados para construir tres diferentes biosensores (fluorescencia, electroquímica y SPR).

# Design of biosensors by exploiting conformational changes in biomolecules

## *Abstract:*

The present study exploits two different molecules as biorecognition elements for biosensing. In the first case, a protein biosensor was performed using maltose-binding protein (MBP). The ability to manipulate protein function rationally also offers the possibility of creating new proteins of biotechnological value. Our design has been used to test the understanding of allosteric transitions in proteins. Here we examined a simple conformational change that can represent the biorecognition principle for a reagentless biosensor. Previously, modular strategies for transducing ligand-binding events into fluorescent and electrochemical responses have been reported. Starting with a study of the conformational changes of MBP this research will further develop electrochemical maltose biosensors. The responses of four individual mutations (K46C-MBP-MT, N282C MBP-MT, Q72C-MBP-MT; and K25C-MBP-MT) were evaluated using square wave voltammetry. The possibility of using this type of transduction mechanism for sensor configurations and analyte specificity is discussed.



The second part of this work involves SELEX (systematic evolution of ligands by exponential enrichment) and aptamers as biorecognition molecules. As a result of the SELEX method, we can obtain oligonucleotide sequences (aptamers) with recognition properties similar to antibodies. These synthetic elements play an important role in molecular recognition because of their capability for specifically binding of a target molecule. A new approach for the separation step has been performed, termed Soluble-SELEX. This new SELEX method uses hybridization as partitioning mechanism for separating the bound and unbound DNA members from the target-molecule. Hybridization procedure has been evaluated by fluorescence studies as partitioning mechanism for SELEX method. Herein, we exploited the incorporation of an aptamer for biosensing detection of a specific target molecule. Three different transduction methods such as fluorescence, electrochemistry and surface plasmon resonance (SPR) were evaluated. In all three cases, the biosensing procedure was successful.

In conclusion, this research has evaluated the translation of a fluorescent biosensor into an electrochemical biosensor using maltose-binding protein as biorecognition element. On the other hand, a new SELEX method has been developed. However, future improvements are required in order to optimize the method. As result of SELEX a new avidin-aptamer was selected and three different transduction systems were employed to construct fluorescent, surface Plasmon resonance and electrochemical biosensors.

# ***CHAPTER 1***

## ***Critical Points in Biosensor Development***

### **1.1 Introduction: Biosensors: history and definition**

Although the canaries used in coal mines could qualify as the first biosensors, the area of biosensors research started in the year 1962 with the development of enzyme electrodes by L.C. Clark. Since then, scientists from the fields of physics, chemistry, biochemistry, molecular biology and material science have contributed to this multidisciplinary field developing more reliable and robust biosensing devices for applications in the fields of medical/clinical analysis (1,2), veterinary (3), agriculture (4), food quality (5), environmental analysis (6), and bioterrorism prevention (7). As per definition of the IUPAC: *A chemical sensor is a device that transforms chemical information, ranging from the concentration of a specific sample component to total composition analysis, into an analytically useful signal. Chemical sensors usually contain two basic components connected in series: a chemical (molecular) recognition system (receptor) and a*

*physicochemical transducer. Biosensors are chemical sensors in which the recognition system utilizes a biochemical mechanism (8).*

Biosensing takes advantage of the biorecognition elements such as whole-cells, cell organelles, tissues, enzymes, antibodies, nucleic acids and proteins (8). The fast developments in molecular biology and biomolecular engineering expand the list of possible biological and semisynthetic biorecognition elements with great speed. The biological recognition event needs to be transformed into a measurable signal in conjunction with a physicochemical transduction mechanism. Both elements, the high specificity of the biomolecules and the sensitivity of the transducer mechanism (electrochemical, optical, electrical, piezoelectric, thermal and magnetic) (9), make possible to recognize and quantify specific molecules in a complex solution. The advances in transduction are closely linked to the accelerated technological breakthroughs related to electronics, informatics, data mining, and computer technologies. Signal transduction and data analysis research, oriented to lowering the cost and portability of biosensor analysis, are areas of high activity in electrical and electronic engineering, and analytical chemistry and lead in accelerated pace to more reliable and easy to use biosensors. The coupling between the biorecognition molecule and the transducer is often a critical step in biosensor development and can be performed by membrane entrapment, physical adsorption, matrix entrapment, or covalent binding among others. It is important to maintain the biorecognition capacity during such procedures while at the same time guarantee the robustness and reproducibility of the sensor.

In this thesis, the work is concentrated on the affinity biosensors based on receptor proteins (periplasmic binding proteins) and aptamers, whose interaction with the analytes is transduced electrochemically. It also explores the possibility of taking advantage of molecular biology to create generically biorecognition elements that can readily transduce their biomolecular interactions in electrochemical signals.

The introduction presents a general overview of the field with emphasis on the implications of the state of the art in each area to this work.

## **1.2. Biosensor classification:**

From the definition of biosensors, they can be classified either by their biological recognition element or their signal transduction mechanism. However, additional biosensor features could be analyzed. For example, the immobilization method of the biological element or the operational mode (simple measurement, multi-measurement, short or long term), can be another alternative for the classification of biosensor devices.

### **1.2.1. Biosensors according to the biorecognition element:**

In this case, the biosensors are classified according to the nature (molecules, whole-cells, etc.) or function (affinity or catalysis) of the biorecognition element. Isolation and/or purification are required in order to obtain the best performance of the sensor. Several molecules or whole cells can be used as biorecognition elements and the most relevant are discussed below:

### **1.2.1.1 Enzymatic biosensors:**

This class of biosensors employs enzymes as biocatalysts. Enzymes react with the analyte or the substrate producing a detectable signal through this biorecognition process (10). The most famous practical device for determination of blood glucose content is an enzymatic biosensor and it was developed by Yellow Springs Instruments in the early 1970s (11).

### **1.2.1.2 Immunosensors:**

Immunosensors are based on the antibody-antigen interaction and the transduction of the biorecognition event into a physical signal. The design and preparation of an optimum interface between the biological element and the detector material is the key part for this kind of sensors (12).

### **1.2.1.3 Whole-Cells or organelles based biosensors:**

Whole-cell bacterial biosensors are bacteria engineered to recognize a specific analyte. The signal-transduction is performed by the production of an easily quantifiable marker protein. In most cases, an existing regulatory system in the bacterial cell is exploited to drive expression of a specific reporter gene, such as bacterial green fluorescent protein, beta-galactosidase and others (13)

### **1.2.1.4 DNA based biosensors:**

DNA biosensors are commonly employed to detect specific sequences of DNA. They can reach high levels of selectivity and affinity based on the hybridization between a DNA

target and its complementary probe, which is present either in solution or on a solid support (14). Homogeneous assays allowing the determination of DNA sequences have been developed. These systems can be based on optical (15, 16) or electrochemical (17, 18) detection.

#### **1.2.1.5 Protein based biosensors:**

Protein-based sensors require that the proteins undergo conformational changes upon ligand binding. Then, the signal-transduction can be monitored quantitatively. Fluorescence detection (19, 20) and/or electrochemical measurements (21) have been reported. Thus, to develop compact, light weight, portable sensors considerable attention has been focused on this kind of recognition molecules for biosensor development.

#### **1.2.1.6 Aptamer based biosensors:**

Aptamers can be defined as *in vitro* selected functional oligonucleotides that bind a specific target molecule. Due to their inherent selectivity, affinity, and their advantages over traditional recognition elements, they represent an interesting alternative for biosensing. Aptamers are small in size in comparison to other biorecognition molecules such as antibodies, protein and enzymes. This allows efficient immobilization at high density. Therefore, production, miniaturization, integration, and automation of biosensors can be accomplished more easily with aptamers than with antibodies (22). As for the protein-based biosensors, the significant conformational change of most aptamers upon target binding offers great flexibility in the design of biosensors.

## **1.2.2 Biosensors according to the transduction method**

### **1.2.2.1 Optical biosensors**

Several optical properties, such as light absorption, fluorescence, bio/chemiluminescence, reflectance, Raman scattering, and refractive index have been exploited as transduction mechanisms for biosensor development (9). However, surface plasmon resonance (SPR) has recently been used as the basis for the optical signal transduction for the biosensor development.

*Surface plasmon resonance:* The binding of soluble target-molecules to the surface-immobilized ligands changes the refractive index of the medium near the surface. This change can be monitored in real time to measure accurately the amount of bound analyte, its affinity for the receptor and the association and dissociation kinetics of the interaction. An extremely wide range of molecules can be analyzed, from targets with low-molecular-weight to complex molecules and even whole cells, with interaction affinities from millimolar to picomolar concentrations. Advantages of SPR technique involve real time detection and reproducible measurements for the binding reactions of chemical compounds. This feature allows kinetic evaluation of affinity interactions, typically between antibodies and antigens. A variety of optical immunosensors have been configured using direct and indirect formats with and without optical labels. The main drawback of optical measurements is the high cost of the apparatus. (23).

### **1.2.2.2 Electrochemical biosensors**

The biochemical signals can be used to generate a current/charge or may change conductivity between two electrodes. The corresponding transduction device can be

described as potentiometric, amperometric, conductometric/impedimetric. A briefly description of these three signal-transduction mechanisms will be discussed.

#### **1.2.2.2.1 Potentiometric**

As per definition of the IUPAC: *Potentiometric measurements involve the determination of the potential difference between either an indicator and a reference electrode or two reference electrodes separated by a permselective membrane, when there is no significant current flowing between them. The transducer may be an ion-selective electrode (ISE), which is an electrochemical sensor based on thin films or selective membranes as recognition elements.*

The main advantage of such devices is the wide concentration range for which ions can be detected, generally between  $10^{-6}$  to  $10^{-1}$  mol/l. Their continuous measurement capability is also an interesting possibility for environmental applications. The apparatus is inexpensive, portable, and it is well suited for *in situ* measurements. The main disadvantage is that the limit of detection for some environmental samples can be high ( $10^{-5}$  mol/l or 1 ppm) and the selectivity can be poor.

#### **1.2.2.2.2 Amperometric**

As per definition of the IUPAC: *Amperometry is based on the measurement of the current resulting from the electrochemical oxidation or reduction of an electroactive species. It is usually performed by maintaining a constant potential at a Pt-, Au- or C-based working electrode or an array of electrodes with respect to a reference electrode, which may also serve as the auxiliary electrode, if currents are low ( $10^{-9}$  -to  $10^{-6}$  A). The*



*resulting current is directly correlated to the bulk concentration of the electroactive species or its production or consumption rate within the adjacent biocatalytic layer. As biocatalytic reaction rates are often chosen to be first-order dependent on the bulk analyte concentration, such steady-state currents are usually proportional to the bulk analyte concentration.*

This signal-transduction mechanism is frequently used for enzymatic and catalytic biosensors. The main advantage of this class of transducer is the low cost, therefore disposable electrodes are often used with this technique. The high degree of reproducibility that is possible for these (one time use) electrodes eliminates the cumbersome requirement for repeated calibration. The type of instrument used for these measurements is also very easy to obtain and can be inexpensive and compact, this allowing for the possibility of *in-situ* measurements. Limitations for this signal-transduction mechanism include the potential interferences to the response if several electroactive compounds can generate false current values. These effects have been eliminated for clinical applications through the use of selective membranes, which carefully control the molecular weight or the charge of compounds that have access to the electrode.

#### **1.2.2.2.3 Conductimetric / impedimetric**

The measured parameter for this signal-transduction mechanism is the electrical conductance/resistance of the solution. The large applicability of conductimetric detection is due to the observation that almost all enzymatic reactions involve either consumption or a production of charged species, and therefore lead to change in the ionic

composition of the enzymatic membrane. The electric field is generated using a sinusoidal voltage (AC) which helps in minimizing undesirable effects such as Faradic processes, double layer charging and concentration polarization (24).

The primary advantage of this technique is the use of inexpensive, reproducible and disposable sensors. The main disadvantage is that the ionic species produced must significantly change the total ionic strength to obtain a reliable measurement. This requirement increases the detection limit to unacceptable levels and results in potential interferences from variability in the ionic strength of the sample.

### **1.3 Biorecognition process**

Binding studies between two biomolecules are important in order to understand the molecular recognition process (25). Molecular recognition can be defined as the capability of a biomolecule to interact specifically with a particular target molecule although a huge variety of different but structurally similar competitor molecules are present (26). In nature, the binding between two bio-molecules is often accompanied by large conformational changes which are essential for cell function (27–30). Recognition processes are governed by the interplay of non-covalent interactions of comparable strengths such as ionic binding, van der Waals interactions, formation of hydrogen bonds and hydrophobicity. The non-covalent interactions between the residues of the biomolecules lead to the formation of a complex where the two biomolecules form a mutual interface consisting of one or more patches on their surfaces. In addition, long-range electrostatic interactions are believed to pre-orient the molecules so that the probability of a contact of the interface patches upon a collision of the molecules is

increased (31, 32). The simultaneous presence of different types of interactions and the fact that the associated energy scales do not separate leads to a complicated interplay among them. Therefore a detailed description of recognition processes poses a challenging problem. An understanding of the principles of molecular recognition processes is not only important from a scientific point of view but also for biotechnological and biomedical applications. The knowledge of these principles is a necessary input for the design of synthetic elements with molecular recognition ability to interact in a biological environment, with different kinds of molecules such as tissue, whole cells, molecular targets, etc. (33). An important feature of the molecular recognition processes is the phenomenon of selectivity, which is basically the ability of biomolecules to bind to each other in the presence of competing molecules. The selectivity of biomolecular recognition is thus only achieved if a large number of functional groups of the two molecules contribute co-operatively to a sufficient number of corresponding non-covalent bonds. This principle is often called complementarity in the literature (34). Thus, selectivity is a genuinely cooperative effect.

#### **1.4 Integrated biosensor development**

The development of standard biosensors is based on two steps: a) selection of a biological element with high level of affinity and selectivity for the target, and b) the adaptation of this biorecognition molecule to a desired signal-transduction mechanism.

Because each molecule presents different properties, the integration process has to be carried out for every single molecule used as biorecognition molecule for biosensing. In addition, the optimization procedure is required. All these factors become important

because there is not yet a generical method for the development of biosensors. In order to find a biomolecule for generic biosensing one requirement has to be fulfilled; that is, an integrated signal-transduction function (e.g. conformational changes) and the pocket or recognition site have to be connected and work together after the recognition step. If the reporter function is intrinsic to the biomolecule, additional modifications or assembly of several macromolecular components are not required.

Some researchers have tried, with more or less success, to introduce generic biosensors as an alternative to the conventional biosensing production. Hellinga's group has been reported that a superfamily of proteins called periplasmic binding proteins (PBPs) could be used as generic biorecognition molecules (35). The modification of the loops or recognition pocket offers the possibility to recognize different targets using the same scaffold protein. By this engineering process, the wild recognition site can be transformed into a new pocket for a different target by the change of aminoacid that confirms that recognition region (12 to 16 aminoacids). In addition, PBPs have another interesting characteristic, that is the conformational change after the target recognition. Through the allosteric changes two different forms of the protein were identified: a) open; without target and b) closed; after target recognition. This conformational change can be useful for the designing of generic biosensors. Although PBPs has been proven to be very flexible, a realistic generic biosensor can not be yet developed using these biomolecules. The principal reason is in relation with the limitation of targets that can be recognized by the loops transformation of PBPs. Only a couple of examples have been recognized as non-natural targets, which provides a clear evidence of this limitation. More specifically,

rational desing used for the pocket recognition site, which emulated the combinatorial chemistry process, is not a guarantee for the success.

On the other hand, anticalins have been reported as interesting generic biomolecules by Skerra group. (36). They are single chain peptides with around 180 amino acids full length, with a rigid structure based on B-barrel as central element. This B-barrel scaffold supports 4 loops that form the pocket or recognition site on the biomolecule. The loops are formed by 16 amino acid residues that can be replaced in order to recognize non-natural targets. The anticalins were described as a new class of engineered ligand-binding proteins. Therefore, the wide flexibility of anticalins for different kind of targets (size, nature, charge, etc) confirms their roll as important alternatives for antibodies. Similar affinity as for the monoclonal antibodies has been recorded as well. In fact, anticalins as generic recognition molecules offer an attractive alternative for clinical and medical applications. They have been proven to have potential applications as recognition molecules. However, the rigid scaffold structure limits the possibility of an intrisical tranduction mechanism. In this sense, the use of anticalins as recognition molecules for generic biosensors is limited. Only mass deposition biosensors (SPR, QCM) can be obtained basd on these type of biomolecules.

For the last two decades, other interisting biomolecules involved in biosesing have been the nucleic acids (DNA and RNA). Nucleic acids can be selected by SELEX (systematic evolution by exponential enrichment) to raise sequences with high affinity and selectivity for a specific target. These oligonucleotide sequences, referred to as “aptamers” have been evidenced attractive properties for biosensing. A wide range of targets with different features can be recognized by aptamers. Theoretically, there is no target limitation for

aptamers, which suggests that they constitute the most generic molecule for biorecognition in nature. Several transduction mechanisms based on aptamers have been reported, such as electrochemistry (37, 38), fluorescence (39), SPR (40), QCM (41), atomic force microscopy (AFM) (42) and others. Therefore, some aptamers have shown conformational changes after the recognition process in different transduction mechanisms. In addition, structural studies for aptamers were performed using NMR and the results have revealed important structures such as G-quadruplex. Here, the presence of conformational changes works as intrinsic signal-transduction mechanism after the target recognition. These allosteric movements are used for the design of “turn on” or “turn off” biosensor systems. In other words, aptamers could be the best candidate for generic biosensing because of their intrinsic signal-transduction mechanism and the unlimited flexibility for target recognition. However, SELEX is not a guaranteed process for an aptamer with intrinsic transduction mechanism; it could only ensure affinity as the parameter of selection. In this sense, if the development of aptamers with intrinsic transduction mechanism (conformational changes) could be induced, SELEX could be considered an approach that can offer a solution for the generic biosensor development.

An interesting approach called “aptamer switch probe” (ASP) has been reported a couple of months ago (43). The method can be described by selecting 3 elements for the strategy: an aptamer, a small oligonucleotide sequence complementary to part of the aptamer, and a PEG linker, which binds the two previous elements. As reporter mechanism, a fluorophore and a quencher were selected. Both were attached at the extreme of the complementary region of the aptamer and oligonucleotide. In the absence

of target the complementary sequences are close enough to block the fluorophore signal by the quencher. After addition of the target, the biorecognition process performed by the aptamer induces a conformational change in the ASP, which “switches on” the fluorescent signal. The method could be used for any aptamer, suggesting an alternative for generic biosensor development.

In this thesis, we proposed to study conformational changes as the generic transduction mechanism in biomolecules. Taking advantage of the previous studies reported about PBPs, more specifically, the research performed by Benson group about maltose binding protein (MBP) based biosensors, MBP transduction mechanism was chosen as the platform for checking the conformational changes that offers MBP for biosensor design. The transfer of a “turn on” fluorescent biosensor into a “turn off” electrochemical biosensor was performed and the possibility to select conformational changes in biomolecules as intrinsic transduction mechanism for generic biosensor development was also evidenced.

After the selection of conformational changes as generic transduction mechanism for biosensors, aptamers were chosen as the generic biomolecules, which offers a wider range of target recognition. Then, a design of SELEX with some variant, in order to induced intrinsic transduction by conformational changes was studied. A new SELEX library was constructed to induce a conformational change in aptamers after the recognition process. A 102-mer single DNA was designed with 22 and 29 nucleotides primer flanking sequences at the 3' and 5' ends respectively, an arbitrary complementary sequence of 12 nucleotides (hairpin region, 6 nucleotides in each extreme following by

the primer regions) and a randomized 49 nucleotide internal sequence (See Figure 1). In addition, two primer sequences were designed according with the library template.

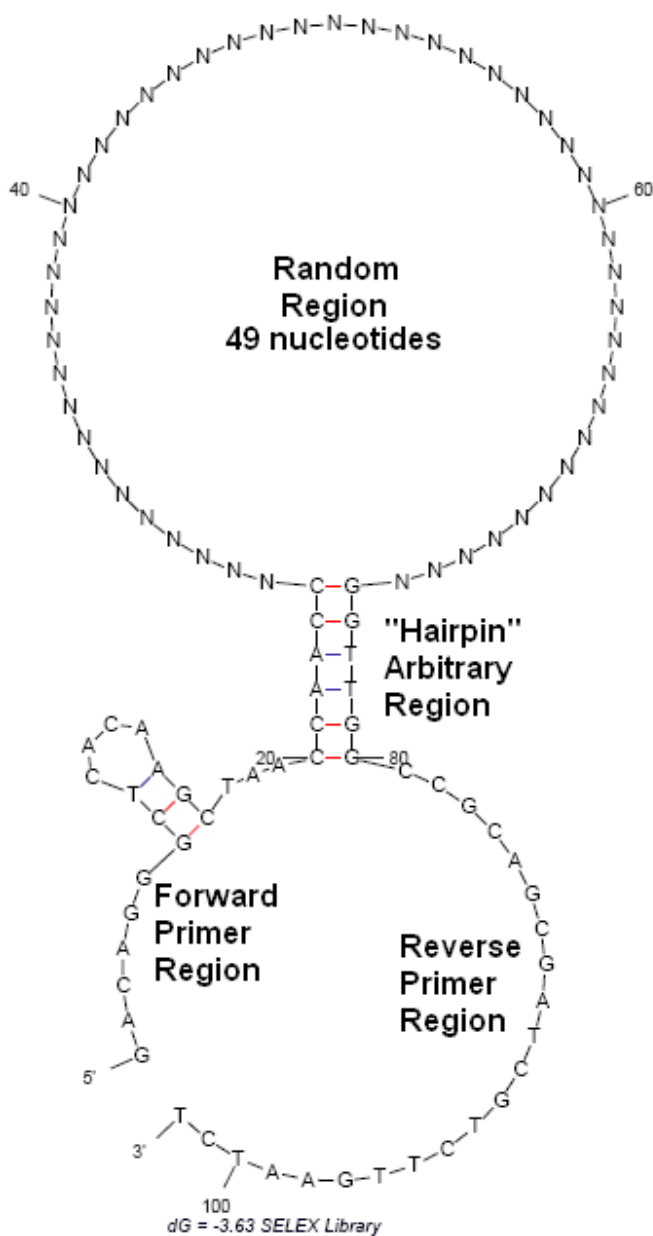


**Figure 1.** Design and prediction of the SELEX library. The prediction was performed by mfold software.



We have included the hairpin region in the library before the starting point of SELEX method. As result of this new library, an increase in the affinity and conformation change will be expected. Therefore, if a member of the library binds the target, the binding energy is expected to be higher than the hairpin energy formation and it would constitute a requirement for the binding event. The free energy ( $\Delta G$ ) necessary to open up the hairpin region has to be higher than the calculated (mfold) energy of -15.19 kJ/mol (-3.63 kcal/mol). Thus, after a binding event with a higher energy, the hairpin structure will collapse and will induce conformational changes In conclusion; the principle of generic biosensing will be studied using two different molecules. MBP will be used in order to prove that conformational changes can be a generic transduction mechanism in biomolecules. On the other hand, aptamers will be used as generic recognition molecules that can be involved in biosensor development. The intrinsic transduction mechanism will be induced in aptamer selection by the breakdown of a hairpin structure that will work as an inducer of the conformational changes.

To prove the generic biosensor development principle, different detector system such as electrochemical, fluorescence and SRP platforms will be adapted to the biomolecule properties.

## 1.5 Bibliography

1. Y.Tian, M. Cuneo, A. Changela, B. Höcker, L. Beese and H. Hellinga. *Protein Science*. 2007. 16, 2240.
2. J.Metzger, P. Landenberg, M. Kehrel, A. Buhl, K. Lackner and P. Lippa. *Clinical Chemistry*. **2007**. 53, 1137.
3. J. Xu, D. Suarez and D. Gottfried. *Anal Bioanal Chem*. **2007**. 389, 1193.
4. M. Velasco-Garcia and T. Mottram. *Biosystems Engineering*. **2003**. 84 (1), 1.
5. L. Terry, S. White, L. Tigwell. *J Agric Food Chem*. **2005**. 9 53(5), 1309.
6. S. Rodriguez, M. Lopez and D. Barceló. *Anal Bioanal Chem*. **2006**. 386, 1025.
7. Kim. Donaldson, M. Kramer and D. Lim. *Biosensors and Bioelectronics*. **2004**. 20, 322.
8. D. Thévenot, K. Toth, R. Durst and G. Wilson. *Pure Appl. Chem.*, **1999**. 71 (12), 2333.
9. A. Collings and F. Caruso. *Rep. Prog. Phys*. **1997**, 60, 1397.
10. J. Newman and S. Setford. *Mol Biotechnol*. **2006**. 32(3), 249.
11. M. Choi, W. Panga, D. Xiaob and X. Wu. *Analyst*. **2001**. 126, 1558.
12. G. Tsekenis, G. Garifallou, F. Davis, P. Millner, T. Gibson and S. Higson. *Anal. Chem*. **2008**, 80, 2058.
13. K. DeAngelis, M. Firestone and S. Lindow. *Appl. Environ. Microbiol*. **2007**. 73 (11), 3724.
14. K. Odenthal and J. Gooding. *Analyst*, **2007**. 132, 603.
15. Z. Wu, J. Jiang, L. Fu, G. Shen, R. Yu. *Anal. Biochem* **2006**, 353, 22.
16. V. Laitala, A. Ylikoski, H. Raussi, P. Ollikka, P. I. Hemmila. *Anal. Biochem*. **2007**, 361, 126.
17. J. Wang, G. Liu and A. Merkoçi, *J. Am. Chem. Soc*. **2003**, 125, 3214.
18. M. Castaneda, A. Merkoçi, M. Pumera, S. Alegret, S. *Biosens. Bioelectron*. **2007**, 22, 1961.
19. M. Sandros, D. Gao, D. Benson. *J. Am. Chem. Soc*. **2005**. 127 (35), 12198.
20. J. Kohn and K. Plaxco. *PNAS*. **2005**. 102(31), 10841.
21. D. Benson, D. Conrad, R. de Lorimier, S. Trammell, H. Hellinga. *Science*. **2001**. 293, 1641.
22. B. Strehlitz, N. Nikolaus and R. Stoltenburg. *Sensors*. **2008**, 8, 4296.
23. Y. Fang. *Sensors* **2007**. 7, 2316
24. A. Senillou, N. Jaffrezic, C. Martelet and S. Cosnier. *Anal. Chim. Acta*. **1999**. 401(1-2), 117.
25. H. Behringer, T. Bogner, A. Polotsky, A. Degenhard, F. Schmid. *J. Biotechnol*. 2007. 129, 268
26. A. Sarai and H. Kono. *Annu. Rev. Biophys. Biomol. Struct*. 2005. 34, 379
27. DE. Koshland. *Proc. Natl. Acad. Sci.*, 1958. 44, 98
28. A. Dunker. *Biochemistry*. 2001. 41, 6573
29. B. Shoemaker, J. Portman, P. Wolynes. *Proc. Natl. Acad. Sci.*, 2000. 97, 8868
30. Y. Levy, P. Wolynes, J. Onuchic. *Proc. Natl. Acad. Sci.*, 2004. 101, 511
31. J. Janin. 2000. Kinetics and thermodynamics of protein-protein interactions. In: Kleanthous, C. (Ed.), *Protein-Protein Recognition*. Oxford University Press, Oxford. (Chapter 1)

32. S. Wodak, J. Janin. *Adv. Prot. Chem.* 2003. 61, 9
33. N. Peppas, Y. Huang. *Pharm. Res.* 2002, 19, 578
34. L. Pauling, M Delbruck. *Science*, 1940. 92, 77
35. H. Hellinga, J. Marvin. *Trends Biotechnol.* **1998**. 16(4), 183.
36. A. Skerra. *Rev. Mol. Biotech.* **2001**. 74, 257.
37. B. Baker, R. Lai, M. Wood, E. Doctor, A. Heeger and K. Plaxco. *JACS.* **2002**. 124(20), 5642.
38. A. Radi, J. Acero, E. Baldrich, C. O'Sullivan. *J. Am. Chem. Soc.* **2006**. 128(1); 117-124.
39. T. McCauley, N. Hamaguchi and M. Stanton. *Anal. Biochem.* **2003**. 319 (2), 244.
40. S. Lee, B. Youn, J. Park, J. Niazi, Y. Kim, M. Gu. *Anal Chem.* **2008**. 80(8), 2867.
41. J. Lee, S. Hwang, J. Kwak, S. Park, S. Lee, K. Lee. *Sensors and Actuators B.* **2008**. 129, 372.
42. L. Lin, H. Wang, Y. Liu, H. Yan, and S. Lindsay. *Biophys J.* **2006**. 90(11), 4236.

# ***CHAPTER 2***

## ***Towards Direct Electrochemical Detection of Maltose-Dependent Conformational Changes of Maltose Binding Protein***

### **2.1 Abstract**

Protein design is an emerging tool for testing general theories of protein structure and function. The ability to manipulate protein sequences rationally offers the possibility of also manipulating protein function and therefore of creating new proteins of biotechnological value. In this work, protein design has been used to produce biosensors based on the understanding of allosteric transitions in proteins. A simple conformational change has been exploited as a biorecognition principle for a reagentless biosensor. Modular strategies for transducing ligand-binding events into fluorescent and electrochemical responses have been reported. In this thesis, electrochemical maltose biosensors based on mutants of the maltose binding protein (MBP) are developed. A

ruthenium<sup>II</sup> complex (Ru<sup>II</sup>), which is covalently attached to MBP, serves as an electrochemical reporter of MBP conformational changes. Biosensors were made through direct attachment of Ru<sup>II</sup> complex modified MBP to gold electrode surfaces. The responses of four individual mutants were evaluated (K46C-MBP-MT, N282C MBP-MT, Q72C-MBP-MT; and K25C-MBP-MT) using square wave voltammetry. A maltose-dependent change in Faradic current (3%, 25%, 0.9% and 3.2% respectively) and capacitance was observed. It is therefore demonstrated that biosensors using generically this family of bacterial periplasmic binding proteins (bPBP) can be made lending themselves to facile biorecognition element preparation and low cost electrochemical transduction.

## 2.2 Introduction

Biosensors are compact analytical devices that incorporate a biological or biologically-derived sensing element that is either integrated within or intimately associated with a physicochemical transducer. The common aim of biosensor development is to produce either discrete or continuous digital electronic signals that are proportional selective to a single analyte concentration (1). The development of most biosensors involves the identification of naturally occurring macromolecules that provide the desired analyte specificity (typically an enzyme or antibody). Once identified, a suitable signal transduction and detection methodology needs to be adapted to the macromolecule in question (2). This is especially true for affinity biosensors, since catalytic biosensors usually are based on the detection of a ubiquitous reaction product. Although cumbersome, effective affinity biosensors have been developed in this way but each device is unique and requires substantial development time since transduction of conformational changes is not straightforward and needs to be adapted to the biorecognition molecule. To overcome this limitation, new approaches are being developed in which protein engineering is used to adapt the signal-transduction properties

of biological molecules to the detector instrumentation and the transduction chemistry of the configuration, rather than adapting instruments and chemistry to the unique requirements of each natural molecule (3). This is achieved by integrating functional groups that provide a simple signal-transduction mechanism between the detector and the protein. Protein engineering has been used to construct fluorescent (4) and electrochemical (5) sensors based on the maltose binding protein that is known to undergo significant conformational changes upon maltose binding. The aim of this work is to further examine the adaptation of fluorescent semiconducting nanoparticle-based biosensors for maltose to electrochemically transduced maltose biosensors.

Three types of changes illustrate the remarkable degree of functional control displayed by some proteins and therefore the properties that can be taken advantage of for transducible biorecognition. First, structurally dissimilar “allosteric” ligands can influence the activity of one another. Such allosteric interactions are responsible for controlling most metabolic and cellular signal transduction pathways. Therefore, allosteric transitions play a central role in regulating cellular physiology (6). Secondly, some proteins bind their ligands following a sigmoidal saturation behavior, which results in a transition between fully bound and ligand-free forms over a relatively short concentration range. This allows exquisite control over ligand loading, as illustrated by the efficient transport of oxygen by hemoglobin between tissues with high partial oxygen pressure to metabolically-active, oxygen-starved tissues (6).

Finally, some proteins are capable of transmitting conformational changes across membranes to different cellular compartments. For instance, the binding of a hormone to a receptor at one side of a membrane results in a change of receptor activity at the other side (7). Previously, it has been demonstrated how a protein design strategy can be derived from simple structural principles to introduce a heterotropically cooperative interaction between ligand binding at one site and activity at another site (in this case, the fluorescence of a fluorophore) in a monomeric protein, *Escherichia coli* maltose-binding protein (8). The spatial separation of the two sites allows modular engineering at such

linkages to create biosensor platforms that can be adapted for fluorescence (8, 9) and electrochemical detection (5, 8) of the ligand.

### 2.3 Review of related literature

The bacterial periplasmic binding proteins (bPBP) are representative members of a widely distributed protein superfamily (10). These bacterial receptors mediate chemotaxis and solute uptake (10, 11). bPBP and a wide variety of ligands have been identified, including carbohydrates, amino acids, anions, metal ions, dipeptides and oligopeptides (10). Additionally, the bPBP fold has been identified in domains of eukaryotic receptors such as GluR2, and DNA repressors (*e.g.* LacI) (10, 11). Sequence diversity within the superfamily is moderate, but the general structural fold is conserved (8). bPBP consist of two domains connected by a hinge region, with a ligand-binding site located at the interface between the two domains, which can adopt two different conformations (12) ((Figure 1d): a ligand-free open form and a ligand-bound closed form, which interconvert through a relatively large bending motion around the hinge. Two structural subclasses have been recognized in the bPBP family, which differ in the polypeptide distribution between the two domains (13). Over 100 PBP structures have been crystallographically determined from a wide variety of sources (*e.g.* *E. coli*, thermophilic bacteria, and eukaryotes) (8).

The remarkable adaptability of this superfamily is likely to have arisen from positioning of the binding site at the domain-domain interface to produce a large ligand-mediated conformational change. When bound to the protein, ligands are in an environment that resembles a protein interior. The binding site environment is made up of residues from

the domain surface. In the absence of ligand, these binding site residues are exposed to solvent, leaving hydrogen bonding residues stabilized by water. This conformational switch provides the adaptability necessary to rationally evolve ligand binding sites. Furthermore, the ligand-mediated conformational change allows conformational changes to be coupled to additional functions. Protein engineers have taken advantage of the intrinsic properties of this protein fold to engineer biosensors, allosteric control elements, biologically active receptors, and enzymes (8).

Ligand-mediated structural changes have been exploited to construct reagentless optical (figure 1a) and electrochemical (figure 1b) biosensors. Environmentally-sensitive thiol-reactive organic reporter groups provide the readout signal (figure 1c and 1e) that links conformational changes with the detection element. Surface cysteine mutations provide the attachment strategy for thiol reactive reporting groups. All successful signaling attachment must have differential association of the organic reporting group and the protein. Most of these ligand-dependent associations stem from crevices that open and close in concert with the global conformational change (14).

Protein engineering also allows the equilibrium between the open and closed states to be altered. Less bulky binding pocket mutations have been shown to weaken the maltose affinity of MBP (4). Bulky allosteric pocket mutations (*e.g.* Trp) strengthen the maltose affinity of MBP (15). Additionally, bulky non-natural amino acids can be added to these allosteric sites to strengthen the maltose affinity of MBP to  $1 \cdot 10^9 \text{ M}^{-1}$ . Therefore, allosterically positioned reporter groups not only report the conformational changes, but also affect the intrinsic equilibrium between the open and closed states (4, 16). Differential interactions between self assembled monolayer immobilized bPBP and the



monolayer surface also alter the open-closed bPBP equilibrium. In the case of the electrochemical assemblies, the open state is favored, consistent with the designed geometry of the assembly. If immobilized bPBP-surface interaction is weak, there should be no effect on ligand binding (17). Recently, maltose biosensors that use MBP attached to CdSe (18) and ZnS coated CdSe nanoparticles (19) were reported that show minimal perturbation of the MBP open-closed equilibrium.

The direct integration of the signal-transduction into the protein fulfils an important design parameter and provides a facile method for biosensor development. Once appropriate modification sites have been chosen and optimized, the synthesis and attachment of sensing element(s) to the protein should be straightforward and biosensors should be effortlessly produced. In this respect, the simplest system is to site selectively attach the reporter molecule to the protein, producing a unimolecular (reagentless) element. The synthetic method should be adaptable to generate a panel of biosensors selective for different analytes. To design a modular protein-engineering system for biosensor development, one of two strategies can be adopted. The first strategy is to find a protein with the appropriate specificity and introduce a signal-transduction system. Alternatively, a protein with a particularly well-behaved intrinsic signal-transduction function can be identified and an appropriate binding site can be engineered into the protein. This work uses the first strategy, where the signal transduction mechanism of MBP (chemotaxis) has been reengineered to provide an electrochemical response.

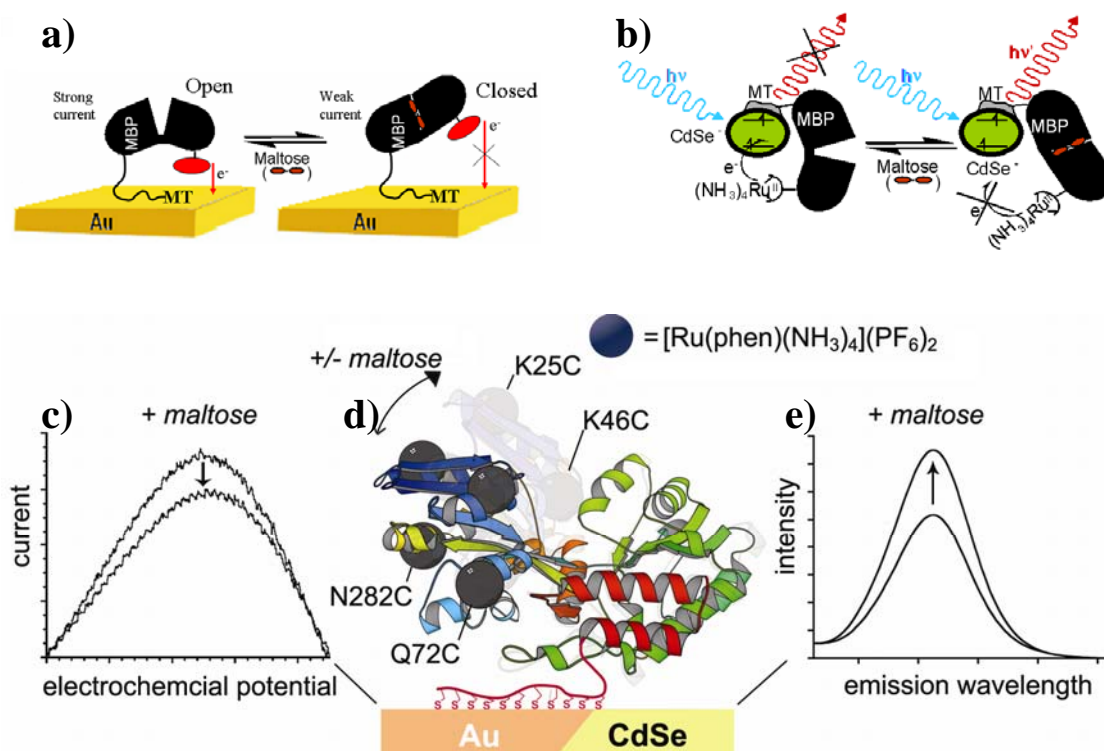


**Figure 1.** The use of MBP as biorecognition molecule for biosensing. The biorecognition of maltose by electrochemical a) and fluorescent b) transduction platforms. d) The advantage of the mediated hinge-binding motions as intrinsic transduction mechanism offers the possibility of generic transduction mechanism. c) Electrochemical “turn off” and e) fluorescent “turn on” signals have been recorded. A redox reporter group is covalently attached to a cysteine, such that it is positioned between the electrode and MBP surfaces (gold electrode or CdSe nanoparticles). In the absence of maltose, the open conformation permits strong electronic coupling between the electrode surface and the reporter group (Figure d, colorful), whereas in the closed form (figure d, shadow), this interaction is weakened.

The ultimate goal of these systems is to simplify the detection scheme and manipulate protein structure at the genetic level. Extensive genetic manipulation of the protein structure can be performed and rapidly produce the protein due to recombinant DNA technology.

## 2.4 Hypothesis

The present study will test if the fluorescence response of Ru<sup>II</sup>-modified MBP attached to CdSe nanoparticles can be translated to an electrochemical response through square wave voltammetry (SWV) using Ru<sup>II</sup>-modified MBP directly adsorbed to bare gold electrodes. While the maltose-dependent signal in CdSe fluorescence is a “turn-on” response, the Faradic electrochemical response to maltose is expected to be “turn-off”.

The adsorption of G174C-MBP-MT on electrode by modifying the gold surface with a self-assembled monolayer of hydroxyl- and Ni<sup>II</sup>-nitrilotriacetate-terminated headgroups has been reported [5]. Here, direct adsorption of Ru<sup>II</sup> modified N282C-MPB-MT, K25C-MBP-MT, K45C-MBP-MT and Q72C-MBP-MT on bare gold electrodes will be evaluated. Previous detection methods have relied on AC voltammetry [5, 24]. However, square wave voltammetry requires less expensive electronics than AC voltammetry.

## 2.5 Objectives

The principal goal of this work is to develop a reagentless electrochemical biosensor using maltose-binding protein (MBP) directly adsorbed to bare gold electrodes and SWV as a detection method. To achieve this objective the following partial objectives will be fulfilled. The MBP-MT plasmids will be expressed in *E. coli*, the COOH-terminus (near the hinge-region) of MBP will be tethered to the electrode through a 33-mer fusion domain, referred to as MBP-MT and Ru<sup>II</sup> (1,10-phenanthroline-5-maleimide)(NH<sub>3</sub>)<sub>4</sub>[(PF<sub>6</sub>)<sub>2</sub>] complex will be attached specifically to a mutant surface cysteine on the amino-terminal domain of MBP, using reported protein modification

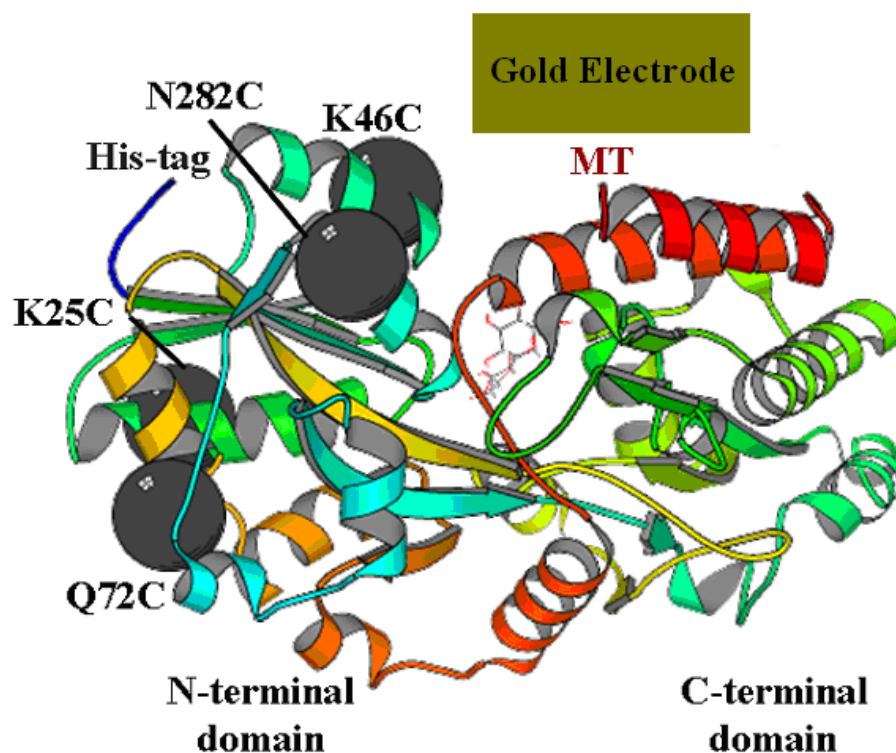


**Figure 2.** Four different mutations sites where cysteine is used to attach  $\text{Ru}^{\text{II}}$  complex on the MBP-MT surface in order to study the effect of reporter location on transduction efficiency.

chemistry [18]. This arrangement is designed to orient the maltose-binding site toward the bulk solution, and link the maltose-mediated conformational changes to the MBP-electrode interface (Figure 2). Alterations in electronic coupling between the  $\text{Ru}^{\text{II}}$  reporter group and the electrode will allow maltose binding to be measured electrochemically.

## 2.6 Experimental Methods

### 2.6.1 Protein Expression

The MBP-MT plasmids were transformed into BL21-DE3 *E. coli* competent cells. The transformed cells were grown on LB/ampicillin plates, incubated overnight at 37°C. A single colony was selected from these plates and inoculated into a 50 mL LB (with

ampicillin) culture. The 50 mL culture was grown overnight and placed in 1 L of LB media. The 1 L culture was grown to optical density of 0.4-0.5. Subsequently, the inducer (IPTG) was added (1 mM) to the cell culture and incubated for four hours. Cells from the 1 L culture were harvested by centrifugation and stored at -80°C.

### **2.6.2 Protein Purification**

The cells were lysed using a French pressure cell. The lysate was treated with polyethyleneimine (10%) (w/v), chilled on ice for 10 minutes, and the lysed cells were removed by centrifugation. The supernatant was loaded on an amylose column (New England Biolabs) that was equilibrated with 20 mM Tris and 200 mM NaCl (pH 7.5). The protein was washed with the equilibration buffer and eluted with elution buffer that contained 10 mM maltose. Protein-containing fractions were dialyzed exhaustively against the equilibration buffer to remove the maltose.

### **2.6.3 Additional Biosensor Reagents**

[Ru<sup>II</sup>(1,10-phenanthroline-5-maleimide)(NH<sub>3</sub>)<sub>4</sub>][(PF<sub>6</sub>)<sub>2</sub>] has been synthesized as previously reported [18]. Four surface cysteine mutant MBP-MTs were generated previously K25C, K46C, Q72C, and N282C-MBP-MT (18, 20).

### **2.6.4 Attachment of the ruthenium complex to MBP-MT**

Attachment of the Ru<sup>II</sup> complex to mutant MBP-MTs was performed as previously reported (18). Briefly, a surface cysteine mutant MBP-MT in 20 mM 3-(N-morpholino)propanesulfonic acid (MOPS) buffer (pH= 7.5) was treated with 5 mM DTT, 10 mM EDTA, and 1 mM 1,10-phenanthroline overnight at 4°C. The complex was purified by gel filtration chromatography (10-DG, Pharmacia). The resulting solution was

incubated immediately with 100  $\mu\text{M}$   $\text{CdCl}_2$  at room temperature for 30 minutes.  $[\text{Ru}^{\text{II}}(1,10\text{-phenanthroline-5-maleimide})(\text{NH}_3)_4][(\text{PF}_6)]_2$  (1.0 equivalents, 10 mM stock in acetonitrile) was added to the  $\text{Cd}^{2+}$  ion-protected protein solution and reacted for two hours. The ruthenated protein sample was quenched with 100  $\mu\text{M}$  2-mercaptoethanol and purified by gel filtration chromatography. The  $\text{Cd}^{2+}$  ions were removed by treatment with 0.1 mM EDTA and 0.1 mM 1,10-phenanthroline at 4°C for 2-24 hours, followed by purification with gel filtration chromatography. The resulting proteins were analyzed by absorbance spectrophotometry monitoring the ratio of the  $\text{Ru}^{\text{II}}$  complex 490 nm and the protein 280 nm (Figure 3). Only one  $\text{Ru}^{\text{II}}$  complex can be linked to the protein surface. The protein labeled percentage can be estimated using the absorbance values of both, protein and  $\text{Ru}^{\text{II}}$  complex (1:1 ratio). Subsequently the MALDI-TOF mass determination (Figure 4) was carried out, as previously reported (19).

### **2.6.5 Attachment of the MBP-MT-Ru to gold electrodes**

Gold ball electrodes were produced by the method of Creager (21). Gold wire (0.25 mm diameter) was threaded through a pulled glass capillary and flame annealed. The gold ball-capillary junction was sealed with non-conducting epoxy. The gold ball electrode was immersed in 2 mL of supporting electrolyte solution (0.2 M sodium phosphate, pH 7.5, 100 mM KCl). After the addition of 0.5 mL protein solution (10 $\mu\text{M}$ ), incubation proceeded under stirring, for 20 minutes. During this process, the metallothionine domain (MT) attached the  $\text{Ru}^{\text{II}}$ -MBP-MT to the gold surface.

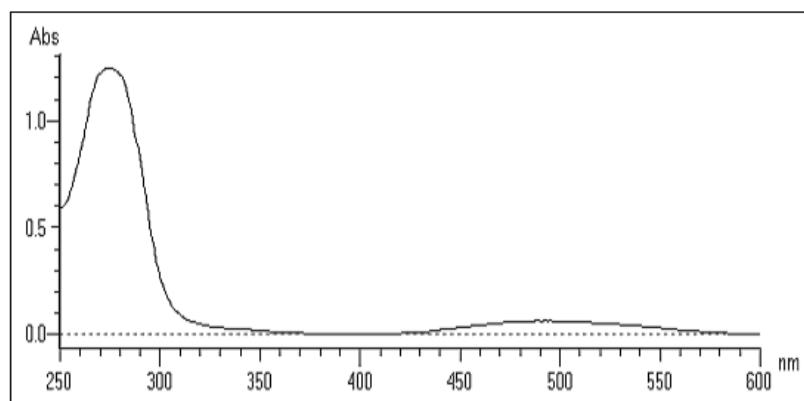


**Figure 3.** Optical properties of MBP-MT ruthenium attached. The protein and  $\text{Ru}^{\text{II}}$  complex concentrations were evaluated by absorbance at 280 nm and 490 nm respectively. The percentage of protein labeling can be estimated in relation with both values. Experimental conditions have been described previously.

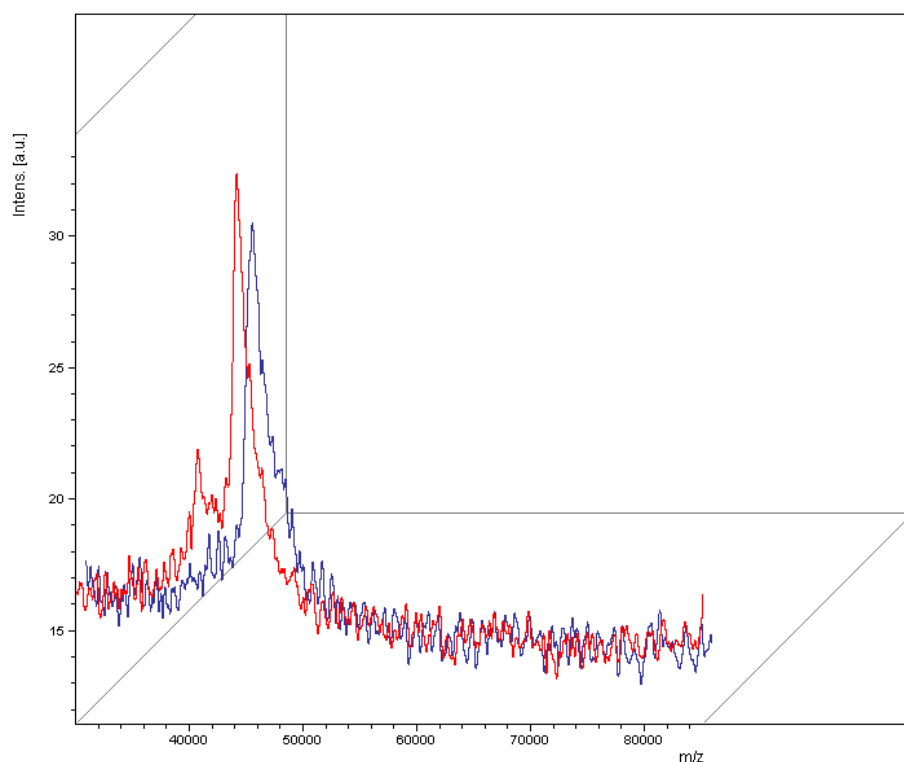


**Figure 4.** MALDI-TOF mass determination. Masses of N282C-MBP-MT (red) and N282C-MBP-MT modified with  $[\text{Ru}^{\text{II}}(1,10\text{-phenanthroline-5-maleimide})(\text{NH}_3)_4][(\text{PF}_6)_2]$  (blue) were analyzed. The MALDI determined  $[\text{M}+\text{H}]^+$  masses were  $44159 \pm 5$  m/z for N282C-MBP-MT samples and  $44621 \pm 15$  m/z for N282C-MBP-MT-Ru complex samples. The masses were consistent with the theoretical calculation of 44161 m/z and 44605 m/z for N282C-MBP-MT and N282C-MBP-MT-Ru respectively.

### 2.6.6 Electrochemical measurements

Electrochemical experiments using a three-electrode one-compartment cell were conducted using a potentiostat (CH Instruments, Model 812A). The electrochemical measurements were conducted using an Ag/AgCl reference electrode and a platinum-counter electrode (Cypress systems: 66-EE008 and 66-EE011, respectively). The potential range of cyclic voltammetry was between 0.0 and 0.6 V (*vs.* Ag/AgCl) with a scan rate of 50 mV/s. Square wave voltammograms (SWV) were registered in the potential interval 0.0 – 0.6 V (*vs.* Ag/AgCl), under the following conditions: potential increment, 1 mV; potential amplitude, 10 mV; pulse frequency, 15 Hz which was optimized in relation with the peak definition. SWV currents of Ru<sup>II</sup> complex modified MBP-MTs were subtracted from unmodified MBP-MT SWVs and linear interpolations between +100 and +550 mV *vs.* Ag/AgCl were used to enhance Faradic current in order to calculate the correlated current (Fig. 6).



## 2.7 Results and discussion

The cyclic voltammogram of gold electrode in 0.1 mM  $[\text{Ru}^{\text{II}}(1,10\text{-phenanthroline-5-maleimide})(\text{NH}_3)_4][(\text{PF}_6)]_2$  shows anodic and cathodic peaks located at 383 and 296 mV (vs. Ag/AgCl), respectively. The formal potential ( $E^\circ$ ) is 340 mV (vs. Ag/AgCl) which is in agreement with the literature value for this complex (22). The peak separation of 120 mV is indicative of a quasi-reversible one-electron heterogeneous electron transfer process (Figure 5). Cyclic voltammetry experiments were performed on the Ru-MBP-MT system. Only a weak Faradic response was observed suggesting minimal Ru-MBP-MT loading on the gold electrode surface. Square wave voltammetry did show a significant Faradic response and was used to characterize the Ru-MBP-MT system in this report. The amplitude and increment of potential used in this study were reported previously [23] and were not optimized, although the frequency was optimized in relation to the peak definition.

Four different mutations of maltose binding protein were evaluated in this work. Each mutation has shown different electrochemical response using SWV. This technique has been found to be useful for the electrochemical analyses of diffusionless systems (23) and, in this report, for studies of conformational changes of a protein adsorbed to a solid surface. When the protein is adsorbed, the current response of the Faradic electrochemical signal should depend on the distance of the electrochemical label from the surface, while the peak potential should be directly correlated to the electrochemical label reduction potential.

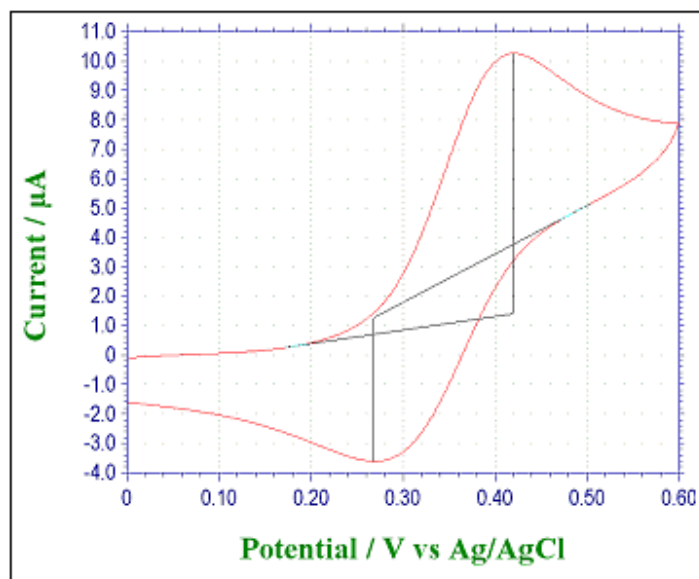


**Figure 5.** Cyclic voltammogram of  $[\text{Ru}^{\text{II}}(1,10\text{-phenanthroline-5-maleimide})(\text{NH}_3)_4][(\text{PF}_6)_2]$  complex 1 mM in supporting electrolyte solution (0.2 M sodium phosphate, pH 7.5, 100 mM KCl). The CV potential range was performed between 0.0 and 0.6 V (vs. Ag/AgCl) with a scan rate of 50 mV/s.

The individual mutations (K46C-MBP-MT, N282C MBP-MT, Q72C-MBP-MT, and K25C-MBP-MT) are depicted in figure 2. These mutants were used to modify gold electrodes as described in the experimental section. SWV experiments were performed with two types of modified electrodes: MBP-MT with (sample) and without (control) the  $\text{Ru}^{\text{II}}$  complex. For each type of electrode, SWV was recorded before and after the addition of 10  $\mu\text{M}$  maltose, which was determined previously to be a saturating concentration. The following observations can be made for each mutant:

*N282C- MBP-MT:* A significant decrease in the signal of 25 % (16.3 nA) was obtained with N282C-MBP-MT modified with  $\text{Ru}^{\text{II}}$  complex after the addition of maltose (Figure 6A). The unruthenated MBP-MT did not show a significant Faradic signal at 340mV. In

the present study N282C-MBP-MT has shown the best electrochemical response, however the system could be optimized to eliminate any capacitance effect in the signal. In this case, a good electro-to-electrode reproducibility was determined (normalized data) as evidenced by the low standard deviation of 3.1% ( $n = 3$ ).

*K25C- MBP-MT*: The surface cysteine mutant K25C- MBP-MT had the most robust maltose-dependent Faradic current change. A clean Faradic signal change of 1.1 nA was observed upon the addition of saturating maltose (Figure 6B). The control in this case, did not exhibit any significant changes upon maltose addition. The analysis of absolute current has confirmed a maltose-mediated change of 3.2%, corresponding to Faradic current. There was an acceptable electrode-to-electrode reproducibility (normalized data) as evidenced by the standard deviation of 9.2% ( $n = 3$ ).

*Q72C-MBP-MT*: The electrochemical response for Q72C-MBP-MT mutation has shown a significant Faradic response (figure 6C), but an insignificant maltose dependent change of signal. It should be noted that the peak potential for the Faradic response is shifted by  $\sim 30$ -50 mV to a more negative potential. Negative shifts in reduction potential can be interpreted as indicative of a more hydrophobic environment and suggest that the Ru<sup>II</sup> modified Q72C-MBP-MT may be denatured on the electrode surface. In presence of maltose, a current change of 0.6 nA was recorded, corresponding to 0.9% decrease. This change was at the lower level of detectability. On the other hand, after the addition of maltose, the control has reported higher values than expected. The analysis of normalized data has not shown the presence of a small maltose-dependent Faradic current change.

Reproducibility was not determined because only one of three electrodes showed a measurable signal. Additional experiments should be performed in order to determine the reproducibility in this case.

**K46C- MBP-MT:** The electrochemical response of MBP-MT-Ru<sup>II</sup> has shown a significant capacitance effect. After the addition of maltose, a 5.2% decrease (9 nA) in signal was observed (figure 6D). On the other hand, the decrease in the signal for the control MBP-MT in presence of maltose was 3% (1.7 nA). Current normalization between ruthenium-modified and unmodified protein electrodes made possible to appreciate more clearly the Faradic current maltose response. The maltose-mediated response with the normalized current showed a 1.25% decrease. This decreased normalized current response is proposed as a Faradic current dominated response. An acceptable reproducibility was obtained (normalized data) as evidenced by the standard deviation of 9.8% ( $n = 3$ ).

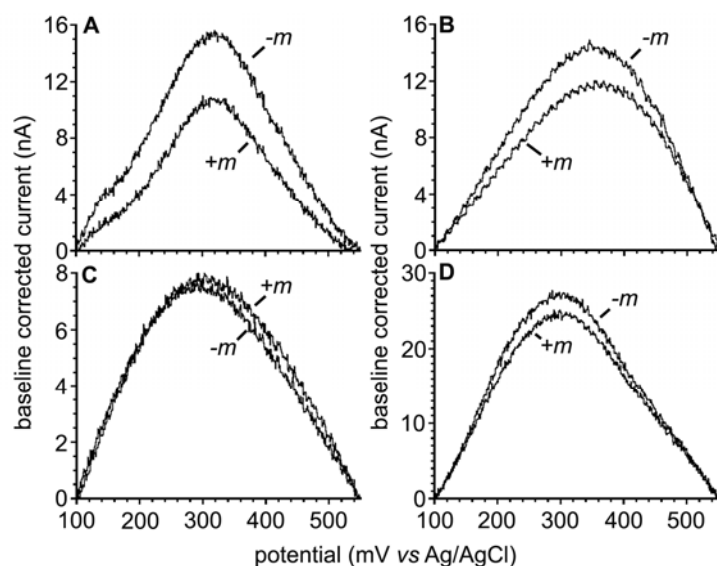


**Figure 6.** Square wave voltammograms of Ru<sup>II</sup> modified MBP-MTs (**A**, N282C; **B**, K25C; **C**, Q72C; **D**, K46C) adsorbed to the Au electrode: -m) initial scan before maltose addition; +m) after maltose addition (10  $\mu$ M, final). Baseline corrected current calculation outlined in the experimental section.

Maltose titration studies were also performed. Amperometric titration data using SWV showed discernible response even to small variations of maltose concentration (Figure 7A). The corresponding titration curve has shown progressive decrease of current as a function of maltose concentrations (Figure 7B), which is in accordance with the literature (18). The binding affinity based interactions between maltose and MBP-MT will be evaluated. In figure 8A) the peak current,  $I$ , is plotted as a function of the bulk concentration  $c_o$ . Under this conditions the dissociation constant ( $K_D = 44$  nM) was obtained from the curve fitting (Figure 8B) using the Langmuir isotherm (19).

$$\theta = K_A c_o / (1 + K_A c_o) \quad (1)$$

Where,  $\theta$  is the fractional coverage defined as  $\Gamma/\Gamma_m$  ( $\Gamma_m$  is the Ru-MBP-MT maximum coverage),  $c_o$  is the bulk maltose concentration, and  $K_A$  is the affinity constant. The coverage  $\Gamma$  of binding maltose is inversely proportional to the current  $I$ . In this case eq. 1 can be expressed as:

$$I = I_m (K_D + c_o) / c_o \quad (2)$$

Where  $I_m$  is the maximum current of Ru-MBP-MT on bare gold electrode and  $K_D$  is the dissociation constant.  $K_D = 1/K_A$ .

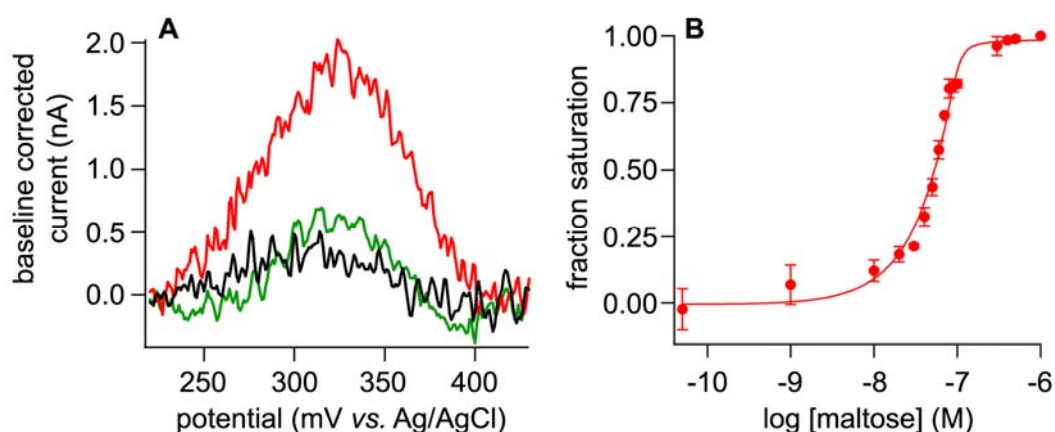


**Figure 7.** Maltose-dependent changes in baseline corrected current observed from  $\text{Ru}^{\text{II}}$ -modified N282C MBP-MT adsorbed Au working electrodes. A) representative corrected voltammograms (bare Au, black;  $\text{Ru}^{\text{II}}$ -modified N282C MBP-MT, red;  $\text{Ru}^{\text{II}}$ -modified N282C MBP-MT with 1  $\mu\text{M}$  maltose, green). B) Mean fraction saturation of integrated current response with standard deviations shown in error bars (line, tight binding model fit to this data).

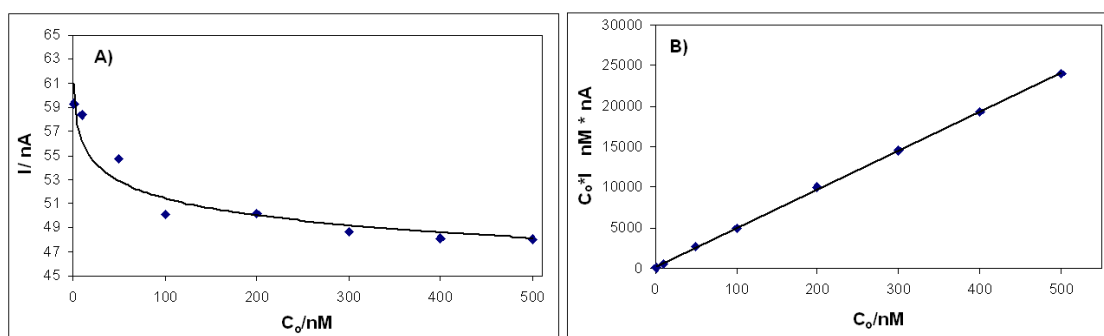


**Figure 8. Maltose titration:** A) Amperometric titration data using SWV was able to detect small variations of maltose concentration. The corresponding titration curve has shown progressive decrease of current as a function of maltose concentrations. B) Maltose-dependent change current, which was fit to the Langmuir isotherm to derive  $K_D = 44 \text{ nM}$ .

The selectivity of the sensor was studied by SWV using as baseline, for this experiment, the signal recorded after the immobilization of MBP-MT-Ru on gold surface electrode. After the addition of different sugars (lactose, glucose and maltose respectively) a SWV was obtained (Figure 9). The MBP biosensor showed better selectivity for maltose

(66.8%) when compared to other substrates (insignificant signal for lactose and 7.1% for glucose). This finding confirmed the substrate selectivity of MBP-based electrochemical biosensor.

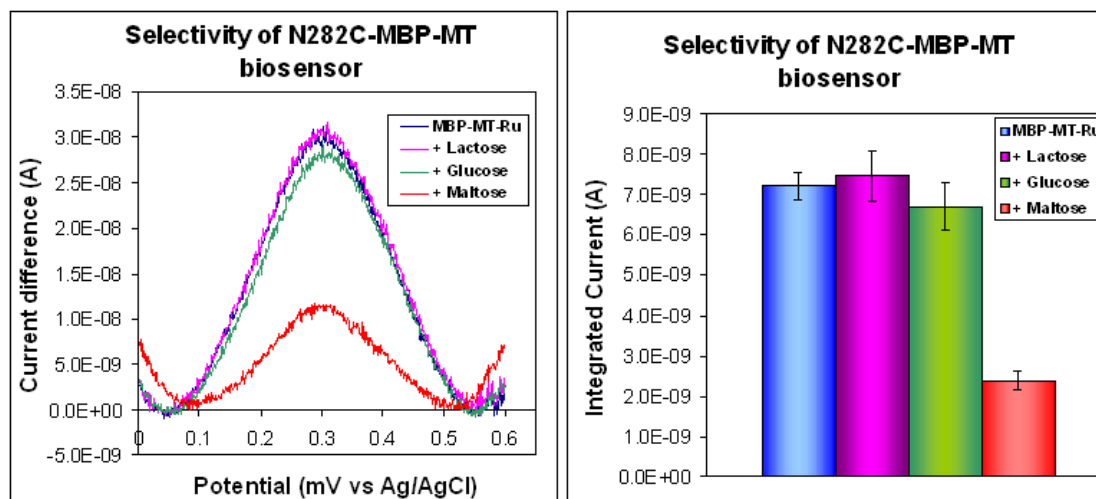


**Figure 9.** The selectivity of the sensor was obtained by SWV. The baseline for this experiment was the signal recorded after the immobilization of MBP-MT-Ru (blue) on gold surface electrode. After the addition of each sugar (lactose; pink, glucose; green and maltose; red respectively) the signal decrease was analyzed. The selectivity for maltose is 66.8% in comparison with other substrates (insignificant signal for lactose and 7.1% for glucose)

These findings are significant, in that a maltose-dependent electrochemical response with square wave voltammetry was observed. Previous detection methods have relied on AC voltammetry (5, 24). Square wave voltammetry requires less expensive electronics than AC voltammetry. This analytical advance stems from, purposely, improved electron transport between the Ru<sup>II</sup> complex and the gold electrode provided by the metallothionin domain attachment chemistry.

## 2.8 Conclusion

Four different Ru<sup>II</sup> complex attachment sites on the MBP-MT surface Reported in the present work were surveyed using SWV. Each position has shown a different electrochemical signal according to the distance dependence effect, wherein, the conformational change was involved after the biorecognition process. More specifically, K46C-MBP-MT showed only a maltose-dependent capacitive effect, while, Q72C-MBP-MT showed a defined square wave voltammetry peak with no maltose-dependent changes. K25C-MBP-MT showed only a maltose-dependent Faradic contribution (1.1 nA). N282C-MBP-MT showed a significant maltose-dependent signal (16.3 nA) that had a combined capacitive and Faradic contribution. Therefore, Ru-N282C-MBP-MT represents the best system for maltose biosensing with the electrochemical detection system employed. In addition, the direct adsorption of Ru<sup>II</sup> modified MBP-MT on bare gold electrodes was tested with satisfactory results. This suggests that the coupling between the modified proteins and gold electrode surface is a successful method for electrochemical detection. The previous results suggest that N282C mutant has shown the best electrochemical signal, due to its reporter group location and the dynamic interaction between the reporter and the gold electrode surface. For the other cases, several factors such as distance, charge, hydrophobic conditions, could be responsible of a decrease in the signal.

The conformational changes involved in MPB-MT have been evaluated by SWV technique. The results suggest that SWV could be an attractive alternative for biosensing compared to the more complicated and expensive techniques such as *ac* voltammetry (5).



The apparent disassociation constant ( $K_D$ ) reported by these studies, have shown a significant value of 44 nM, which represents an important improvement in affinity (10-15 fold increase) in comparison with previous electrochemical (5) and fluorescence (26) MBP biosensors. Previously, the surface of the gold electrodes used to be covered by a monolayer (linker), which increased the capacitance effect. In contrast, in our approach, the direct absorption of MBP-MT over the surface electrode reduces the capacitance effect and the Faradic current can be recorded without interferences.

The maltose selectivity and the non-specific interaction for two additional targets have been studied. The signal at saturated condition of maltose has shown a significant signal of 68% of the total maximum signal. The evaluation of non-specific targets has revealed a 7% of the total signal for glucose and an insignificant signal for lactose. The non-specific signal for glucose could be explained by the fact that glucose is the monomer of maltose, thus some partial signal could be expected.

In summary, this work provides a high affinity maltose-dependent biosensor for studying the allosteric mechanism of maltose binding protein adsorbed to gold surfaces using electrochemical techniques. The results suggest that conformational changes represent a successful intrinsic transduction mechanism for biomolecules. In addition, this type of intrinsic transduction could be applied to the design and development of generic biosensors.

## 2.9 Bibliography

1. A.P. Turner, I. Karube, G.S. Wilson. *Biosensors: Fundamentals and Applications*. 1987.
2. Gopel, *Sensors: A Comprehensive Survey*. **1994**.
3. H.W. Hellinga, J.S. Marvin. *Trends Biotech.* **1998**, 16, 183-189
4. J.S. Marvin, E. E. Corcoran. *PNAS*. **1997**, 94 4366-4371
5. D.E. Benson, D. W. Conrad, H.W. Hellinga. *Science*. **2001**, 293, 1641-1644
6. M.F. Petutz. *Mechanisms of Cooperativity and Allosteric Regulation in Proteins*. **1990**
7. D.E. Koshland, G. Nemethy. *Biochem.* **1966**, 5, 365-385
8. M.A. Dwyer H.W. Hellinga. *Curr. Opi. Struc. Biol.* **2004**, 14, 495-504
9. Daunert, S. *Optical Biosensors: Present and Future*. **2002**
10. R. Tam, M.H. Saier. *Micro. Rev.* **1993**, 57, 320-346
11. C.B. Felder, R.C. Graul. *AAPS Pharm. Sci*, **1999**
12. M. Gerstein, A. M. Lesk. *Biochem.* **1994**, 33, 6739-6749
13. K.K. Fukami, Y. Tateno. *J. Mol. Biol.* **1999**, 286, 279-290
14. J.D. Dattelbaum, L.L. Looger. *Prot. Scien.* **2005**, 14, 284-291
15. J.S. Marvin, H.W. Hellinga. *Nat. Struc. Biol.* **2001**, 8, 795-798
16. R.M. De Lorimier, J.J. Smith. *Prot. Scien.* **2002**, 11, 2655-2675
17. Wada and M. Mie. *JACS*. **2003**, 125, 16228-16234
18. M.G. Sandros, D. Gao, D.E. Benson. *JACS*. **2005**, 127, 12198-12199
19. C.H. Fan, K.W. Plaxco and A.J. Heeger. *PNAS*. **2003**, 100, 9134-9137
20. M.G. Sandros, D. Gao, C. Gokdemir, D.E. Benson. *Chem. Comm.* **2005**, 22, 2832-2834
21. S.E. Creager, T.T. Wooster. *Anal. Chem.* **1998**, 70, 4257-4263
22. S.A. Trammell, H.M. Goldston. *Bioconj. Chem.* **2001**, 12, 643-647
23. J.J. O'Dea, J.G. Osteryoung. *Anal. Chem.* **1997**, 69, 650-658
24. C.H. Fan, K.W. Plaxco. *PNAS*. **2003**, 100, 9134
25. S.A. Jaffari, A.P. Turner. *Physiol. Measur.* **1995**, 16, 1
26. M.G. Sandros, V. Shete, D.E. Benson. *The Analyst*, **2006**, 131, 229

# CHAPTER 3

## *Selection of transduction-incorporating avidin-aptamer by a novel partitioning mechanism termed “Soluble-SELEX”*

### 3.1 Abstract

SELEX (Systematic Evolution of Ligands by EXponential enrichment) has proven to be a useful tool in finding nucleotide sequences with high affinity for a specific target molecule from a random synthetic library with around  $10^{15}$  members of certain length (20 to 80 nucleotides) (1-2). SELEX can be performed inexpensively *in vitro* with only routine equipment of a molecular biology laboratory and for these reasons it has been gaining acceptance as a tool for the isolation of biorecognition elements of intracellular and extracellular targets (1). The method involves three principal steps: **interaction** between a mixture of candidates and the target molecule, **partitioning** of the mixture candidates with high and low affinity for the target molecule, and **amplification** of the bound members. One of the critical steps in SELEX method is the partitioning, i.e. the

separation of unbound and bound oligonucleotides to the target molecule. The selection of an appropriate separation method has been the subject of the work of several researchers in the recent years (3-7). Separation methods in use include nitrocellulose membrane filtration (8), affinity surfaces (9), affinity tags (10), column matrices (11), gel electrophoresis (12), centrifugation (13), surface plasmon resonance (14), flow cytometry (15), and capillary electrophoresis (16). Limitations still exist for most of the methods used and are of two types. Primarily, the library interacts with the immobilization matrix used for facile target separation or with the separation media (for example membranes) leading to a certain degree of non specific selection. Secondly, most separation methods are limited by the size of the target in case the target is not immobilized, for example small (a few Da) targets are difficult to be selected against. On the other hand, when aptamers are used for biosensing it is not always guaranteed that the immobilized form of the aptamer will still provide recognition. The problem is more severe that in the case of immobilization of antibodies because aptamers are relatively short nucleotide sequences that can lose their capacity to induce a 3-D structural change when derivatised. A similar failure can easily result when aptamers are modified with a fluorescent or redox label to facilitate transduction. For this reason it is important to obtain aptamers that incorporate the transduction and immobilization chemistries as much as possible already during selection.

For these reasons herein, a new approach for the separation step has been invented, termed Soluble-SELEX. This new SELEX method uses hybridization as partitioning mechanism for separating the bound and unbound DNA members from the target-molecule. The hybridization procedure has been evaluated by fluorescence studies as

partitioning mechanism for SELEX method. Furthermore, a primary structure has been incorporated into the library design that allows the facile transduction and immobilization of the resulting aptamer candidates, namely a hairpin-like structure with an interaction potential of about -15,2 kJ/mol. It is hypothesized that by introducing this restriction in the primary structure of the aptamer, all members selected for recognition will be inducing a breaking of the hairpin-like structure that will at the same time serve for facilitating a non-interfering immobilization site and facile transduction.

Herein, we developed an avidin-aptamer using this new partitioning mechanism termed “Soluble-SELEX” starting with a library that incorporates a hairpin-like primary structure and we characterized the obtained biorecognition elements using fluorescence, electrochemistry and surface plasmon resonance methods. To do so, we develop the new SELEX method.

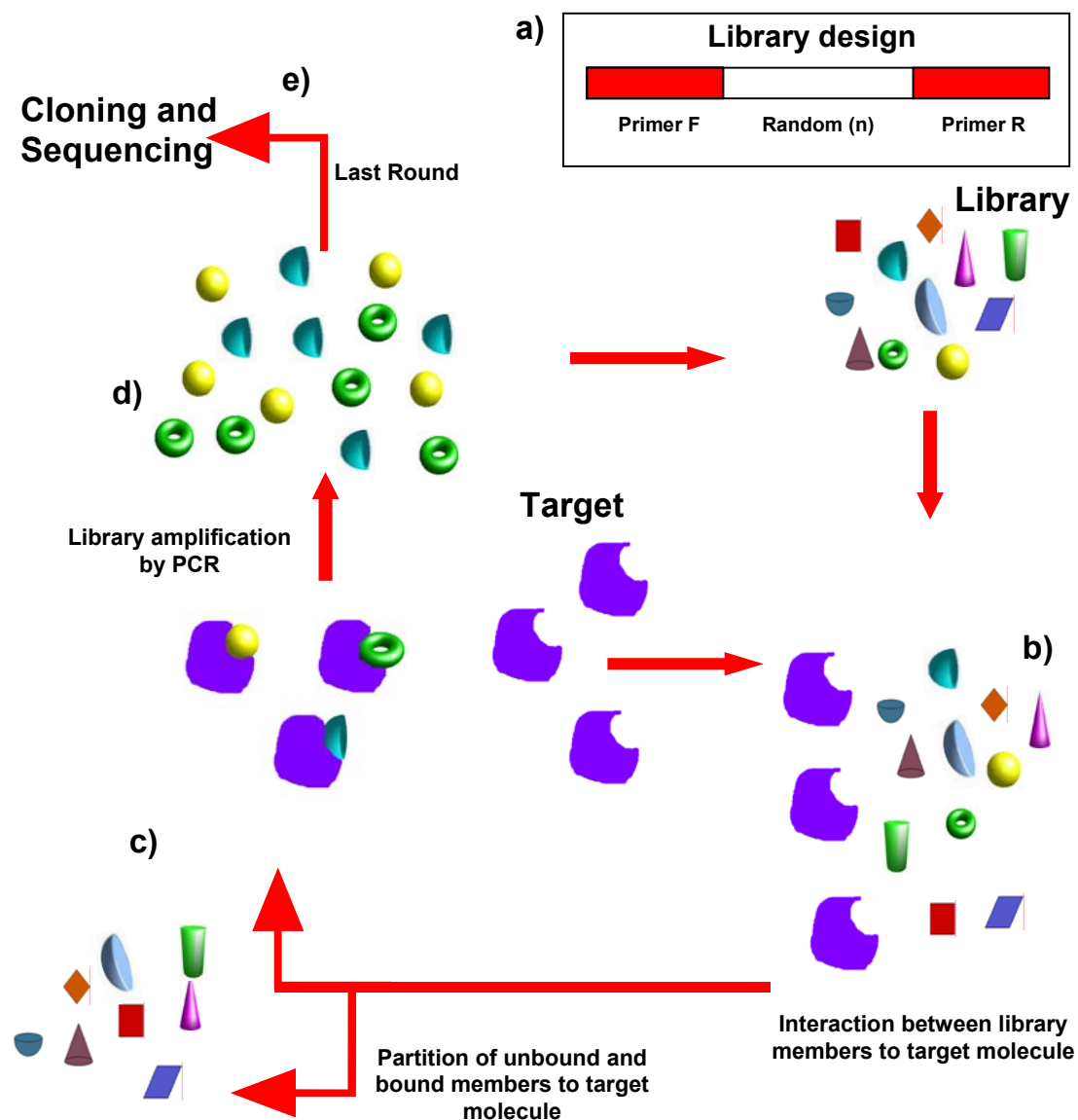
### **3.2 Introduction**

SELEX (Systematic Evolution of Ligands by EXponential enrichment) can be defined as a combinatorial oligonucleotide chemistry tool that has been proven to be an important technology for the production of synthetic molecules with biorecognition properties termed “aptamers”. Etymologically, the term aptamer is derived from the Latin “aptus” meaning “to fit” (9) and from the Greek “meros” which means particle. The SELEX method consists in the screening of a large member library down to a single target molecule (1, 9). A wide variety of molecular targets with different features such as inorganic compounds, small organic molecules, nucleotides and derivatives, cofactors,

amino acids, carbohydrates, antibiotics, peptides and proteins, and complex structures have been previously described (17). Nucleic acids offer an extraordinary alternative as biorecognition molecules (RNA/DNA). Millions of possible conformers, structures and interactions of the library members to the target molecule are involved in SELEX technology. In addition, the possibility of nucleic acids amplification by PCR and the synthesis of complex libraries with about  $10^{15}$  different molecules convert SELEX in an attractive technology for biosensing, diagnosis, drug discovery, biotechnology and pharmaceutical research.

### 3.2.1 SELEX principle

Since its first description by Gold (1) and Ellington (9) in 1990, SELEX technology has become an important tool for *in vitro* selection of oligonucleotides with recognition properties, so called aptamers. The SELEX method has proven to be a useful platform for selecting a large number of aptamers with a wide variety of targets, including simple ions, small molecules, proteins, organelles, viruses and whole cells (18–21). Scheme 1 shows the standard SELEX procedure. Wherein, several steps are involved such as: a) design of the library, b) interaction between a mixture of candidates to the target molecule, c) partitioning of the mixture candidates with high and low affinity for the target molecule, d) amplification of the bound members and e) cloning and sequencing. One of the critical steps in SELEX method is the separation of unbound and bound nucleic acid to the target molecule.



**Scheme 1.** SELEX (systematic evolution of ligands by exponential enrichment). a) design of the library, b) interaction between a mixture of candidates to the target molecule, c) partitioning of the mixture candidates with high and low affinity for the target molecule, d) amplification of the bound members and e) the last step involves cloning and sequencing.

### 3.2.1.1 Target molecule

There are several reports in the literature about aptamers with high-affinity against over 150 different targets (29) including targets with different features such as inorganic components, small organic molecules, nucleotides and derivatives, cofactors, amino acids, carbohydrates, antibiotics, peptides and proteins, and complex structures have been classified (17, see table 1). The previous information confirms the versatility and universal application of SELEX technology for a wide range of molecules. Aptamers are usually developed for therapeutic applications, for example, have been approved for the treatment of wet age-related macular degeneration (30-31).

Target	Size (Da)	Partitioning method	Affinity ( $K_D$ )	Ref.
Ig E	150.000,0	Nitrocellulose filter	10 nM	(37)
Thrombin	36.000	Affinity Column	37 nM	(38)
Streptavidin	60.000,0	Affinity surface (MB)	85 nM	(39)
Zn <sup>2+</sup>	65,41	Affinity Column	1,2 nM	(40)
ATP	573,1	Affinity Column	6 $\mu$ M	(41)
Cyanocobalamin	1.355,39	Affinity Column	88 nM	(42)
A/Panama influenza virus	NA*	Titer plate	0,18 nM	(43)
gap polyprotein from HIV-1	161.772,0	Affinity Tag	0,2 nM	(44)
Integration host factor (IHF)	11,354,0	Gel electrophoresis	0,5 nM	(45)
Prohead RNA of bacteriophage $\phi$ 29	NA*	Centrifugation	NR**	(46)
Avidin	60.000	Soluble-SELEX	1.3 nM	
Ig E	150.000,0	SPR	134 nM	(47)
NF- $\kappa$ B p50 protein	50.000,0	Flow cytometry	NR	(48)
HIV reverse transcriptase	51.330,0	Capillary electrophoresis	0.18 nM	(49)

\* Not applicable, \*\* Not reported.

**Table 1.** List of several aptamer target-molecules and different separation methods.



### 3.2.1.2 Design of the oligonucleotide library

The SELEX method starts with the library design. Up to  $10^{15}$  random sequences are synthesized by solid phase nucleic acid synthesis. Each member of the library contains a randomized internal region (20 to 80 nucleotides) that is flanked by two primer regions at the 3' and 5' ends. In addition, two primer sequences are designed according to the library template, that are used as primer-binding sites for PCR amplification (17) of the library and subsequent selected sub populations. In this work of particular interest are library designs that incorporate generic features that permit immobilization and transduction. Approaches to this effect have been reported in the literature. One such effort involves the incorporation of complementary regions that immobilize the library members on the surface of magnetic beads (35). Other reports involve the post selection modifications for generic transduction in biosensor development (36).

### 3.2.1.3 Interaction between library members and target molecule

The main goal in this step is to obtain library members with high-affinity to target-molecule. Two categories of interaction methods have been reported (25). First involves a supporting matrix during the interaction (e.g., affinity tags, column matrices) on which the target is immobilized and the second one involves a soluble, matrix-free interaction (e.g. capillary electrophoresis). Herein, the target is exposed directly to millions of library members with a specific incubation period.

#### 3.2.1.4 Partitioning

After an incubation period, the partitioning step has the objective to separate library members that are unbound and bound to the target molecule. This step is crucial in the success of the SELEX method and several strategies have been developed such as: nitrocellulose membrane filtration (8), affinity surfaces (9), affinity tags (10), column matrices (11), gel electrophoresis (12), centrifugation (13), surface plasmon resonance (14), flow cytometry (15), and capillary electrophoresis (16). It is difficult to evaluate their effectiveness, because the optimum partitioning strategy depends on the features of the target and the expected outcome of the SELEX (if for example pharmaceutical or analytical purposes). For the purposes of this work it is important to examine the methods that involve matrix-free partitioning, especially as they are related to their adaptability to recognize small molecules as targets. Such methods include capillary electrophoresis, filtration, gel electrophoresis, centrifugation. Table 2, summarizes the characteristics of these methods. As it can be seen, currently there is no method that generically could be suited for partitioning when small molecules are used as targets. Capillary electrophoresis (CE) is probably a real advance in SELEX technology (26, 27) however, partitioning is based on size and charge parameters, and thus small molecules are not the best target candidates for this system.

#### 3.2.1.5 Amplification

In the first round of SELEX, a large amount of non-specific interactions is expected, because only a small population of the library members (around  $10^{15}$ ) can be bound to the target molecule. In this sense, the primer regions that flank the library member are used

Method	Separation principle	Limitations	Ref.
Capillary electrophoresis	Size and charge	Small molecules	(50)
Nitrocellulose filter	Size	Non-specific interactions, small molecules, and decrease of variability	(1)
Gel electrophoresis	Size and charge	Non-specific interactions and small molecules	(45)
Centrifugation	Sedimentation	Non-specific interactions, small molecules, and decrease of variability	(46)
Soluble-SELEX	Hybridization	No available for nucleic acids as targets	

**Table 2.** Soluble methods for SELEX and their limitations.

in order to enrich the library by PCR technique. In addition, the primers can be modified for functionalizing purposes (e.g. biotin-primer), which provides special features to the library. In the case of DNA libraries of interest here, a simple PCR step is sufficient for member population enrichment. For RNA libraries, the process of enrichment involves reverse transcription PCR (RT-PCR) which produces complementary DNA (cDNA) and finally, a standard PCR to increase the library population.

### 3.2.1.6 Conditioning

Conditioning is the preparation of the library after amplification by different mechanisms, for application in the target interaction step. It has to be performed after the library amplification and before the starting point of the new round of SELEX. For DNA libraries, the PCR product double-stranded DNA has to be separated into single-stranded DNA. Several strategies using the streptavidin/biotin system have been reported. The

modification with biotin of the unwanted strand and the separation of ssDNA by molecular weight using gel electrophoresis has been successfully performed (32). Another option is to allow the biotinylated strand to bind to streptavidin surfaces (plates or magnetic beads). Then, the strand separation is carried out by breaking the hydrogen bonds in alkaline conditions allowing the unmodified strand (wanted) to be recovered in the supernatant (33). Other strategies, such as asymmetric PCR can also be used where one of the primers is in excess in order to amplify mostly the wanted strand. For RNA, the conditioning procedure consists of the *in vivo* transcription of DNA template by T7 RNA polymerase.

#### 3.2.1.7 Cloning and Sequencing

After several rounds of SELEX (6 to 12) the process is completed by cloning and sequencing procedures (17). When the affinity of the enriched library can no longer increase it is the starting point for cloning. The number of library members in the last round can not be estimated. Therefore, the variation in this number involves parameters such as: nature of the target, target concentration, type of SELEX method. The number of library members after a complete SELEX method can be expected to be from 1 to 1.000.000 (34). The main goal of the cloning procedure is to split up the pool of library members into single members. The final pool of library members is cloned into a bacterial vector and individual colonies with single-members are obtained (17). Then, the extraction of the plasmid is performed for the sequencing method that produces the sequence that offers high-affinity against the target molecule. All the isolated sequences

(usually 20 to 50) are analyzed to find consensus motifs between them. The consensus motifs derived from this selection process will become the aptamer-candidates.

#### 3.2.1.8 Analysis of consensus sequences

Bioinformatic tools are necessary for the analysis of the sequences obtained by SELEX. In order to find the consensus sequence, the alignment of all sequences is a requirement to complete the SELEX method. Bioinformatics programs like CLUSTAL W are frequently used for the alignment performance. The analysis of the alignment data is based on the concordance between different sequences and some specific motif sequences that differ by the position of single nucleotides. Using this type of analysis, the consensus sequences can be identified and at the same time, groups based on homology can be observed. When performing a complete SELEX method, the expected positive outcome is the consensus sequences between different library members. In addition, the consensus sequence obtained will be the candidate-aptamer that will be synthesized for the aptamer characterization.

### 3.3 Hypothesis

The idea of a SELEX method, wherein the interaction between nucleic acid-ligand and target molecule is carried out in the absence of surfaces or matrices, will be successful enough to avoid the non-specific interaction. Herein, a new approach for separation step is proposed, termed “Soluble-SELEX”. This new SELEX method uses hybridization as partitioning mechanism for separating the bound and unbound DNA members to the target-molecule. In this new method, beads that are used to provide the library ssDNA

members used for target interaction, are kept and used again to hybridize back all members that do not interact strongly enough with the target. The target-bound members are used directly for PCR while the non bound members are easily separated since they are hybridized to the magnetic beads containing the complimentary part of the library. This “Soluble-SELEX” and its hybridization procedure will be evaluated by fluorescence studies as the partitioning mechanism for SELEX method.

Furthermore it is hypothesized in this work that the incorporation of a primary structure motif in the library (namely a  $-15.19$  kJ/mol hairpin-like structure ) will provide a generic modulation of aptamer structure upon target recognition that leads to an off-mechanism of detection (separation of the hairpin members).

### **3.4 Objectives**

The principal goal of this work is to develop a new SELEX method that avoids the non-specific interaction of surfaces or matrices. This new method termed, “Soluble-SELEX” will be used hybridization as the partitioning mechanism and the interaction between library members and target will be carried out in solution (matrix-free method).

In addition, the design of the library has an arbitrary “hairpin region” that will be an inducer of conformational changes in the library members that bind the target molecule. Hairpin-like structure will provide an intrinsic transduction mechanism for the selected aptamers.

## 3.5 Experimental Methods

### 3.5.1 Design of the SELEX Library:

The method starts with the library design. A 102-mer single DNA was designed with 22 and 29 nucleotides primer flanking sequences at the 3' and 5' ends respectively, an arbitrary complementary sequence of 12 nucleotides (hairpin region, 6 nucleotides in each extreme following by the primer regions) and a randomized 49 nucleotide internal sequence. In addition, two primer sequences were designed according with the library template. The primer sequence at the 3' end was biotinylated for preparation of the single-stranded DNA library.

Library: Blue; primer region, red; hairpin and black; random region (Figure 1).

5'- **GAC AGG GCT CAC AAG CTA ACC AAC C** (AGCT) (AGCT) (AGCT)  
(AGCT) (AGCT) (AGCT) (AGCT) (AGCT) (AGCT) (AGCT) (AGCT) (AGCT)  
(AGCT) (AGCT) (AGCT) (AGCT) (AGCT) (AGCT) (AGCT) (AGCT) (AGCT)  
(AGCT) (AGCT) (AGCT) (AGCT) (AGCT) (AGCT) (AGCT) (AGCT) (AGCT)  
(AGCT) (AGCT) (AGCT) (AGCT) (AGCT) (AGCT) (AGCT) (AGCT) (AGCT)  
(AGCT) (AGCT) (AGCT) (AGCT) (AGCT) (AGCT) (AGCT) (AGCT) (AGCT)  
(AGCT) **G GTT GGC AGC GAT CGT CTT GAA TCT** - 3'

Primer forward (biotynalated):

5'- AGA TTC AAG ACG ATC GCT G -3'

Primer reverse:

5'- GAC AGG GCT CAC AAG CTA A -3'

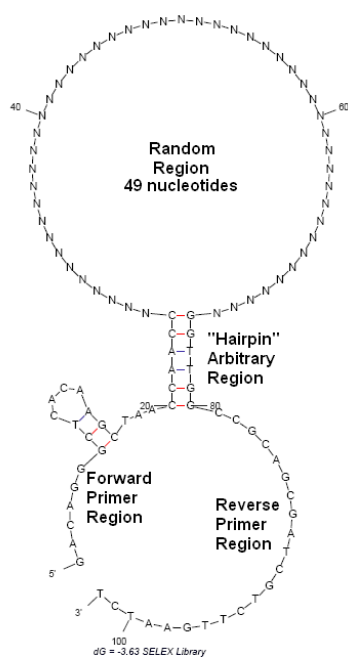


**Figure 1.** Design and prediction of the SELEX library. The prediction was performed by mfold software.

### 3.5.2 Soluble-SELEX method:

The strategy of Soluble-SELEX with hybridization as partitioning mechanism is described in 6 different steps (Fig. 2): a) The candidate mixture is amplified by PCR of the initial library. Then, the coupling between streptavidin magnetic-beads and biotinylated PCR product is carried out. b) Separation of single-stranded DNA (ssDNA) is required. Sodium hydroxide (NaOH) has been used to increase the ionic strength and the consequent separation between ssDNA and biotinylated ssDNA bound to magnetic-beads. After the magnetic recovery of ssDNA-magnetic-beads, the candidate mixture (ssDNA) is obtained by extraction of the supernatant. In addition, the ssDNA magnetic-beads are washed and kept in buffer for the hybridization step. c) After a precipitation step of the supernatant, the candidate mixture (ssDNA) was concentrated in water before



incubation with the target-molecule. d) The hybridization as partitioning mechanism is performed by coupling between ssDNA magnetic-beads and ssDNA with low affinity for the target molecule. e) The hybridized DNA is magnetically recovered followed by the supernatant extraction that contains ssDNA with high affinity to the target -molecule. f) The next step is the amplification by PCR after the target denaturation using high temperature (95°C).

#### 3.5.2.1 Evolution monitoring of the Soluble-SELEX method.

In order to develop the Soluble-SELEX, the resulting evolution from each round was quantified by fluorescence as has been previously described (18). The detection was carried out by Oligreen. This probe has been designed with high specificity for single-stranded DNA.

Reagents: Quant-iT™ OliGreen® ssDNA reagent (Oligreen), solution in DMSO 20X TE (25 mL of 200 mM Tris-HCl, 20 mM EDTA, pH 7.5) and Ultra pure Water. TE buffer was used for the preparation of Oligreen, oligonucleotide and ssDNA diluted solutions. Because Oligreen is an extremely sensitive detection reagent for ssDNA, it is imperative that the TE solution used be free of contaminating nucleic acids. The Oligreen working solution was prepared with a 200-fold dilution of the Oligreen reagent using the 20X TE buffer.

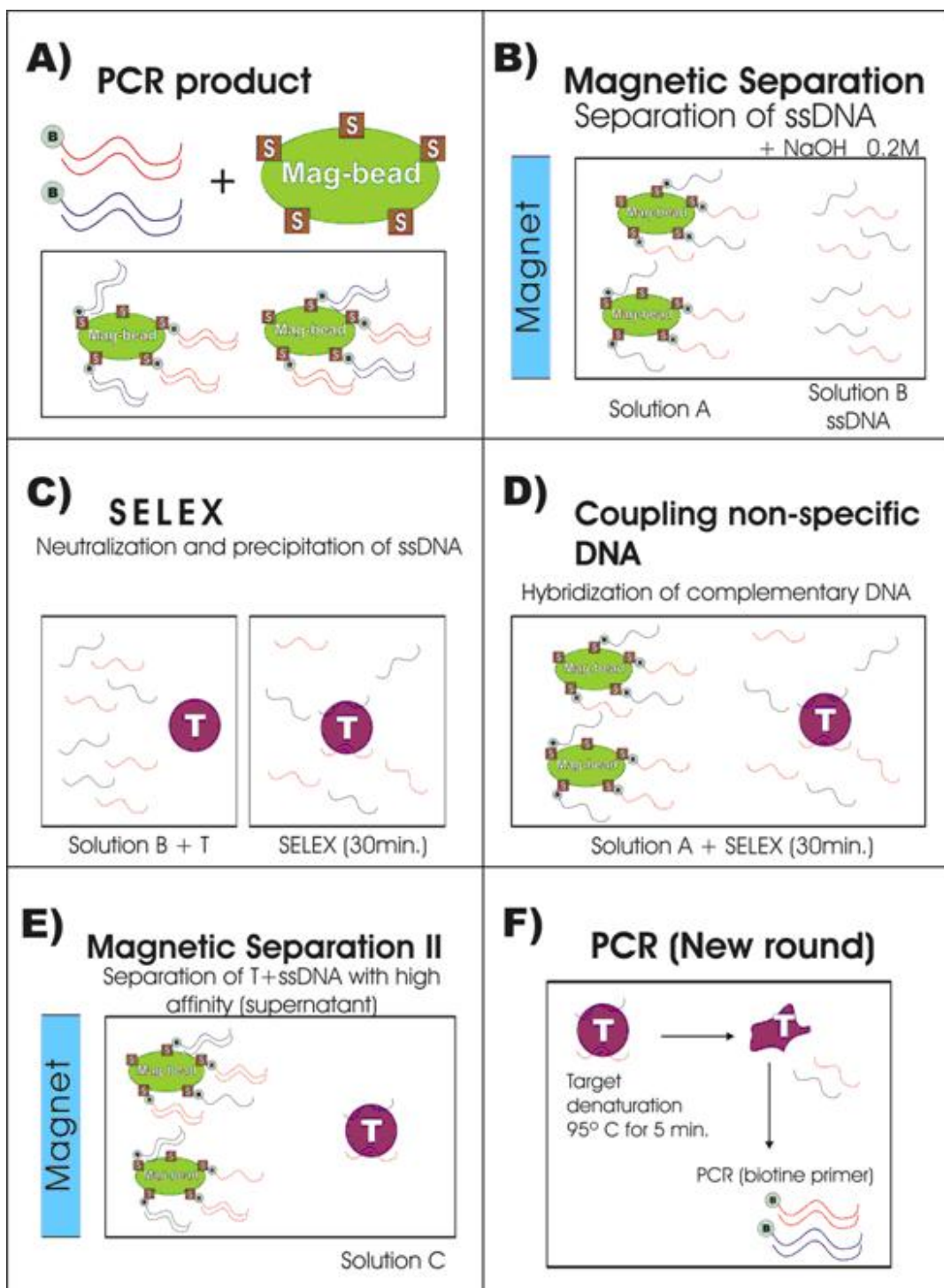


**Fig 2. Soluble-SELEX method:** a) coupling between PCR product and Mag-Beads, b) Separation of ssDNA, c) target bound and unbound ssDNA, d) hybridization between complementary ssDNA attached on Mag-Beads and ssDNA in solution, e) magnetic partitioning of target bound and unbound ssDNA, f) PCR with previous denaturation of the target.

Sample preparation: For every round of Soluble-SELEX, 5 $\mu$ L of solution C (Figure 2, E) were taken for evolution measurements. The samples were diluted in 45 $\mu$ L of ultra pure water and then 50 $\mu$ L of Oligreen working solution was added to the quartz cuvette. All measurements were performed using a Cary Eclipse Fluorescence spectrophotometer with the following parameters: excitation 480nm, emission 520nm and a scanning range from 450 to 600nm.

### 3.5.2.2 Cloning

TOPO TA Cloning® kit has been selected in order to perform the cloning procedure of Soluble-SELEX. TOPO Cloning provides a highly efficient, and one-step cloning strategy ("TOPO® Cloning") for the direct insertion of Taq polymerase-amplified PCR products into a plasmid vector. No ligase, post-PCR procedures, or PCR primers containing specific sequences are required.

The plasmid vector pCR2.1-TOPO is supplied linearized with:

- a) Single 3'-thymidine (T) overhangs for TA Cloning®
- b) Topoisomerase I covalently bound to the vector (referred to as "activated" vector)

Taq polymerase has a non template-dependent terminal transferase activity that adds a single deoxyadenosine (A) to the 3' ends of PCR products. The linearized vector supplied in this kit has single, overhanging 3' deoxythymidine (T) residues. This allows PCR inserts to ligate efficiently with the vector. Topoisomerase I from Vaccinia virus binds to duplex DNA at specific sites and cleaves the phosphodiester backbone after 5'-CCCTT in one strand (Shuman, 1991). The energy from the broken phosphodiester backbone is

conserved by formation of a covalent bond between the 3' phosphate of the cleaved strand and a tyrosyl residue (Tyr-274) of topoisomerase I. The phospho-tyrosyl bond between the DNA and enzyme can subsequently be attacked by the 5' hydroxyl of the original cleaved strand, reversing the reaction and releasing topoisomerase (Shuman, 1994). In order to complete the procedure, additional steps have been carried out.

#### 3.5.2.2.1 Bacteria Transformation:

After cloning TOPO reaction, the transformation of *E. coli* competent cell was performed by the addition of 2  $\mu\text{L}$  of the TOPO® cloning reaction into a vial of *E. coli*. The reaction was mixed gently and incubated on ice for 5 to 30 minutes. Heat-shocking step (30 seconds at 42°C without shaking) is required before immediately transferring the tubes to ice.

#### 3.5.2.2.2 Inoculation on media-LB agar plates:

- a) Add 25 grams of LB powder and 15 grams of agar to 1 L of distilled water. Autoclave and allow the LB agar solution to cool until it can be safely handled. Add ampicillin and kanamycin (50  $\mu\text{g}/\text{mL}$ ). Pour the LB agar solution containing antibiotics into Petri dishes and cover. Let stand overnight to harden and dry.
- b) Warm selective plates at 37°C for 30 minutes.
- c) Spread 40  $\mu\text{L}$  of 40 mg/mL X-gal on each LB ampicillin and kanamycin plate and incubate at 37°C until ready for use.
- d) Add 250  $\mu\text{L}$  of room temperature S.O.C. medium to the transformed cells
- e) Cap the tube tightly and shake the tube horizontally (200 rpm) at 37°C for one hour.
- f) Spread 10-50  $\mu\text{L}$  of transformed cells solution on a pre-warmed selective plate.

- g) Incubate plates at 37°C overnight.
- h) After the observation of white (library member insertion) and light blue colonies (no insertion), the selection of singles colonies was performed.

#### 3.5.2.2.3 Inoculation of single colonies in LB liquid media.

A small part of a white colony was carefully harvested and cultured in a tube with 10 mL LB medium containing 50 µg/mL ampicillin and 50 µg/mL kanamycin for 12 hour at 37°C. This step was repeated for at least 30 colonies. The bacterial growth has been evaluated by the pellet formation in the LB media.

#### 3.5.2.2.4 Plasmid extraction

The plasmid extraction procedure was performed by PureLink™ Quick Plasmid Miniprep Kit. The cells were lysed using an alkaline/SDS procedure. The lysate was then applied to a silica membrane column that selectively binds plasmid DNA. Contaminants were removed with wash buffers. The plasmid DNA was eluted in TE Buffer and is suitable for all routine downstream applications. The PureLink™ Quick Plasmid Miniprep Kit was used with a centrifuge method. The complete procedure is described below:

- a) Pellet 1 to 5 mL of an overnight culture (1–2 x 10<sup>9</sup> *E. coli* in LB medium). Thoroughly remove all medium from the cell pellet.
- b) Completely resuspend the pellet in 250 µL resuspension buffer (R3) with RNase A. No cell clumps should remain.
- c) Add 250 µL lysis buffer (L7) to cells. Mix gently by inverting the capped tube 5 times. Do not vortex.

- d) Incubate the tube for 5 minutes at room temperature. Do not exceed 5 minutes.
- e) Add 350  $\mu\text{L}$  Precipitation Buffer (N4). Mix immediately by inverting the tube until the solution is homogeneous. For large pellets shake more vigorously. Do not vortex.
- f) Centrifuge the mixture at  $\sim 12,000 \times g$  for 10 minutes at room temperature using a microcentrifuge to clarify the lysate from lysis debris.
- g) Load the supernatant from step f) onto a spin column.
- h) Centrifuge at  $\sim 12,000 \times g$  for 1 minute. Discard the flow-through and place the column back into the wash tube.
- i) Add 700  $\mu\text{L}$  wash buffer (W9) with ethanol to the column.
- j) Centrifuge the column at  $\sim 12,000 \times g$  for 1 minute. Discard the flow-through and place the column back into the wash tube.
- k) Centrifuge the column at  $\sim 12,000 \times g$  for 1 minute to remove any residual Wash Buffer (W9). Discard the wash tube with the flow-through.
- l) Place the spin column in a clean 1.5 mL recovery tube.
- m) Add 75  $\mu\text{L}$  of preheated TE Buffer (TE) to the center of the column.
- n) Incubate the column for 1 minute at room temperature.
- o) Centrifuge at  $\sim 12,000 \times g$  for 2 minutes.
- p) The recovery tube contains your purified plasmid DNA. Discard the column.
- q) Store the DNA at  $-20^\circ\text{C}$  or use DNA for the desired downstream application.

#### 3.5.2.2.5 Plasmid analysis by PCR

Before starting with the sequencing method, a simple confirmation of the purification of the plasmid was carried out by standard PCR. Using the commercial M13 primers the PCR was performed. Then, the band (around 300 bp) that corresponds to the specific plasmid segment was observed by gel electrophoresis.

### 3.5.2.3 Sequencing

Sequencing data was obtained by capillary electrophoresis in a Beckman Coulter CEQ 8000 device. The sample preparation was performed using 0.5  $\mu\text{L}$  of purified plasmid solution and genomelab™ dye terminator cycle sequencing with quick start kit- Beckman coulter. The list of reagents and complete procedure are described below:

Reagents: Dye Terminator Master Mix, pUC18 Control Template (0.25  $\mu\text{g}/\mu\text{L}$ ), M13 Sequencing Primer (1.6 pmol/ $\mu\text{L}$  or 1.6  $\mu\text{M}$ ) Glycogen (20 mg/mL).

PCR reaction:

- a) Heat the template (purified plasmid) at 96°C for 1 minute.
- b) Cool to room temperature.
- c) Sequencing reaction was prepared as follows: 0.5  $\mu\text{L}$  template, 2  $\mu\text{L}$  of M13 primer, 8  $\mu\text{L}$  master mix and 20  $\mu\text{L}$  ultrapure water.
- d) PCR thermal cycling program: denaturation 96°C for 20 sec, annealing 50°C for 20 sec and extension at 60°C for 4 min. For 30 cycles followed by holding at 4°C.

Ethanol precipitation: Precipitation in Individual Tubes

- e) Prepare a labeled, sterile 0.5 mL tube for each sample.
- f) Prepare fresh Stop Solution/Glycogen mixture as follows (per sequencing reaction): 2  $\mu\text{L}$  of 3M Sodium Acetate (pH 5.2), 2  $\mu\text{L}$  of 100 mM Na<sub>2</sub>-EDTA (pH 8.0) and 1  $\mu\text{L}$  of 20 mg/mL of glycogen (supplied with the kit). To each of the labeled tubes, add 5  $\mu\text{L}$  of the Stop Solution/Glycogen mixture.
- g) Transfer the sequencing reaction to the appropriately labeled 0.5 mL tube and mix thoroughly.

- h) Add 60  $\mu\text{L}$  cold 95% (v/v) ethanol/dH<sub>2</sub>O from -20°C freezer and mix thoroughly. Immediately centrifuge at 14,000 rpm at 4°C for 15 minutes. Carefully remove the supernatant with a micropipette (the pellet should be visible). Note: For multiple samples, always add the cold ethanol/dH<sub>2</sub>O immediately before centrifugation.
- i) Rinse the pellet 2 times with 200  $\mu\text{L}$  70% (v/v) ethanol/ dH<sub>2</sub>O from -20°C freezer. For each rinse, centrifuge immediately at 14,000 rpm at 4°C for a minimum of 2 minutes. After centrifugation carefully remove all of the supernatant with a micropipette.
- j) Dry for 30 minutes in the dark.
- k) Resuspend the sample in 40  $\mu\text{L}$  of the Sample Loading Solution and charge in capillary electrophoresis machine.
- l)

#### 3.5.2.4 Alignment and analysis of sequence:

Sequencing data was analysed by ClustalW2 and T-Coffee. ClustalW2 is a general tool for multiple sequence alignment programs for DNA. It calculates the best match for the selected sequences (one clone), and the primer regions that are used in the library. After the identification of the random sequence (49n) for each clone by Clustal program, T-Coffee was used for the multiple sequence alignment of multiple clones sequencing data. Both tools allow the identification of the consensus sequence present in different clones. According to the alignment data, the synthesis of several aptamer candidates was performed by VBC Biotech services (Austria).

#### 3.5.2.5 Evaluation of aptamer-candidates



The evaluation of aptamer candidates was performed by a BIAcore 3000. In order to analyse all the candidates, the target (Avidin) was immobilized on the BIAcore chip surface (CM5) and the binding affinity of the aptamer candidates was evaluated. Then, the best aptamer candidate was modified with a thiol-group at 5' and immobilized on the BIAcore chip (Au surface). A titration with different concentration of the target was evaluated in order to obtain the dissociation constant  $K_D$ . The reagents and complete procedure is described below:

Reagents: TBS-T (1 L deionized water, 0.05 M Tris, 0.138 M NaCl, 0.0027 M KCl, pH 8.0, 25°C, 0.05% Tween 20), EDC: (1-Ethyl-3-(dimethylaminopropyl)carbodiimide HCL) 0.2 M, NHS: (N-Hydroxysuccinimide) 0.05 M, 10 mM sodium acetate pH 4.4, Ethanolamine (1 M, pH 8.5),  $KPO_4$  1M, avidin 1 mg/mL (100  $\mu$ L), CM5 sensor chip and Au sensor chip (BIAcore, GE Healthcare, Sweden).

CM5 chip Procedure:

- a) Add a mixture of 50  $\mu$ L of each EDC and NHS to the Au side of a CM5 chip mix.
- b) Incubate for 20 minutes.
- c) Wash chip with buffer.
- d) Add 100  $\mu$ L of 1 mg/mL avidin to the chip.
- e) Incubate for 30 minutes.
- f) Wash chip with buffer.
- g) Add 50  $\mu$ L of 1M ethanolamine for blocking.
- h) Wash chip with buffer.
- i) Add 35  $\mu$ L of 50 nM candidate aptamer to the avidin-modified chip.

Au Chip Procedure:

- j) To the Au side of a CM5 chip add 50  $\mu\text{L}$  of 2  $\mu\text{M}$  candidate-aptamer, dissolved in  $\text{KPO}_4$  1M.
- k) Incubate for 20 minutes.
- l) Wash chip with buffer.
- m) Add 35  $\mu\text{L}$  of avidin (target) from 100 to 1000 pM.

#### 3.5.2.6 Thermodynamics by BIAcore T100:

The SPR assays were performed according to the same coupling method as described previously. Using a BIAcore T100 instrument, the H18hp avidin-aptamer was modified with a thiol group at 5' end, in order to bind the surface of the Au sensor chip (BIAcore). The H18hp avidin-aptamer was immobilized to  $\sim 500$  RU<sup>in</sup> flow cell by thiol coupling in binding buffer  $\text{KPO}_4$  (pH 3.4) at a flow rate of 15  $\mu\text{L}/\text{min}$  at 25°C for 5 min by the INJECT program (BIAcore). The running buffer (TBT-t) was passed through flow cells of the sensor chip for 1 min at the KINJECT program (BIAcore). The data was obtained by subtracting the signals for H18hp avidin-aptamer on the Au sensor chip (flow cell 2) from the signal for Au sensor chip unmodified (flow cell 1), thereby showing the net interaction between aptamer and target molecule (Figure 7). To regenerate the sensor chip, bound materials were completely removed by injecting 20  $\mu\text{L}$  of 0.05 M NaOH at a flow rate of 15  $\mu\text{L}/\text{min}$ . Close-fitting curves to the sensograms were calculated by global fitting curves (1:1 Langmuir binding) generated using BIAcore T100 evaluation software.

## 3.6 Results and discussion

### 3.6.1 SELEX

This new SELEX method uses hybridization as partitioning mechanism for separating the bound and unbound DNA members to the target-molecule. The hybridization procedure has been evaluated by fluorescence. First of all, a measurement of the hybridization recovery by streptavidin magnetic beads at three different times (15, 30, 45 min) was performed (Fig 3) in order to determine the optimum incubation time for this step. After coupling of dsDNA-biotinylated with streptavidin magnetic beads (Figure 1a), the elution of ssDNA by NaOH was carried out. The facile magnetic-bead separation allows the extraction of the supernatant. The supernatant analysis by Oligreen permits the ssDNA concentration determination (Fig. 3b). Subsequently, the hybridization between the biotinylated-ssDNA attached on the magnetic bead surface from the previous step and the ssDNA in solution was carried out for 15min (Fig 3c), 30min (Fig 3d) and 45 min (Fig. 3e) in order to determine the incubation time that is sufficient for this step. After the magnetic separation, the supernatant is evaluated and insignificant difference between 30 and 45 minutes is observed. The previous experiment confirms the usefulness of the hybridization using magnetic-bead for the extraction of ssDNA in solution, and 30 minutes was chosen as the optimal separation time.

In order to prove that hybridization can be used as the partitioning mechanism for SELEX, a hybridization experiment was performed using SELEX conditions. Figure 4 shows the hybridization after a simulated SELEX round.

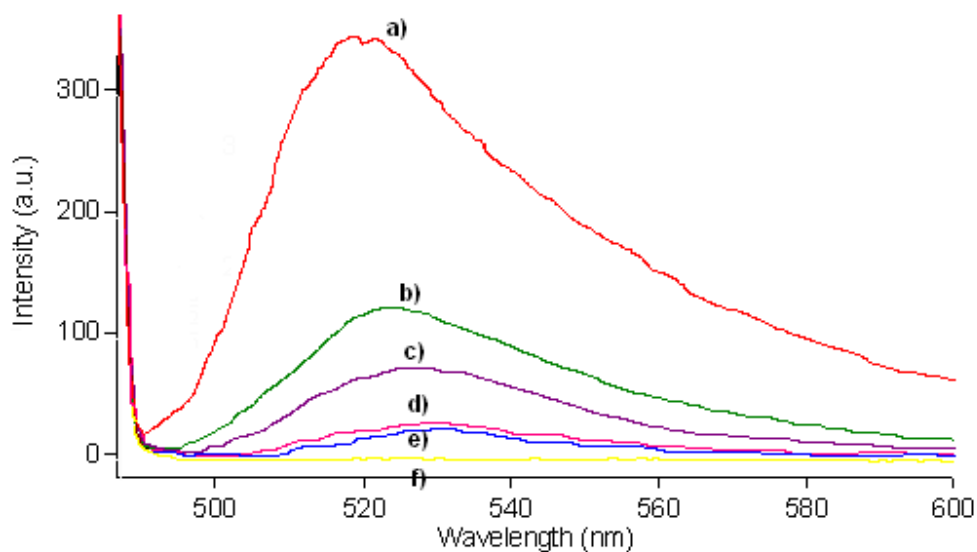


Figure 3. **Hybridization analysis by fluorescence (Oligreen dye).** Streptavidin-magnetic bead was attached to biotinylated dsDNA, then the supernatant (dsDNA) has been evaluated (a). After elution of ssDNA (NaOH) the sample was collected and analysed (b). Then, the hybridization was carried out at different times 15 min (c), 30 min (d) and 45 min (e). negative control (f). Conditions as described in the text.

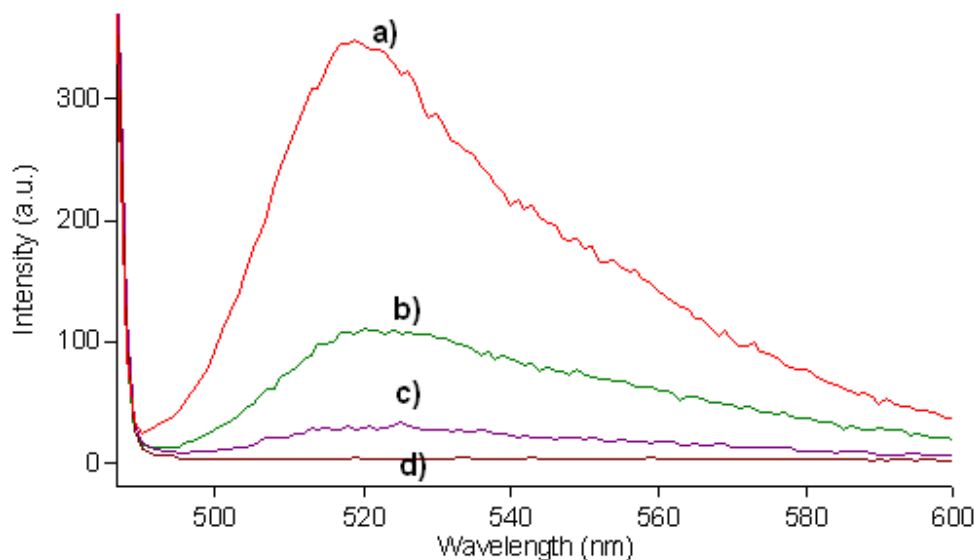
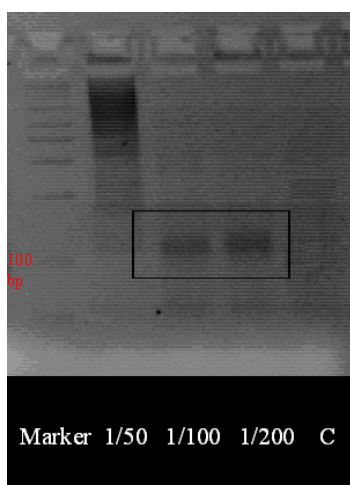


Figure 4. **Hybridization analysis by fluorescence (Oligreen dye).** Streptavidin-magnetic bead was attached to biotinylated dsDNA, then the supernatant (dsDNA) has been evaluated (a). After elution of ssDNA (NaOH) the sample was collected and analysed (b). Finally, after hybridization (ssDNA magnetic-beads and ssDNA solution) the supernatant has been collected and evaluated (c). Negative control (d). Conditions as described in the text.

Following the same methodology as before (Figure 3) we proceeded with the evaluation of dsDNA (Fig. 4a) and ssDNA extraction (Figure 4b). The hybridization between modified magnetic bead and ssDNA was carried out after precipitation of DNA (simulation of SELEX). Finally, the evaluation of the supernatant after magnetic separation was performed (Fig. 4c). The last step in proving that the hybridization could be incorporated in SELEX method would be to do a complete round of SELEX and analyse the result. Figure 5 shows the DNA band as a result of amplification from different dilutions of the sample after the first round of SELEX .



**Figure 5.** Electrophoresis of the first round of “Soluble-SELEX” using hybridization as partitioning mechanism. Three PCRs were carried out for three different dilutions of the first round SELEX product. M: DNA marker; the band that corresponds to 100 base pairs (bp) is highlighted. 1/1: 1  $\mu$ L of undiluted sample as template for PCR, 1/50 1  $\mu$ L of 50 times diluted sample, 1/100 1  $\mu$ L of 100 times diluted sample and C, negative control for PCR.

To validate the approach, 12 rounds of Soluble-SELEX were performed against the target PSA (0.01 mg/mL). No evolution was observed for the original target. After the analysis of SELEX samples, it was found by ELISA that some avidin (0.03  $\mu$ g/mL) was leaking out from the magnetic beads. This avidin was present at all times in the

SELEX process and working as a non-specific target. Evolution studies were performed then against avidin employing fluorescence spectroscopy (Figure 6) as reported previously (18). After performing the analysis of the results, it was confirmed that SELEX method evolved against avidin instead of the original target PSA even when the PSA was three orders of magnitude more concentrated. Currently we have no explanation for this observation. However, it has to be noted that there are no reports in the literature about aptamers for PSA and parallel experiments in our laboratory (M. Svobodova, C. Ozalp and C. O'Sullivan: unpublished results) using "traditional" SELEX partition methods have failed to yield a PSA aptamer. Although a non-specific aptamer was obtained with the first "Soluble-SELEX", the objective of this study was to prove the concept that the soluble SELEX partition method is valid. In this sense, the target is not as important. Still, it is desirable for the "Soluble-SELEX" to be improved in order to avoid the non-specific selection against the immobilisation chemicals of the bead. Preliminary experiments (results not shown) have demonstrated that if non-specific silanol magnetic beads (-OH) are used for removal of the non-bound ssDNA, no evolution is seen. Therefore, the improvement can be afforded by modulating the time of contact of the library with the beads and all steps where streptavidin might have leaked from the surface. In order to isolate an aptamer (even against avidin) cloning and sequencing procedures were completed using standard methods as described in the methodology section. Sequence alignments are necessary to compare the random region of the library members. The sequence analysis was performed by internet bioinformatic software CLUSTAL W (<http://tcoffee.vital-it.ch/cgi-bin/Tcoffee/tcoffee.cgi/index.cgi>). Based on the

alignment data some of these sequences (12 out of 20) shared common motifs (Figure 7a). Random regions with some motif sequences, but different in some single nucleotide positions were observed.

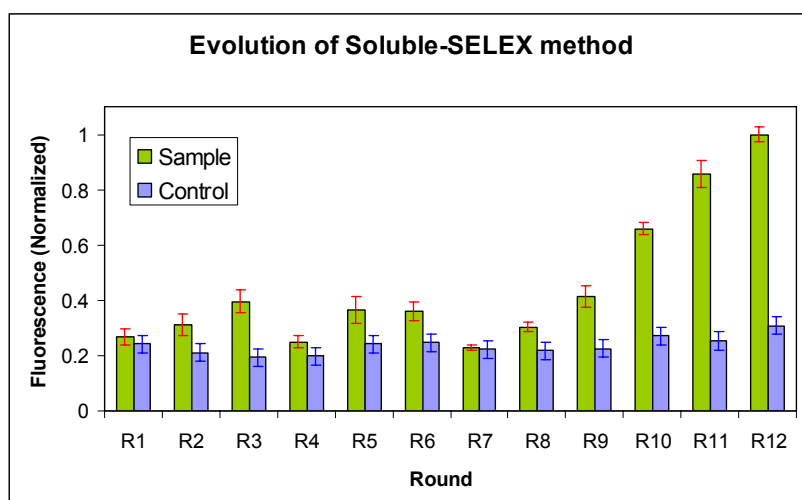


**Figure 6.** Evolution of “Soluble-SELEX” by the binding of DNA library members. Twelve rounds of “Soluble-SELEX” were analyzed using the fluorescent dye oligreen. ssDNA pool from each round were evaluated by incubation with the target (sample) and incubation without target (control). After 30 minutes of incubation, the separation was carried out by hybridization with the complementary sequence immobilized on magnetic beads. Each sample was amplified by PCR and the DNA concentration was determined by oligreen dye (fluorescence measurement). No binding was observed from 0 to 8 rounds. Round 9 has shown a progressive increase until round 12, when the target was present in solution, whereas no evolution in binding was observed in the control (no target).

The sequences were divided in 2 groups, A and B, in order to increase the sequence homology (Figure 7b). After the alignment process, 6 sequences were selected as candidate aptamers and their predicted structures (Figure 8) were carried out by mfold program <http://mfold.bioinfo.rpi.edu/cgi-bin/dna-form1.cgi>. In addition, the sequences were synthesized and their  $K_D$  values were determined using SPR in a Biacore 3000 (Figure 9). One of those sequences 5'-CCAACCGCAATTGTAGTTGACTCAACATAGTACCGGACTCGGCTAATAGACCTGGGGTTGG-3' (H18-hp) has

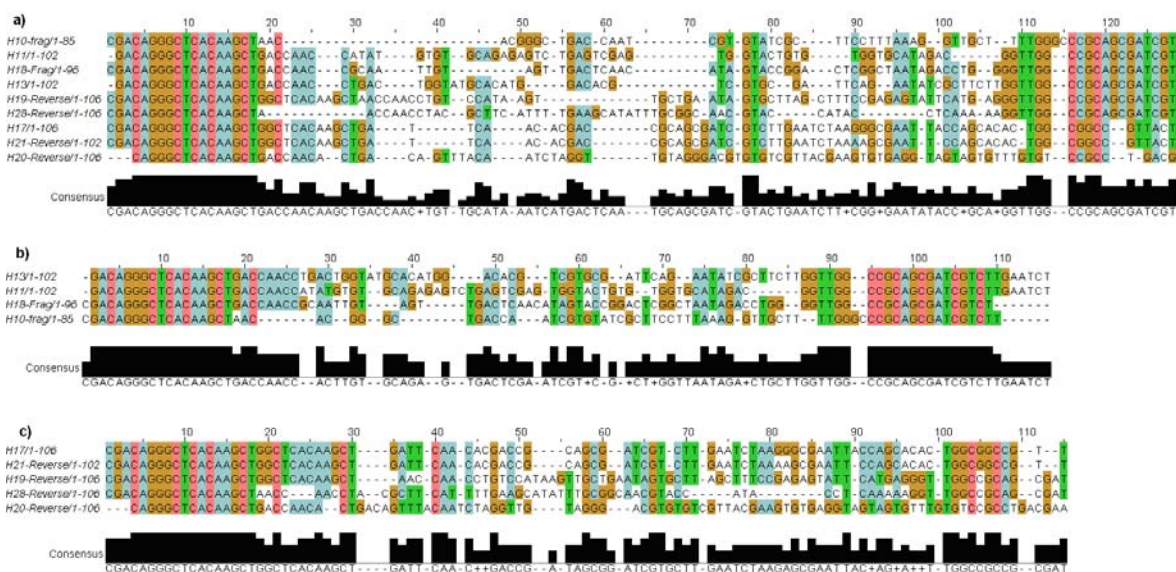


**Figure 7.** Alignments by bioinformatic software T-Coffee. a) all members, b) subgroup 1 and c) subgroup 2. The primer regions are located at the extremities of the sequence alignment and the consensus motifs are located in the middle of the sequence.

shown a representative  $K_D$  value of 1.3 nM to avidin (Fig 10). In order to assess the performance of the method, the sequence and the affinity constant of this aptamer were compared with two streptavidin aptamers that have been reported previously (19-20). The sequence comparison has shown several conserved regions among the aptamers. On the other hand, the dissociation constants ( $K_D$ ) for the three aptamers have been determined to be of the same order of magnitude (Table 3). This suggests that soluble-SELEX is a method that can raise aptamers with similar results as the standard SELEX.

Aptamer Origin	$K_D$ value [nM]
DNA H18-(Soluble-SELEX)	1.3
RNA S1 (Srisawat and Engelke)	70
RNA S19 (Tahiri and co-workers)	7

**Table 3.** Comparison between Soluble-SELEX and two additional aptamers performed by standard SELEX.



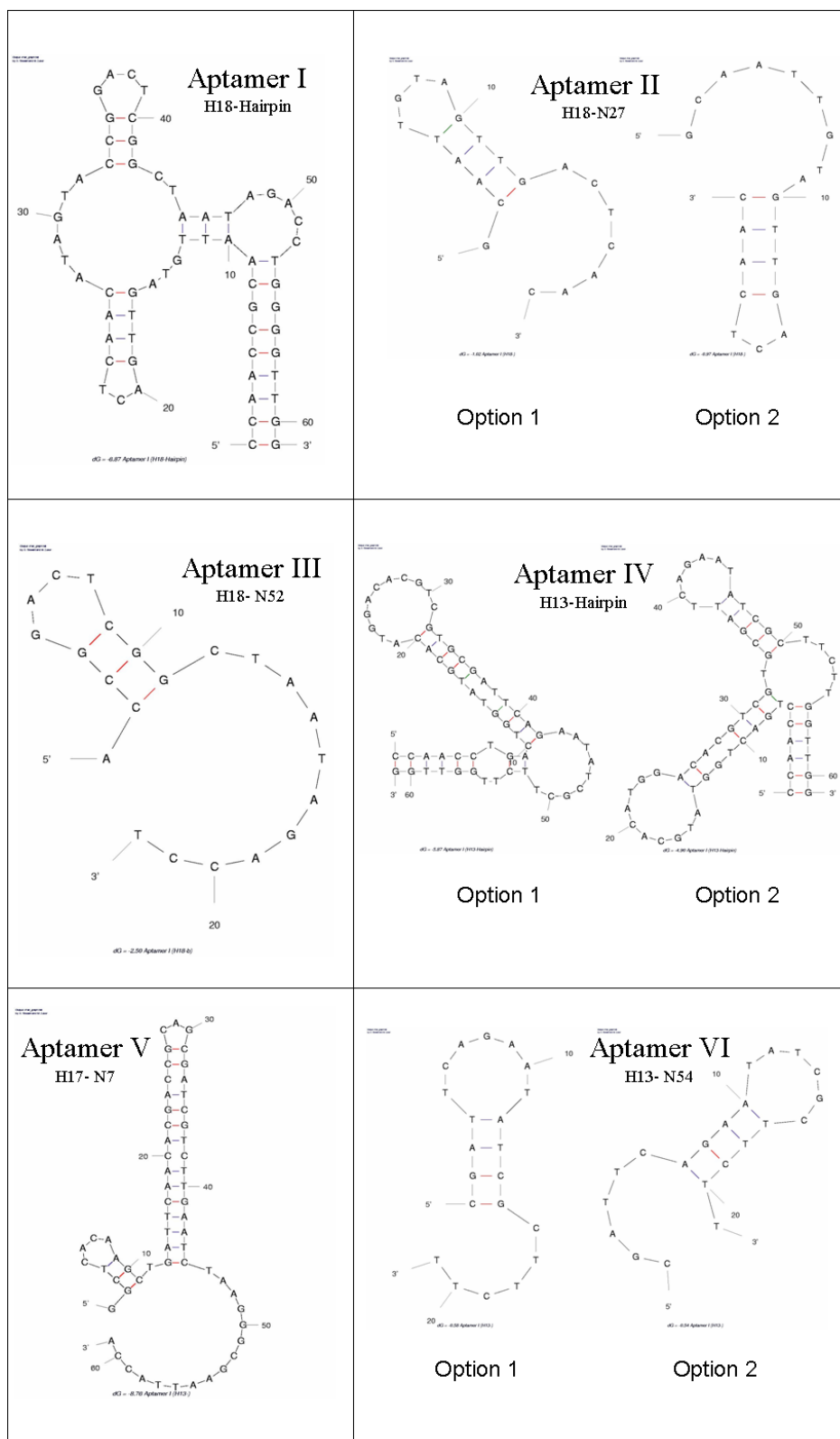


**Figure 8.** Prediction of secondary structure of the six candidate aptamers by mfold program.

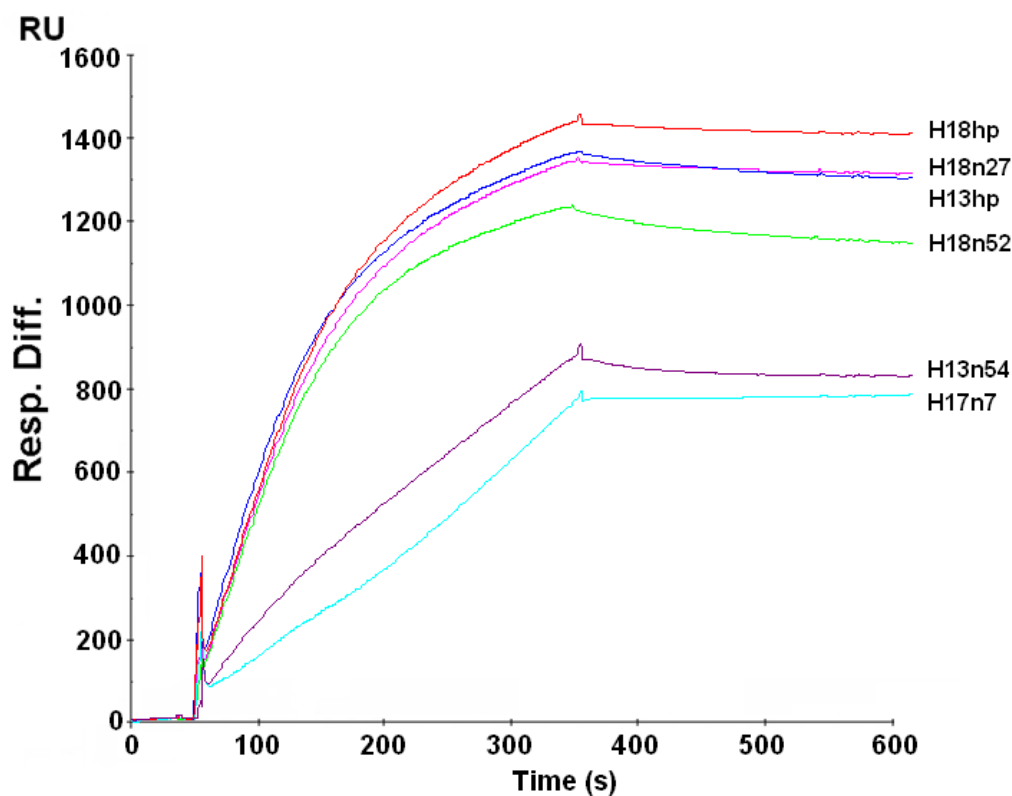


**Figure 9.** BIAcore binding curves for 500 nM of six candidate aptamer. Resonance units (R.U.) are a measure for the number of candidate aptamer molecules retained by the target (avidin) immobilized on the sensor chip. Conditions as described in the text.

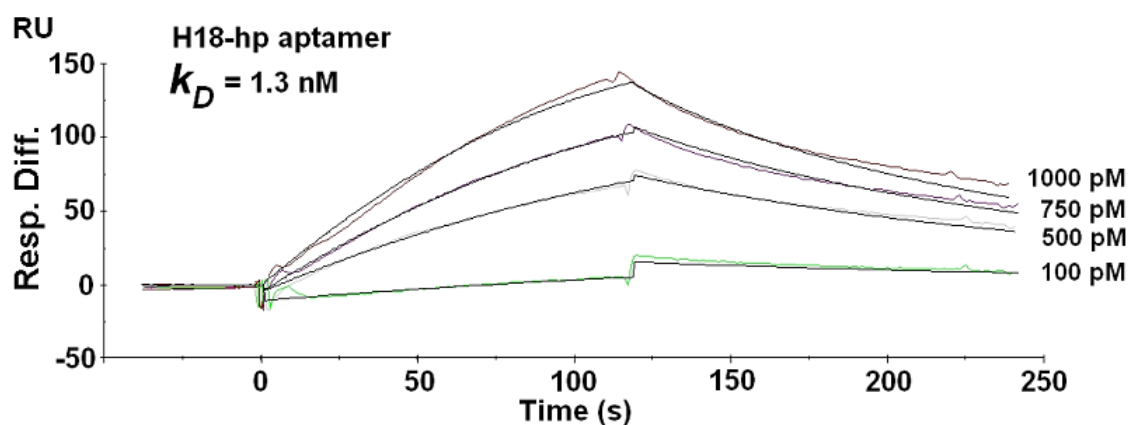


**Figure 10.** High-affinity interaction between immobilized H18-aptamer and avidin. Resonance units (R.U.) are a measure for the number of target molecules (avidin) retained by H18-immobilized aptamer on the sensor chip. Four different avidin concentrations were analyzed (100 pM to 1000 pM) and a significant value of 1.3 nM was reported using a Langmuir fitting model (with mass transfer, as determined by Biaevaluation 2.0 procedures, black lines)

### **3.6.2 Candidate-aptamer evaluation**

In order to characterize the candidate aptamers that were obtained by Soluble-SELEX, SPR was performed in the Biacore 3000 instrument.

#### **3.6.2.1 Surface Plasmon Resonance (SPR)**

After the  $K_D$  determination for H18-avidin aptamer (Figure 10), its selectivity was studied by SPR. The baseline for this experiment is the signal recorded after the immobilization of H18-avidin aptamer (modified with a thiol group at 3') on gold Biacore chip. After the addition of two non-specific proteins (BSA and PSA) the plasmon resonance was recorded for each case (Figure 11). The signal recorded after the addition of non-specific targets was insignificant. In contrast, in the presence of the specific-target, the results have shown an important binding effect between aptamer and the target. These results suggest the high selectivity of H18-aptamer on biacore platform. In addition, the biosensor reproducibility was checked by measuring four replica at three different concentrations each (0, 10 and 30 nM). All errors were below 4% (SD: 1.8%), which verified the robustness of our H18-avidin aptamer based biosensor system. The regeneration protocol consists of an efficient flushing step with a 50  $\mu$ M of NaOH and TBS-T as running buffer (Figure 12).

#### **3.6.2.2 Thermodynamic information by Surface Plasmon Resonance Analysis**

The interactions between avidin and anti-avidin aptamer H18hp were characterized by SPR analysis at different temperatures. A direct measurement of binding thermodynamic parameters are possible with isothermal titration calorimetry. Measuring the temperature

dependence of affinity constants by SPR analysis has been used as an alternative method for determining thermodynamics of binding between biomolecules (51).

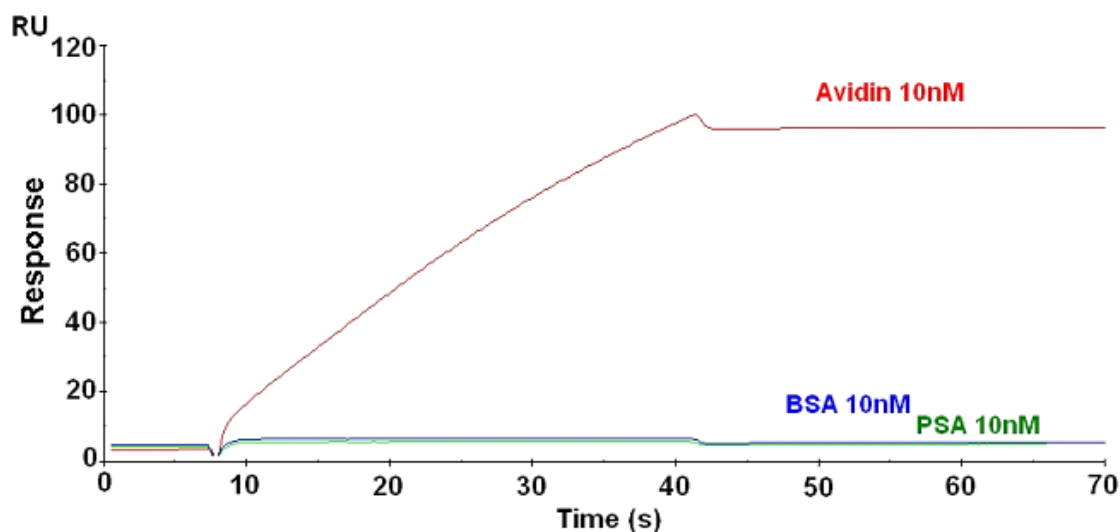


**Figure 11.** Evaluation of specificity of H18-avidin aptamer by SPR: 10 nM of avidin as specific target and 10 nM of PSA and BSA as non-specific targets were passed over the H18-avidin aptamer immobilised on the BIAcore chip sensor. PSA and BSA proteins showed no significant change in the H18-avidin aptamer interaction process whereas avidin binding was greatly enhanced, yielding a response 97 RU above the H18-aptamer interaction.

The thermodynamic parameters of the interaction between H18hp avidin-aptamer and avidin were determined by measuring the temperature dependence of the ratio of its kinetic association and dissociation rate constants. Surface plasmon resonance analysis was used to measure the rate constants at temperatures ranging from 10 to 35°C. Five different target concentrations (10 to 50 nM) were analyzed in order to determine each  $K_D$  value at each temperature. After the kinetic analysis, thermodynamic data, such as free energy  $\Delta G^\circ$  (-46 kJ/mol), enthalpy  $\Delta H^\circ$  (-12 kJ/mol) and entropy  $\Delta S^\circ$  110 [J(K\*mol)] were obtained (See table 4). The functional binding activity of two molecules

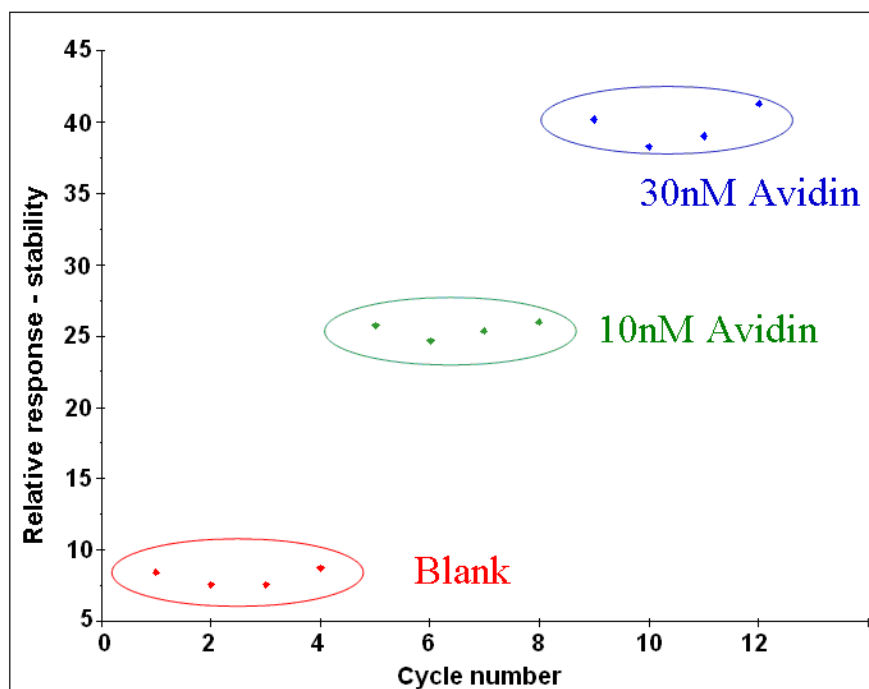


**Figure 12.** Studies of stability and reproducibility of H18hp avidin-aptamer by BIAcore (T100) technology. Three different concentrations of avidin were used (0, red; 10, green; and 30, blue at nM range). Four repeated measurements at each concentration were performed. Conditions as described in the text.

can be described by the kinetic rate constants and equilibrium constants. In addition, the binding interaction can be estimated from the thermodynamic parameters as well. The changes in enthalpy ( $\Delta H^\circ$ ) and entropy ( $\Delta S^\circ$ ) are related to the free energy of binding ( $\Delta G^\circ$ ) and the equilibrium association constant ( $K^\circ$ ) in the van't Hoff equation[eq. 1] (52)

$$\Delta G^\circ = -RT \ln 1/K_D = RT \ln K_D \quad [\text{eq. 1}]$$

where,  $\Delta G^\circ$  is the standars free energy change

R is the universal gas constant

T is the absolute temperature (K)

$K_D$  is the equilibrium dissociation constant,

Substituting in the expression

$$\Delta G^\circ = \Delta H^\circ - T \Delta S^\circ$$

and rearranging gives:

$$\ln K_D = \Delta H^\circ/RT - \Delta S^\circ/R$$

where,  $\Delta H^\circ$  is the standard enthalpy change and  $\Delta S^\circ$  is the standard entropy change.

If the enthalpy change  $\Delta H$  does not vary with temperature, the van't Hoff plot of  $\ln K$  versus  $1/T$  results in a straight line of slope  $-\Delta H/R$ . However, for  $\Delta S$  values corresponding to the binding of biomolecules very often a significant change in temperature is reported. As a result, heat capacity change,  $\Delta C_p$ , different from zero can be expected (53). In such cases, the plot of  $\ln K_D$  against  $1/T$  is not linear, and the relationship becomes [eq. 2]:

$$RT \ln K_D = \Delta H^\circ_{T_0} - T \Delta S^\circ_{T_0} + \Delta C_p^\circ (T - T_0) - T \Delta C_p^\circ \ln (T/T_0) \quad [\text{eq. 2}]$$

where,  $\Delta C_p^\circ$  is the heat capacity change under standard conditions and  $T_0$  is the reference temperature ( $25^\circ\text{C} = 298.15 \text{ K}$  for standard conditions)

**Table 4.** Thermodynamic parameters of the interaction between H18hp avidin-aptamer and its target

Parameter Name	Parameter Value	Standard Error
$\Delta H^\circ$ [kJ/mol]	-12	1.8
$\Delta S^\circ$ [J/(K*mol)]	110	5.9
$T\Delta S^\circ$ [kJ/mol]	34	1.8
<b><math>\Delta G^\circ</math> [kJ/mol]</b>	<b>-46</b>	<b>0.013</b>
$\Delta C_p^\circ$ [kJ/(K*mol)]	-4	0.35

Importantly, the value of  $\Delta G^\circ = -46 \text{ kJ M}^{-1} \pm 0.013$  for the H18hp avidin-aptamer obtained by these experiments has been compared with the antigen-antibody interaction that was characterized by BIAcore technology and the thermodynamical data was evaluated. The  $\Delta G^\circ$  value obtained in those studies was  $-49 \text{ kJ/mol}$  (53). This result suggests that H18hp –avidin aptamer has a similar thermodynamical behaviour as the antigen-antibody interaction. The analysis of the van't Hoff plot (Figure 13) shows a non-linear slope, suggesting that the enthalpy change  $\Delta H^\circ$  varies with the temperature. The heat capacity change  $\Delta C_p$  in our case has been reported with a value of  $(-4 \text{ kJ/(K mol)})$  which is in agreement with the non-linear behaviour of the van't Hoff plot.

. Single dissociation constants ( $K_D$ ) at each temperature were calculated by global fitting of five concentrations of avidin (10 to 50nM) over a constant density aptamer surface (Figure 14). A 1:1 Langmuire fitting was used for each temperature with  $\chi^2$  values below 5. A reliable data for  $K_D$  has been assumed by a  $\chi^2$  value less than 10 in literature.

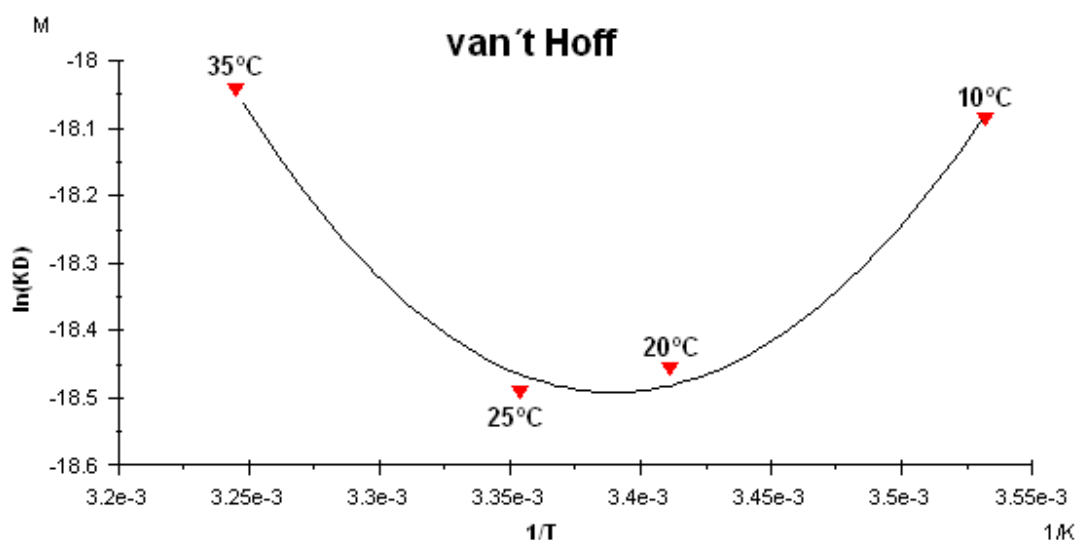


**Figure 13.** van't Hoff plot of H18hp avidin-aptamer at 10, 20, 25 and 35°C. The plot shows the effect of temperature in the enthalpy change  $\Delta H^\circ$  according to a non-linear behaviour.

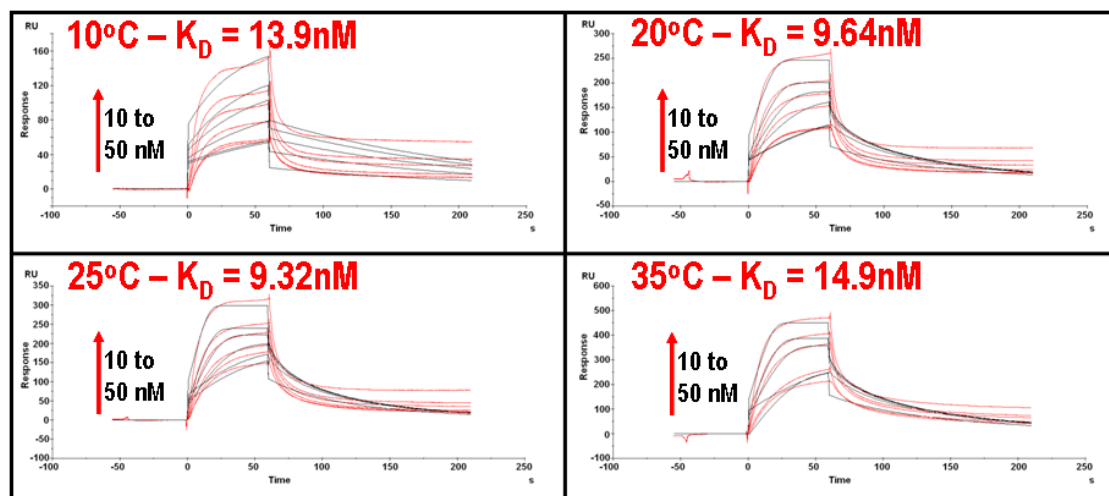


**Figure 14.** High-resolution kinetic analysis of the binding of avidin to H18hp avidin-aptamer surface using BIAcore T100. Red lines show biosensor data collected at 10, 20, 25 and 35°C. Five different concentrations (10 to 50 nM) were tested. Significant  $K_D$  values in the range of nM were reported using a Langmuir isotherm fitting model. (black lines).



### 3.7 Conclusions

In summary, the hybridization procedure has been evaluated as partitioning mechanism that can be incorporated into SELEX method. “Soluble-SELEX has been optimized and a complete SELEX round was performed and confirmed by gel electrophoresis (Figure 3). After 12 successful rounds of SELEX, the evolution against the original target (PSA) was evaluated with negative results. However, after the analysis of SELEX samples by ELISA, we found out that some leaking of avidin from the magnetic beads was present at all times in the SELEX process. After the evolution studies against avidin, the results have shown a significant evolution of the library to avidin. Cloning and sequencing were carried out successfully in order to complete the SELEX method. After the alignment, several consensus sequences have been found and the structures of 6 candidate aptamers have been predicted. Therefore, the synthesis of the sequences has been ordered. The binding studies performed by BIAcore have shown an important binding effect for some of the 6 avidin candidate-aptamers. H18hp-aptamer has revealed the best binding signal according to the preliminary screening results (binding interaction with the immobilized target). In addition, affinity studies were performed in order to obtain the  $K_D$  for H18hp-aptamer. A significant  $K_D$  value of 1.3 nM was recorded. Moreover, the  $K_D$  value was compared with the aptamers reported in the literature against avidin, Srisawat and Engelke ( $K_D = 70$  nM) and Tahiri and co-workers ( $K_D = 7$  nM). Here we concluded that “Soluble-SELEX” is a method that can raise aptamers with similar results as the standard SELEX technology. In order to avoid the SELEX selection against avidin as non-specific target, two strategies can be performed. a) To use magnetic beads with a different

immobilization system for the library such as NHS/EDC conjugation chemistry by coupling amino-labeled library to carboxylated magnetic beads or b) After the analysis of the “Soluble-SELEX” samples, it was realized that some steps in the previous procedure have to be carried out more carefully. For example, the leaking of avidin usually occurs when the magnetic beads with the complementary sequences are kept at 4°C (store conditions). In this case, several washing steps have to be performed in order to eliminate the avidin present in the solution by magnetic separation.

Collectively, the selectivity and robustness of the biosensor was reported. The selectivity results showed that H18hp avidin-aptamer has a high selectivity against avidin and insignificant recognition properties for BSA and PSA as non-specific targets. The H18hp avidin-aptamer biosensor based on surface plasmon resonance was performed in order to confirm the stability, reproducibility and reusable properties of the aptamer. Figure 12 shows the stability and the capability of the aptamer for regeneration. These results suggest the presence of one of the most interesting features of the aptamers versus antibodies, namely the regeneration and reusable capabilities.

On the other hand, kinetic and thermodynamic studies were performed. Thermodynamic parameters can be calculated by SPR technique using the van't Hoff equation (52), which correlated the kinetics ( $K_D$ ), temperature and free energy. In our case, the temperature dependence of the interaction between H18-avidin aptamer and avidin was evaluated. As a result, the determination of the binding free energy of -46 kJ/mol was reported. This thermodynamic value was calculated at temperature ranging from 10 to 35°C.

The kinetic data was obtained by five different concentrations of the target (10 to 50 nM) for each temperature analysis. The kinetic information is plotted as depicted in Figure 14,

where the values of  $K_D$  at 10°C (13.9 nM), 20°C (9.64 nM), 25°C (9.32 nM) and 35°C (14.9 nM) were reported. After the kinetic analysis, additional thermodynamic data, such as enthalpy  $\Delta H^\circ$  (-12 kJ/mol), entropy  $\Delta S^\circ$  (110 [J/ (K\*mol)]) and  $\Delta C_p^\circ$  (-4 [kJ/ (K\*mol)]) were obtained. In addition, van't Hoff plot shows a non-linear tendency which is correlated with the temperature dependence. The enthalpy  $\Delta H^\circ$  at 25°C shows the best free energy of binding, this value being in accordance with the selection conditions of the aptamers by SELEX. According with our previous free energy calculation for the hairpin structure (-15.19 kJ/mol), the binding free energy of H18-avidin aptamer is three times higher (-46 kJ/mol). The previous results suggest that only library members with a free energy higher than -15.19 kJ/mol were selected. In this case, the hairpin library design could be involved in this selecting process. However, future analyses have to be carried out in order to confirm this hypothesis.

On the other hand, the hairpin design and free energy calculation (-15.19kJ/mol) were based on the most recent and complete report of thermodynamic studies of L-argininamide aptamer (54), wherein, a binding free energy value of -21.3 kJ/mol was reported. The difference between these two binding free energy values could not be explained only by the hairpin structure function. The nature of the target can be an important factor for the thermodynamic analysis. In our case, the target is a protein with a molecular weight of 60.000 Daltons (Da) and L-argininamide has 246 Da as molecular weight. Herein, we hypothesized that more interaction points between aptamer and target (hydrogen binding, hydrophobic, electrostatic interaction etc) could produce a variation in the temperature dependence. In thermodynamic terms, we suggest that the enthalpy change  $\Delta H^\circ$  could vary according to the target molecule features (i.e. size). In this sense,

the binding free energy could be expected to be higher for avidin than L-argininamide. This hypothesis could be supported by the antibody thermodynamic information previously reported. Wherein, by SPR technique a value of -49 kJ/mol was reported for Hen Egg Lysozyme (HEL), a protein target with a molecular weight of 14.388 Da. However, the most interesting feature of the hairpin structure as inducer of conformational changes has to be evaluated by the construction of at least two different biosensor platforms with “on” and “off” mechanisms (see Chapter 4).

In conclusion, a new method termed “Soluble-SELEX” has been developed. However, a different setup has to be designed in order to avoid the non-specific selection. With some minor modifications, “Soluble-SELEX” could constitute an effective tool for raising aptamers. The method is not optimized but the principle of hybridization as partitioning mechanism in SELEX has been proven. The H18-avidin-aptamer developed by “Soluble-SELEX” method has shown a significant specificity ( $K_D = 1.3\text{nM}$ ) and selectivity. The robustness of the system evaluated by SRP and high levels of reproducibility and stability has been reported.

The thermodynamic analysis of the interaction between H18-avidin aptamer and avidin has revealed a high binding free energy (-46 kJ/mol). This high value is similar to an antigen-antibody interaction previously reported (-49 kJ/mol). In order to evaluate the effect of the hairpin structure as a mechanism for selecting high binding free energy library members, a complete SELEX process has to be carried out for a small target or a longer hairpin region for a big target.

### 3.8 Bibliography

1. C. Tuerk and L. Gold, *Science*, **1990**, 249, 505.
2. K. Marshall and A. Ellington., *Methods Enzymol.*, **2000**, 318, 193.
3. P. Kumar, K. Machida, P. Urvil, N. Kakiuchi, D. Vishnuvardhan, K. Shimotohno, K. Taira, N. Nishikawa, *Viol.*, **1997**, 237, 270.
4. R. Yamamoto, K. Murakami, K. Taira, P. Kumar., *Gene Ther. Mol. Bio.*, **1998**, 1, 451.
5. J. Cox and A. Ellington., *Bioorg. Med. Chem.*, **2001**, 9, 2525
6. S. Mendoza and M. Bowser., *Anal. Chem.*, **2004**, 76, 5387
7. T. Misono and P. Kumar, *Anal. Biochem.*, **2005**, 342, 312.
8. T. Pristoupil and M. Kramlova, *J. Chromatogr.*, **1968**, 32, 769
9. A. Ellington and J. Szostak, *Nature*, **1990**, 346, 818
10. M. Dobbelstein, T. Shenk, *J. Virol.*, **1995**, 69, 8027.
11. J. Ciesiolka, J. Gorski, M. Yarus, *RNA*, **1995**, 1, 538.
12. D. Smith, G. Kirschenheuter, J. Charlton, D. Guidot, J. Repine, *Chem Biol.* **2005**, 2, 741.
13. F. Zang and D. Anderson., *J. Biol. Chem.*, **1998**, 273, 2947.
14. S. Park, D. Myszkka, M. Yu, S. Litter, I. Laird-Offringa, *AMol. Cell. Biol.* **2000**, 20, 4765
15. M. Blank, T. Weinschenk, M. Premier, H. Schluesener, *J. Biol. Chem.* **2000**, 276, 16464.
16. A. Drabovich, M. Berezovski, V. Okhonin, and S. Krylov, *Anal. Chem.* **2006**, 78, (9) 3171
17. R. Stoltenburg, C. Reinemann, B. Strehlitz, *Biomolecular Engineering*, **2007**, 24, 381
18. S. Gopinath, *Arch. Virol.*, **2007**, 152: 2137
19. L. Gold, B. Polisky, O. Uhlenbeck, and M. Yarus. *Annu. Rev. Biochem.* **1995**, 64, 763
20. S.E. Osborne and A.D. Ellington. *Chem. Rev.* **1997**, 97, 349
21. D.S. Wilson and J.W. Szostak. *Rev. Biochem.* **1999**, 68, 611
22. H. Ueyama, M. Takagi and S. Takenaka. *J. Am. Chem. Soc.*, **2002**, 124, 14286
23. C. Song, Y. Xia, M. Zho, X. Liu, F. Li, Y. Boda, H. Yin. *J Mol Model.* **2006**, 12, 249
24. A. Radi and C. O'Sullivan. *Chem. Commun.*, **2006**, 32, 3432
25. S. Gopinath. *Anal Bioanal Chem* **2007**, **38**(7), 171
26. M. Berezovski, M. Musheev, A. Drabovich, J. Jitkova, S. Krylov. *Nature Protocols*, **2006**, 1, 1359.
27. R. Mosing, S. Mendonsa, M. Bowser. *Anal. Chem.*, **2005**, 77 (19), 6107.
28. James W.. Aptamers. *Encyclopedia of Analytical Chemistry* **2000**, 4848
29. S. Shamah, J. Healy, S. Cload. *Acc. Chem. Res.*, **2008**, 41 (1), 130
30. J. Chapman, C. Beckey. *Ann. Pharmacother.* **2006**, 40, 1322.
31. Ng, E. W. D. Shima, P. Calias, E. Cunningham, D. Guyer, A. Adamis. *Nat. Rev. Drug Discovery* **2006**, 5, 123.
32. T. Fitzwater, and B. Polisky, *Methods Enzymol.* 1996, **267**, 275.
33. M. Naimuddin K. Kitamura, Y. Kinoshita, Y. Honda-Takahashi, K. Nishigaki. *J. Mol. Recognit.* **2007**, 20, 58
34. R. Conrad S. Baskerville, A. Ellington. *Mol. Div.* **1995**, 1, 69
35. R. Nutiu and Y. Li. *Angew. Chem. Int. Ed.* **2005**, 44, 1061
36. Z. Tang, P. Mallikaratchy, R. Yang, Y. Kim, Z. Zhu, H. Wang, W. Tan. *JACS.* **2008**, 130(34), 11268
37. Wiegand TW, Williams BP, Dreskin SC, Jouvin M, Kinet J Tasset D. *J Immunol.* **1996**, 157,221
38. Kubik MF, Stephens AW, Schneider D, Marlar R, Tasset D. *Nucleic Acids Res* **1994**, 22, 2619
39. Stoltenburg R, Reinemann C, Strehlitz B. *Anal Bioanal Chem* **2005**, 383,83
40. Ciesiolka, J., Gorski, J., Yarus, M., *RNA*. **1995**, 1, 538
41. Huizenga, D.E., Szostak, J.W., *Biochem.* **1995**, 34, 656
42. Lorsch, J.R., Szostak, J.W. *Biochem.* **1994**, 33, 973
43. S. Gopinath, T. Misono, K. Kawasaki, T. Mizuno, M. Imai, T. Odagiri, P. Kumar. *J Gen Virol.* **2006**, 87, 479
44. M. Lochrie, S. Waugh, D. Pratt, J. Clever, G. Parslow, B. Polisky. *Nucleic Acids Res* **1997**, 25, 2902
45. S. Goodman, N. Veltm, Q. Gao, S. Robinson, A. Segall. *J Bacteriol.* **1999**, 181, 3246
46. F. Zhang, D. Anderson. *J Biol Chem* **1998**, 273, 2947
47. J. Wang, R. Lv, J. Xu, D. Xu, H. Chen. *Anal Bioanal Chem.* **2008**, 390, 1059
48. X. Yang, X. Li, T. Prow, L. Reece, S. Bassett, B. Luxon, N. Herzog, J. Aronson, R. Shope, J. Leary, D. Gonstein. *Nucleic Acids Res* **2003** 31, e54
49. R. Mosing, S. Mendonsa, M. Bowser. *Anal Chem.* **2005**, 77, 6107
50. S. Mendonsa and M. Bowser *JACS.* **2004**, 126 (1), 20
51. Y. Day, C. Baird, R. Rich, D. Myszkka. *Protein Sci.* **2002**, 11, 1017
52. T. Wiseman, S. Williston, J. Brandts, L. Lin. *Anal. Biochem.* **1989**, 179, 131
53. G. Zeder-Lutz, E. Zuber, J. Witz, M Van Regenmortel. *Anal. Biochem.* **1997**, **246** (1), 123
54. G. Bishop, J. Ren, B. Polander, B. Jeanfreau, J. Trent, J. Chaires, *Biophys. Chem.* **2007**, 126, 165

# *CHAPTER 4*

## **H18-avidin aptamer based biosensors**

### **4.1 Abstract**

One important step in developing a biosensing system that exploits aptamers as biorecognition elements is to establish effective methods capable of transducing a binding event into an easily recordable signal. Strategies have been developed for transducing aptamer–target interactions into fluorescence, electrochemical, mechanical, piezoelectric, or surface plasmon resonance signals. Within these methods, fluorescence signaling is very desirable because of the convenience of detection, the diversity of measurement methods, and the availability of a large selection of fluorophores and quenchers for nucleic acid modification (25). Herein, we exploited the incorporation of H18hp avidin-aptamer to a fluorescent platform. H18hp avidin-aptamer has been modified with a fluorophore (FAM at 5' end) and a quencher (BHQ at 3' end). The titration results showed a “turn off” biosensor mechanism with a relevant specific signal of 91.2% corresponding to avidin and a lower value of 23.9% as non-specific signal against BSA. In order to complete the H18hp avidin-aptamer, electrochemical

transduction was performed as well. The electrochemical H18hp-avidin aptamer-based biosensor for rapid and label-free detection of avidin was developed. The 5'-thiol-functionalized end of the H18hp avidin-aptamer sequence was immobilized on a gold electrode, and the 3'-ferrocene (Fc)-functionalized end as the redox reporter group. Upon binding of avidin, the aptamer switches conformation from an open unfolded state to a closed conformation, resulting in a well-defined “turn on mechanism” that increased electron-transfer efficiency between Fc and the gold surface electrode. The electrochemical response, which was measured by square wave voltammetry, reaches saturation within 300 nM avidin; a specific signal of 337 nanoamperes (nA) was recorded. In contrast, BSA as non-specific signal at the same concentration has reported only 76 nA, these results suggesting the high affinity and selectivity of H18hp avidin aptamer. In conclusion, a H18-aptamer-based biosensor for the detection of avidin was developed using two different transduction methods such as fluorescence, and electrochemistry. In both platforms, the biosensing procedure was successful. The intrinsic transduction mechanism present in H18-aptamer, observed by the “turn off” and “turn on” mechanism for fluorescence and electrochemistry platform respectively, suggests that the hairpin structure can be an important element to induce conformational changes in aptamers.

## 4.2 Introduction

*“Aptamers are artificial nucleic acid ligands that can be generated against amino acids, drugs, proteins, and other molecules. They are isolated from complex libraries of synthetic nucleic acid by an iterative process of adsorption, recovery and reamplification. They have potential applications in analytical devices, including biosensors, and as therapeutic agents”.* **Willian James.**

Aptamers are synthetic nucleic acids that bind different kind of targets (1) such as inorganic compounds, small organic molecules, nucleotides and derivates, cofactors, amino acids, carbohydrates, antibiotics, peptides and proteins, complex structures and other molecules (2). The range in size from approximately 6 to 40 kDa and secondary (3) and tertiary (4) structures have been reported. The natural composition of aptamers includes RNA and single-stranded DNA molecules. However, sequences with non-natural nucleotides or combination of nucleic acids have been exploited. Aptamers are selected by SELEX method (See chapter 3). “Aptamer” is derived from the latin word “aptus” (meaning “to fit”) (5) and the Greek suffix “mer” which means particle (6). Aptamers bind to their targets with  $K_D$  typically in the low nanomolar range and can distinguish enantiomers of small molecules or minor sequence variants of macromolecules with frequently several orders of magnitude  $K_D$  ratio (1). In addition, aptamers have the capacity to distinguish target molecules from minimal structural differences, such as the existence of a methyl or hydroxyl group in the target molecule (7). In most medical applications, high affinity and specific molecular recognition are achieved by antibodies, but there are some limitations, especially in their production, which requires animal or cell lines (8). In contrast with antibodies, *in vitro* selected



aptamers are reproducibly synthesized by conventional methods in short time and easily modified using chemical methods to improve their stability or addition of reporter groups to increase their applicability. Aptamers have been widely used in different research areas and they are involved in applications based on biorecognition events, including diagnostic (9), therapeutics (10) and biosensing (11).

Aptamers are a new class of biorecognition elements that can be an alternative to antibodies. For comparison, Table 1 summarizes the advantages and disadvantages of aptamers versus antibodies.

**Table1.** Comparison between antibodies and aptamers.

<b>Antibodies</b>	<b>Aptamers</b>
Limitations against target representing constituents of the body and toxic substances	Toxins as well as molecules that do not elicit good immune response can be used to generate high affinity aptamers
Kinetic parameters of Ab-Ag interactions can not be changed on demand	Kinetic parameters such as on/off rates can be changed on demand
Antibodies have limited shelf life and are sensitive to temperature and may undergo denaturation	Denatured aptamers can be regenerated within minutes, aptamers are stable to long term storage and can be transported at ambient temperature
Identification of antibodies that recognize targets under conditions other than physiological is not feasible	Selection conditions can be manipulated to obtain aptamers with properties desirable for in vitro assay e.g. non-physiological buffer/T
Antibodies often suffer from batch to batch variation	Aptamers are produced by chemical synthesis resulting in little or no batch to batch variation
Requires the use of animals	Aptamers are identified through an <i>in vitro</i> process not requiring animals
Labeling of antibodies can cause loss in affinity	Reporter molecules can be attached to aptamers at precise locations not involved in binding

The comparison in Table 1 suggests that aptamers have superior features, according with their binding capability to the target molecules, with relatively high affinity and

specificity, are generally small, easy to produce (not animal or cells) and modified. In addition, the reproducibility between different batches and their reusable activity classifies aptamers as an important option for generic biosensor development.

#### **4.1.1 Biosensing**

Certain applications demand analyte detection within a real time evaluation or at least very fast time period. To achieve rapid detection, sensors based on molecular recognition and that are coupled to transducers have been developed. For biosensing, aptamers offer an interesting alternative as biorecognition elements, with a multitude of advantages over the common molecules used for the recognition event, such as antibodies and enzymes (12). One of the common limitations of immunosensors is their poor capacity to regenerate the antibody surface. In contrast, several advantages are apparent in aptamer-based sensors. The ability to regenerate the immobilized aptamer surface would be their most attractive advantage (9). In this sense, reusable and reproducible sensors can be developed, because as nucleic acids, aptamers could be subjected to repeated cycles of denaturation and renaturation. Moreover, aptamers can be modified with a wide range of reporter groups and incorporated in different kinds of detection methods (6). Potyrailo et al (13) designed a biosensor that offered a one-step direct detection of the analyte. A DNA aptamer, specific for human thrombin, was used to detect the binding of the target protein by evanescent wave-induced fluorescence anisotropy. The aptamer was labeled at the 5' end with fluorescein and its 3' end was modified with an alkyl amine linked to a glass surface. The assay was completed in 10 min, and 5 nM of protein could be detected in an addressed volume of 5 nL. Lee and Walt (14) detected thrombin by displacement of

fluoresceinated thrombin from DNA aptamers linked to silica microspheres in a fiber-optic biosensor system. The aptamer beads selectively bound to the target, and could be reused with no sensitivity change. Moreover, aptamers without modifications could be useful for analytical methods such as surface plasmon resonance (SPR). This interesting alternative has been exploited by BIAcore system and several target molecules have been reported (15-17). An interesting area for aptamers constitutes the sensors based on electrochemical detection (18, 19). As polyanionic compounds, aptamers are an attractive biorecognition element for sensing the changes in conductance in the presence or absence of the target molecule binding. Electrochemical biosensing based on aptamers offers a great potential in the area of molecular sensing (6).

A recent class of fluorogenic probes termed “molecular beacons” has been introduced for the homogeneous detection of nucleic acid sequences. Molecular beacons are simple hairpin-loop probes, in which a fluorophore is linked to the 5' or 3' end of an aptamer and a quencher to another end (9). The nucleic acid sequence in the loop of the molecular beacon is designed to be complementary to the target of interest. When ligands bind, the conformational changes of the aptamer removes the quencher from the fluorophore, resulting in an easily detected signal (20). In summary, biosensors are dependent on the power of a molecular recognition element. Therefore, it seems logical to explore the use of aptamers as recognition molecule. In other words, the emerging capabilities of aptamers offer a great opportunity to be classified as the most interesting biorecognition element for diagnosis, therapy and, in the future, for biosensing.

## **4.3 Experimental Methods**

### **4.3.1 Fluorescence experiment:**

#### **4.3.1.1 Synthesis of the oligonucleotide:**

The synthesis of the H18-hp 5'- CCA ACC GCA ATT GTA GTT GAC TCA ACA TAG TAC CGG ACT CGG CTA ATA GAC CTG GGG TTG G-3' – (61n), labeled at 5' end with FAM (fluorophore) and 3' end with black hole quencher (BHQ) was performed by VBC Biotech services (Austria).

#### **4.3.1.2 Reagents:**

Avidin, bovine serum albumin (BSA), TBS-T (1 L deionized water, 0.05 M Tris, 0.138 M NaCl, 0.0027 M KCl, pH 8.0, 25°C, 0.05% Tween 20), potassium chloride and sodium chloride were obtained from Sigma-Aldrich.

#### **4.3.1.3 Measurement of fluorescence spectra:**

Fluorescence spectra were measured on a Cary Eclipse Fluorescence spectrophotometer equipped with a programmable temperature control unit. The following parameters were set up for all the measurements: excitation 480nm, emission 520nm and a scanning range from 450 to 600nm.

### **4.3.2 Electrochemical experiments:**

#### **4.3.2.1 Synthesis of the oligonucleotide:**

The synthesis of the H18-hp 5'- CCA ACC GCA ATT GTA GTT GAC TCA ACA TAG TAC CGG ACT CGG CTA ATA GAC CTG GGG TTG G-3' – (61n), labeled at 5' end

with thiol group (SH) and 3' end with a ferrocene (electrochemical reporter group) was performed by BIOSYNTHESIS company (United States).

#### **4.3.2.2 Reagents:**

Gold electrode CHI101 (2 mm diameter) from CH Instruments, Inc, potassium phosphate ( $\text{KPO}_4$ ) at pH 3.4, avidin, BSA, PSA, TBS-T buffer were obtained from Sigma – Aldrich.

#### **4.3.2.3 Modification of gold electrode:**

The gold electrode surface was cleaned by exposing it to warm piranha solution for 20 minutes. Then, the electrodes surface was prepared by mechanical polishing and electrochemical cleaning with sulfuric acid. The aptamers immobilization was carried out by 100  $\mu\text{L}$  of 2  $\mu\text{M}$  of H18hp modified avidin-aptamer (5' Thiol and 3' Ferrocene) in 1 M  $\text{KPO}_4$  buffer solution at pH 3.4. The gold electrode surface was incubated in the aptamers solution overnight at room temperature. The unmodified spaces in the electrode were blocked with 2-mercaptoethanol using 50  $\mu\text{L}$  of 0.1 M solution in  $\text{KPO}_4$  buffer for 20 minutes. All electrochemical measurements were performed in TBS-t buffer.

#### **4.3.3.4 Electrochemical measurement:**

Electrochemical experiments using a three-electrode configuration in a one-compartment cell were conducted using a potentiostat/galvanostat PGSTAT 12 Autolab (Ecochemie – Netherlands). The electrochemical measurements were performed using an Ag/AgCl reference electrode and a platinum-counter electrode. The electrochemical cell was filled with 2 mL TBS-t buffer and several additions of avidin and BSA were injected. After

each injection (avidin- BSA), the solution was shacked by magnetic stirring. Square wave voltammetry (SWV) was registered in the potential interval  $-0.1 - 0.4$  V, under the following conditions: potential increment, 1 mV; potential amplitude, 20 mV; pulse frequency, 25 Hz was optimized in relation with the peak definition.

## **4.4 Results and discussion**

### **4.4.1 Aptamer characterization**

The first aptamer characterization was performed by determination of the the  $K_D$  for H18-avidin aptamer with a significant value of 1.3 nM (chapter 3, Figure 10). Additionally, the selectivity of the sensor was studied by SPR as well. After the addition of two non-specific proteins (BSA and PSA) the plasmon resonance was recorded for each case (chapter 3, Figure 11). The signal recorded after the addition of non-specific targets was insignificant. In contrast, in the presence of the specific-target, the results showed an important binding effect between aptamer and the target. These results suggest the high selectivity of H18-aptamer on BIAcore platform. In order to complete the H18hp avidin-aptamer characterization, two different studies have been performed: fluorescence and electrochemistry.

#### **4.4.1.1 Fluorescence**

The H18-aptamer has been selected for the fluorescence studies. By attaching a fluorophore (5'FAM) and a quencher (3'Black Hole) to H18hp avidin-aptamer with high affinity for a target protein, we have combined the high sensitivity given by the fluorescence signals with the specificity of binding of the DNA aptamer to the target protein. We examined the effect of the salt, target, buffer and water on the modified aptamer. Figure 1 shows the signal of fluorescence-quenching assay for each detection case.

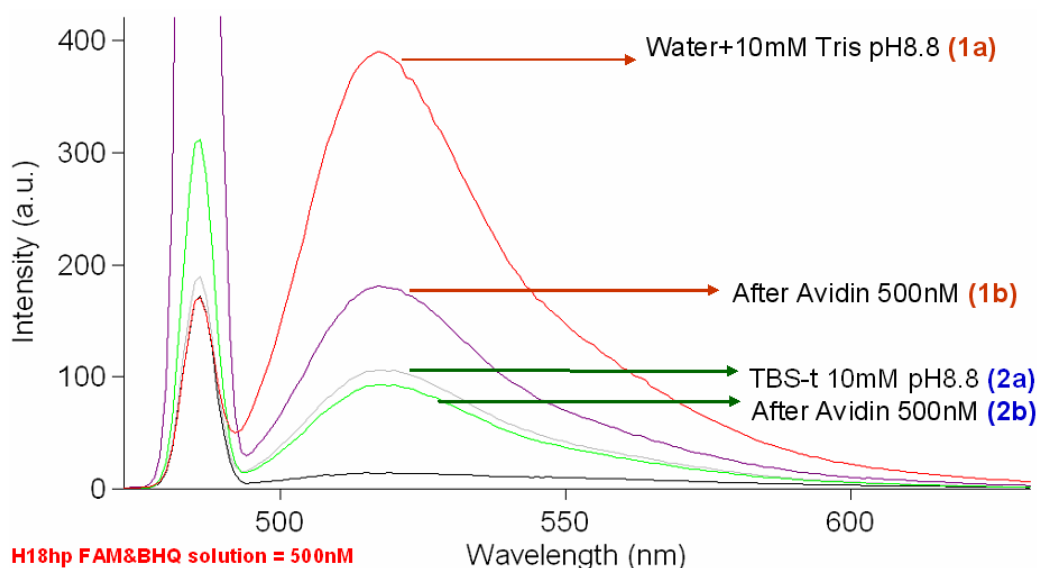


**Figure 1.** Optimization of the H18hp avidin-aptamer (500 nM solution) fluorescence signal at two different conditions: avidin effect in water-Tris solution, before (1a) and after (1b) avidin addition; and avidin effect in TBS-t buffer solution, before (2a) and after (2b) avidin.

Water (10 mM Tris at pH 8.8) and TBS-t (0.05 M Tris, 0.138 M NaCl, 0.0027 M KCl, pH 8.0, 25°C, 0.05% Tween 20) were tested to select the optimal conditions for the H18-avidin-aptamer characterization. All measurements were carried out with 500 nM of aptamer concentration. After the addition of the target (500 nM – avidin), both signals were recorded. In water (Tris 10 mM, pH 8.8), a significant change of 50.9% (quenching) in the fluorescence signal was observed. For TBS-T buffer solution, the change after target addition was only of 12.8% (quenching). These preliminary fluorescence studies showed that water (Tris pH 8.8) gives the best signal using H18-aptamer. Therefore, the system has been characterized as a “turn off” mechanism (signal decreasing in the presence of target). Several dilutions of the buffer (TBS-T) were carried out (1/2, 1/4, 1/8 and 1/16) and the H18-aptamer concentration for all solutions was 500 nM (Figure 2).



The results have revealed that the 1/8 dilution shows an insignificant change compared to the 1/16 dilution. According to previous data, if salt is a requirement to perform an experiment, the 1/8 dilution of TBS-T will be used. This could be the case for the electrochemical experiments where the salt works as supporting electrolyte.

### H18hp F&Q solution = 500nM

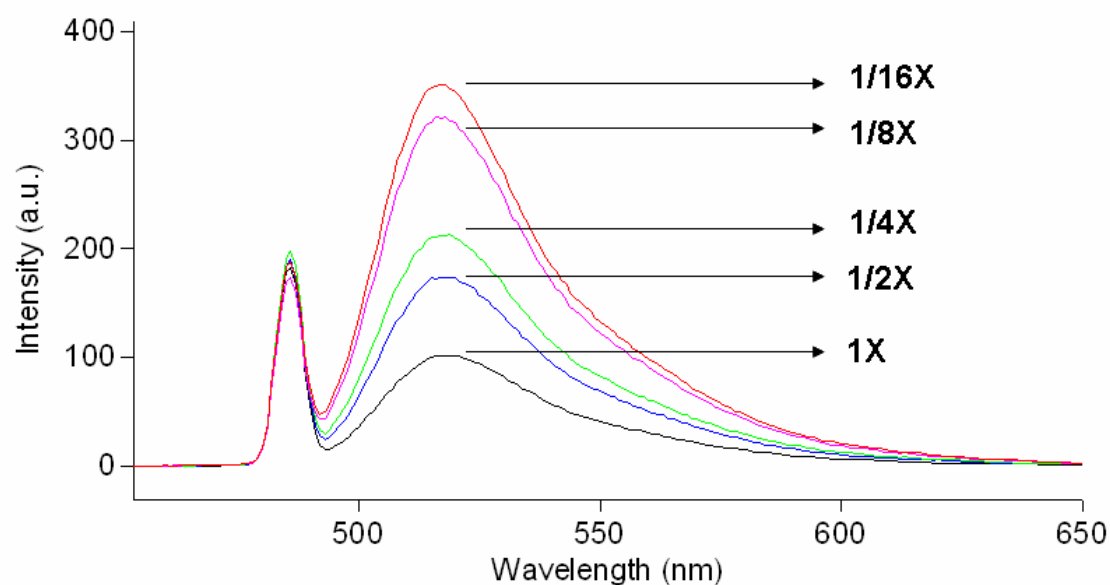


**Figure 2.** Evaluation of buffer TBS-T dilution in the fluorescence-quenching signal. Fluorescence signal for several dilutions of TBS-t. Conditions as described in the text.

H18hp avidin-aptamer titration studies were performed in order to understand the target-dependent system. Fluorescence titration data using the signal of fluorescence-quenching shows significant variations for avidin concentration (Figure 3). The fluorescence quenching technique shows high sensitivity, allowing for small variations in the avidin concentration to be detected.

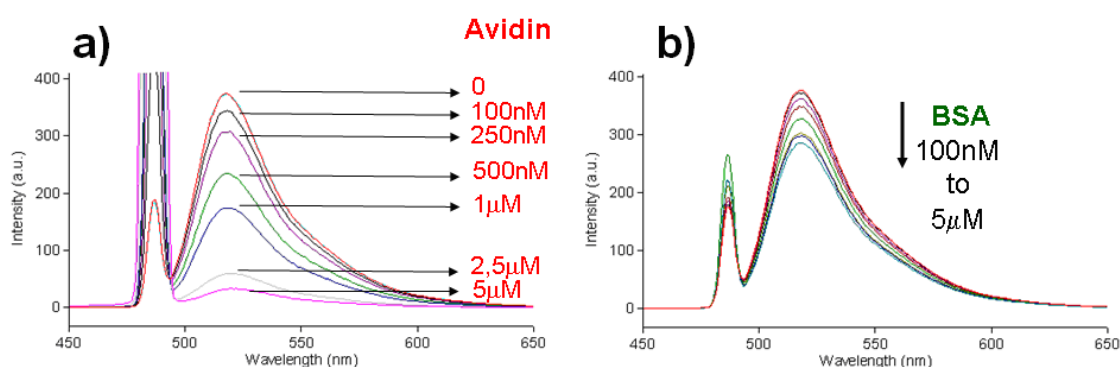


**Figure 3.** Avidin-dependent changes in fluorescence-quenching of H18-aptamer. a) Titration signal of BSA as non-specific target (23.9%). b) Titration of avidin with an important change of fluorescence-quenching of 91.2%.

The above titration curves show progressive decrease of fluorescence as a function of avidin concentrations. In addition, the same experiment was performed for BSA, which works as non-specific target. The titration was performed in a range from 100 to 5000 nM. The results show a specific quenching signal of 91.2% for avidin (Figure 3A) and 23.9% of quenching for BSA as non-specific target (Figure 3B). In addition, the detection limit of the fluorescent biosensor was calculated (320 nM). Previous results confirm the selectivity of H18-avidin aptamer according with BIAcore experiments (chapter 3, Figure 9). The increase of the non-specific fluorescence signal could be due to the salt concentration of both avidin and BSA solutions. However, figure 3 reveals a significant difference between specific and non-specific target. For a more detailed analysis of the effect of salt in H18-aptamer, additional experiments were carried out.

Evaluation of salt effect: the main conformational changes of the oligonucleotides depend on the sequence, ionic environment and hydrophilic conditions (22). Several ions play an important role for the study of allosteric changes in aptamer structure.  $K^+$  ion has been

reported as inducer of G-quadruplex structure (21, 23) and could be used as a preliminary tool for recognizing a G-quadruplex structure in aptamer sequences. Herein, the effect of potassium chloride (KCl) that works as structural G-quadruplex inducer and sodium chloride (NaCl), which can induce allosteric changes at high concentrations, were studied by the fluorescence-quenching of H18-aptamer. Figure 4 shows two important aspects in the characterization of H18-aptamer: A) the effect of KCl is relevant at low concentrations (0.05 to 10 mM) in comparison with NaCl that only produce significant conformational changes at high concentrations. These results suggest the existence of a G-quadruplex structure involved in the aptamer sequence. However, additional experiments, such as nuclear magnetic resonance (NMR), have to be performed in order to confirm the structure of the aptamer. B) Similar quenching effect at high concentrations for both ions was observed (50 to 500 mM) which means that at high salt concentrations the effect of specific ions cannot be observed. In addition, these allosteric changes induced by the increase of ionic strength may explain the increase of the non-specific signal for BSA (Figure 3b) observed for the fluorescence measurements.

#### **4.4.1.2 Electrochemistry**

Herein, we report an electrochemical detection method based on ferrocene-modified aptamer (5'end Thiol and 3'end ferrocene). This approach has revealed that using ferrocene it is possible to detect avidin with high affinity and selectivity. The interaction between the ferrocene-modified aptamer against avidin and BSA has been studied by square wave voltammetry (SWV) technique. This technique has been found to be useful for studies of conformational changes of biomolecules adsorbed to a solid surface (25).

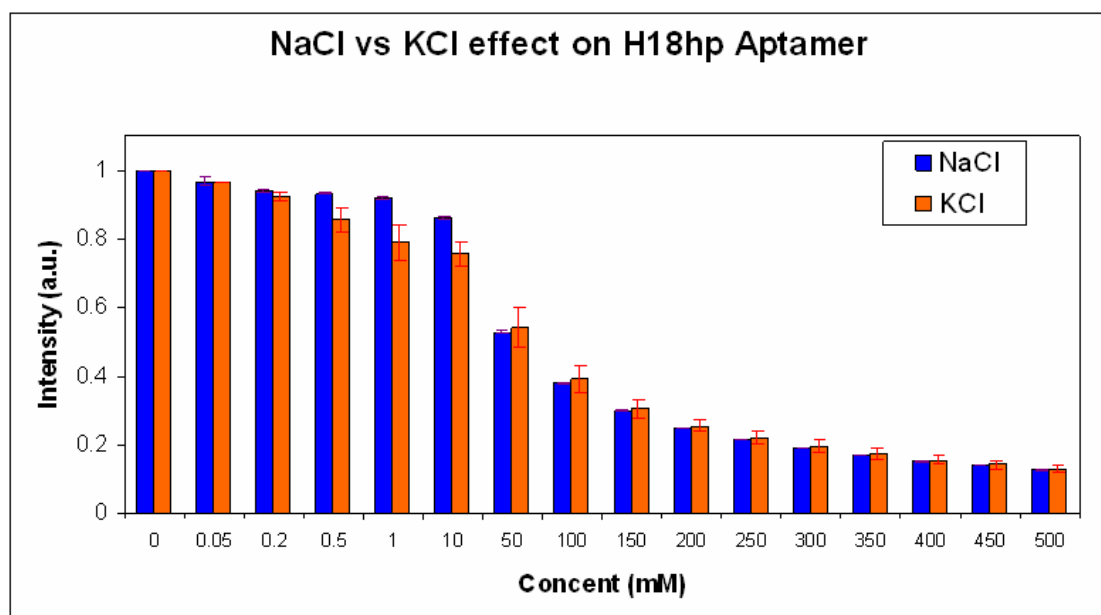


**Figure 4.** Effect of KCl and NaCl on H18 avidin-aptamer. A titration from 0.05 to 500 mM of salt concentration was performed. Conditions as described in the text.

When the ferrocene-aptamer is immobilized on the gold surface, the current response of the Faradic electrochemical signal should depend on the distance of the ferrocene from the surface, while the peak potential should be directly correlated to the ferrocene oxidation potential. The ferrocene-aptamer has been exposed to several additions of avidin and BSA. As result, an anodic peak was observed corresponding to the oxidation of ferrocene on the electrode surface. In the presence of avidin, a proportional correlation between concentration and current was observed as specific signal (Figure 5a) with a detection limit value of 21nM.

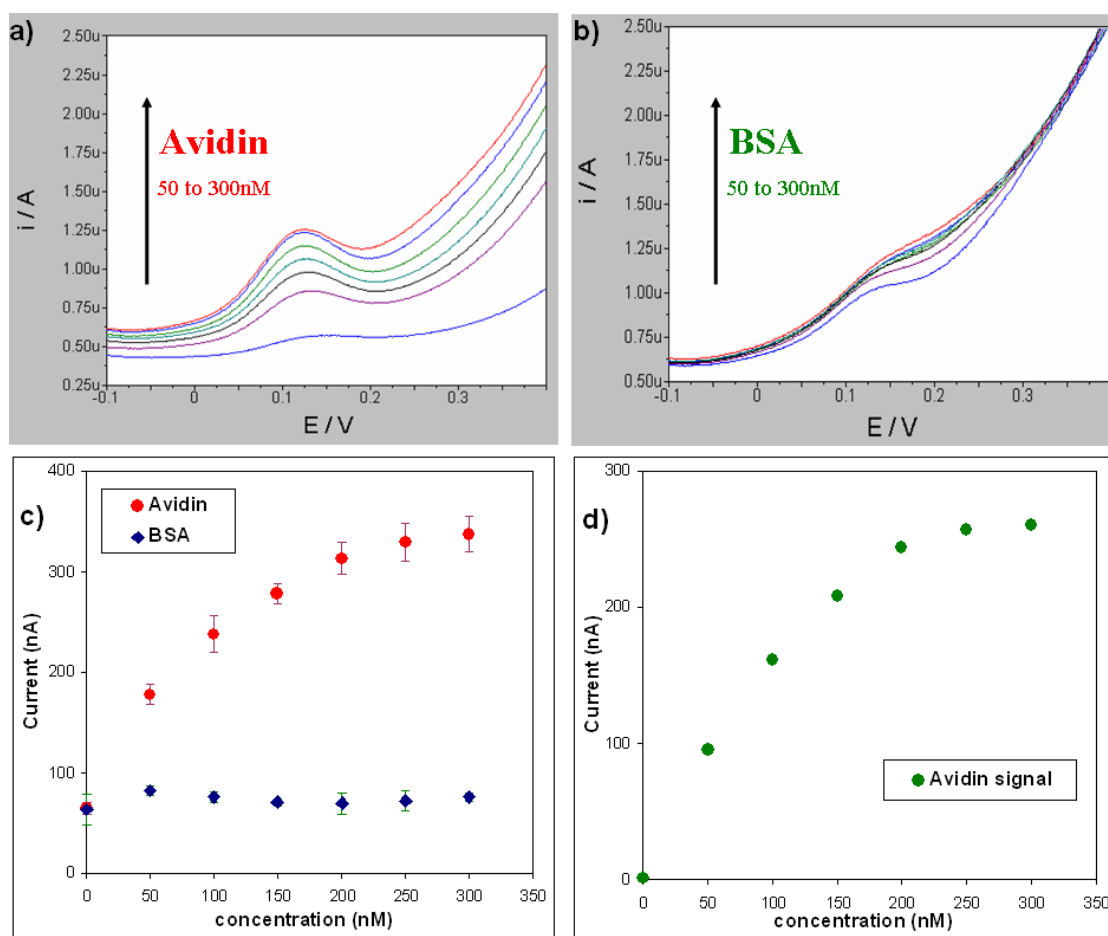


**Figure 5.** Ferrocene-apptamer characterization by SWV. a) Avidin titration from 50 to 300 nM concentration as the specific signal. B) BSA titration in the same conditions as for avidin. BSA represents the negative control. C) Plot of the triplicate measurements for avidin and BSA addition. D) Plot of the subtraction of the non-specific signal (BSA) from avidin. Conditions as described in the text.

According to the previous results, a “turn-on” mechanism has been revealed on this electrochemical platform. In contrast, after the addition of BSA, an insignificant signal was recorded as non-specific signal (Figure 5b). The results obtained are in agreement with the literature, where the same strategy was performed for the electrochemical characterization of thrombin aptamer (24).

## 4.5 Conclusion

In summary, two biosensors based on H18hp avidin-aptamer have been developed successfully by two different transduction mechanisms such as fluorescence, and electrochemistry.

The fluorescence biosensor was optimized and the best measurement conditions were selected (water + 10 mM Tris at pH 8.8). After the addition of target molecule, a quenching effect was observed, this approach working as a “turn-off” mechanism for the fluorescence biosensor. Then, the titrations against avidin as specific target molecule and BSA as non-specific target were carried out. It was found that the 91.2% of the signal corresponds to specific signal and the 23.9% was correlated with non-specific signal (Figure 3). In addition, the salt effect for H18hp avidin-aptamer by  $K^+$  and  $Na^+$  ions was evaluated. The  $K^+$  ion has the capability to interact as G-quadruplex inducer, in contrast with  $Na^+$  that can only induce allosteric changes at high concentrations. After the characterization of these two ions by H18hp avidin-aptamer based on fluorescence, it can be suggested that the effect of the  $K^+$  has shown a significant effect at low concentrations (0.05 to 10 mM) compared to  $Na^+$  ion that only induced significant conformational changes at high concentrations. These results suggest the existence of a G-quadruplex structure involved in the H18hp avidin-aptamer sequence. However, additional structural experiments by NMR or crystallography have to be carried out in order to confirm the presence of a G-quadruplex structure in the aptamer sequence.

The H18hp avidin-aptamer biosensor based on electrochemistry has been evaluated and successful information has been recorded. After the addition of avidin, a proportional

increment of current in correlation with concentration was observed as specific signal. The previous results suggest a “turn-on” mechanism for the electrochemical biosensor. The titration experiments for avidin (specific signal) and BSA (non-specific) have shown a relevant difference between specific and non-specific molecules (Figure 5). In the case of avidin, after the addition of 300 nM concentration, 337 nA (nanoamperes) were recorded. In contrast, after the addition of BSA at the same concentration, 76 nA were obtained (close to the base line). According with this result, 22.5% of non-specific signal was observed. Similar results have been reported by fluorescence biosensor as well.

H18hp avidin-aptamer has been characterized by two different platforms: fluorescence and electrochemistry. Relevant information such as quenching, current density, detection limits have been reported. The successful strategy in the design and development of both biosensors confirms the properties of the H18-avidin aptamer conformational changes. These results suggest that the hairpin structure becomes an attractive element to induce conformational changes in aptamer.

In conclusion, studies of the conformational changes were performed to understand their behaviour in biosensing. Moreover, the designs of the hairpin structure suggest an significant inducer system for conformational changes in aptamers. These allosteric changes can be useful as intrinsic transduction mechanism for generic biosensor development. On the other hand, the aptamer properties, such as *in vitro* biorecognition of a wide range of targets and easy production convert this biomolecule in the most promising and attractive element for generic biosensing.

## 4.6 Bibliography

1. James W.. Aptamers. *Encyclopedia of Analytical Chemistry* **2000**, 4848
2. R. Stoltenburg, C. Reinemann, B. Strehlitz. *Biomol. Eng.* **2007**, 24, 381.
3. M. Bozza, R. Sheardy, E. Dilone, S. Scypinski, M. Galazka. *Biochem.* **2006**, 45, 24, 7639.
4. K. Wang, SH. Krawczyk, N. Bischofberger, S. Swaninathan, P. Bolton. *Biochem.* **1993**, 32 (42), 11285.
5. A. Ellington and J. Szostak, *Nature*, **1990**, 346, 818
6. S. Jayasena. *Clin. Chem.* **1999**, 45, 1628
7. J. Kawakami, Y. Yokota and N. Sugimoto. *J. Inorg. Biochem.* **2001**, 82, 197
8. KM.You, SH Lee, A. Im, and SB. Lee. *Biotechnol. Bioprocess Eng.* **2003**, 8, 2:64
9. S. Tombelli, M. Minunni, M. Mascini. *Biomol. Eng.* **2007**, 24 (2), 191
10. Ng, Eugene, D. Shima, P. Calias, E. Cunningham, Jr, D.Guyer, *Nature Reviews Drug Discovery.* **2006**, 5, 123
11. C. O'sullivan. *Anal Bioanal Chem.* **2002**, 372, 44
12. D. Sussman, J. Nix, C. Wilson. *Nat. Struct. Biol.* **2000**, 7, 53
13. R. Potyrailo, R. Conrad, A. Ellington, G. Hieftje. *Anal. Chem.* **1998**, 70, 3419
14. M. Lee and D. Walt. *Anal. Biochem.* **2000**, 282, 142
15. P. Mitchell. *Nat Biotechnol.* **2002**, 20 (3), 225
16. A. Dey, M.Khati, M. Tang, R. Wyatt, S. Lea, W. James. *J Virol.* **2005**, 79 (21), 13806
17. S. Miyakawa, A. Oguro, T. Ohtsu, H. Imataka, N. Sonenberg, Y. Nakamura *RNA.* **2006**, 12, 1825
18. A. Radi, J. Acero, E. Baldrich, C. O'Sullivan, *JACS*, **2006**, 128 (1), 117
19. M.Rodriguez, A. Kawde, J. Wang. *Chem. Commun.*, **2005**, 4267
20. R. Yamamoto and P.K. Kumar. *Genes cells.* **2000**, 5, 389
21. H. Ueyama, M. Takagi and S. Takenaka. *JACS.* **2002**, 124, 14286
22. C. Song, Y. Xia, M. Zho, X. Liu, F. Li, Y. Boda, H. Yin. *J Mol Model.* **2006**, 12, 249
23. A. Radi and C. O'Sullivan. *Chem. Commun.* **2006**, 3432
24. J.J. O'Dea, J.G. Osteryoung. *Anal. Chem.* **1997**, 69, 650
25. J. R. Lakowicz. *Principles of Fluorescence Spectroscopy*, 2nd ed. **1999**, Kluwer Academic/Plenum



# *CHAPTER 5*

## **Overall conclusions and future perspectives**

The main objective of this study was to evaluate the conformational changes as intrinsic transduction mechanism and aptamers as biorecognition molecules for generic biosensor development. Diverse transduction platforms have been used in order to exploit the binding and unbinding of target-ligands by the biorecognition molecules in a biosensor setup. Well-defined structural allosteric changes between two stable conformations (open and closed) of such constructs can serve as a viable signal transduction mechanism for generic biosensing, which should be facilitated by rational design to improve the affinity, selectivity, reproducibility and stability of these sensor devices.

This work contains two parts: (i) Maltose-binding protein based biosensor and (ii) SELEX and aptamer based biosensors.

The first part of this thesis was focused on the translation of a fluorescence biosensor into an electrochemical biosensor using maltose-binding protein as biorecognition element. As a result, conformational changes feature was selected as intrinsic transduction mechanism for the design and construction of generic biosensing approaches. Moreover, a maltose-biosensor with acceptable affinity and selectivity has been reported.

On the other hand, a new SELEX method termed “Soluble-SELEX” has been developed. However, future improvements are required in order to optimize this method. The important aspect however, is that the principle of the hybridization as partitioning mechanism for SELEX has been proven. In addition, as result of “Soluble-SELEX”, a new avidin-aptamer has been selected and three different transduction mechanisms were employed to construct surface plasmon resonance (SPR) fluorescence, and electrochemical biosensors. In all cases, successful signals were recorded with high affinity and selectivity. Moreover, the fluorescence and electrochemical biosensors have reported a significant detection limit values of 320 and 21 nM, respectively and significant thermodynamic information was obtained using SPR technique.

As final conclusion, this work reports an alternative for generic biosensor development. Wherein, conformational changes have been evaluated as intrinsic transduction mechanism for biosensing. Therefore, H18-avidin aptamer has shown affinity properties in the low nM range ( $K_D = 1.3$  nM) and a binding free energy (-46 kJ/mol) three times higher than the hairpin structure calculation (-15.19 kJ/mol). These results suggest that the hairpin structure becomes an attractive element to induce conformational changes in

aptamer. The development of several aptamers by the same methodology it is prerequisite in order to prove the real applications of these improvements in biosensing and SELEX fields.

The future perspectives in generic biosensor development, would be addressed to the identification of the aptamer scaffold structure that involves conformational changes and its stabilization. The stabilization process could be performed by the incorporation of non-natural nucleic acids such as LNA (Locked Nucleic Acids) which have been reported as protectors for enzyme degradation and stabilized agents. In this sense, the library design for SELEX method will be carried out as follows: a) primer region that flanked the library members for PCR amplification, b) an arbitrary scaffold where the intrinsic transduction mechanism will be incorporated and c) the random sequence in order to identified the target. This ambitious plan will be able to obtain molecules by SELEX with similar biorecognition properties as periplasmic binding proteins (PBPs) or anticalins, however the limitations about production or intrinsic transduction mechanism will be overcome.